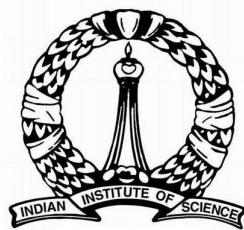


The monopole-dimer model and eccentricities for Cartesian product of graphs

A Dissertation
submitted in partial fulfillment
of the requirements for the award of the
degree of
Doctor of Philosophy

by
Anita Arora



Department of Mathematics
Indian Institute of Science
Bangalore - 560012

Declaration

I hereby declare that the work reported in this thesis is entirely original and has been carried out by me under the supervision of Prof. Arvind Ayyer at the Department of Mathematics, Indian Institute of Science, Bangalore. I further declare that this work has not been the basis for the award of any degree, diploma, fellowship, associateship or similar title of any University or Institution.

Anita Arora

01-01-00-10-11-19-1-17579

Indian Institute of Science,
Bangalore,
June, 2024.

Prof. Arvind Ayyer
(Research advisor)

Dedication

To my beloved father,
Mr. Chandra Shekhar Arora (Lt.).

Acknowledgment

Completing this thesis has been a significant journey, and I am deeply grateful to the many individuals who have supported and encouraged me along the way.

First and foremost, I would like to express my sincere gratitude to my research supervisor *Prof. Arvind Ayyer* for his invaluable guidance, insightful feedback, and continuous support throughout the course of my research. I am thankful to him for allowing me to work under his guidance and introducing me to the beautiful theory of combinatorics and dimers. I am grateful for his patience and understanding. I thank him for providing me with the opportunity to visit some of the best conferences and workshops around the world. I am deeply grateful to him for carefully reviewing all the drafts of my research articles, as well as this thesis, and for providing me with valuable feedback that significantly improved the quality of my work.

I would like to thank the Department of Mathematics at the Indian Institute of Science for providing me with an excellent environment for research. I extend my sincere thanks to the faculty of the Department of Mathematics and Computer Science at the Institute for offering a wide variety of courses for an enriching learning experience. I am grateful to be a teaching assistant of *Prof. Gautam Bharali* and my supervisor. My special thanks to *Prof. L. Sunil Chandran* at the Department of Computer Science and Automation, Indian Institute of Science for introducing me to Krenn's conjecture and for engaging in numerous useful discussions. I thank the technical and administrative staff at the department and Institute for their quick resolution to all the queries and problems.

I would like to thank *Prime Minister Research Funding* (PMRF: PM-MHRD_19_17579) and the DST FIST program - 2021 [TPN - 700661] for supporting the research in this thesis and funding me to present the parts of this thesis at various national and international conferences. My humble gratitude to my comprehensive exam panelists and PMRF review committee members for their fruitful and encouraging remarks. I thank Prof. K. Somasundaram at the Department of Mathematics, Amrita Vishwa Vidyapeetham and Prof. Satyanarayana Reddy at the Department of Mathematics, Shiv Nadar University for giving me an opportunity to carry out my PMRF teaching assistance under their supervision.

I would like to thank my seniors and collaborators *Dr. Hiranya Kishore Dey* and *Dr. Shivani Goel*. They helped me to learn many new things which were useful in various ways in the creation of this thesis. Special thanks to my collaborator *Mr. Rajiv Mishra* at the Department of Mathematics and Statistics, Indian Institute of Science and Research Kolkata. Chapter 7 and Chapter 8 are based on our collaborated work about

the eccentric graphs.

I extend my thanks to my friends, seniors and colleagues at the Department/ Institute Subhajit Ghosh, Digjoy Paul, G.K.V. Teja, Ritul Duhan, Mohd. Irfan, Sumanta Das, Ajay Kumar Nair, Dipnit Biswas, Nimisha Pahuja, Rishikesh Gajjala, Vikas Arora and Abhishek Ranjan for the academic and emotional support.

Finally, I thank my parents for their encouragement and unwavering belief in me. I thank my father (Chandra Shekhar Arora) for envisioning my education, and my brother (Jatin Arora) for consistently supporting and pushing my father and me in this journey. I thank my mother (Shashi Arora) for protecting me from falling and lifting me up whenever I faltered. My husband (Abhishek Lal) for challenging me to do better in each phase of life. Lastly, my heartfelt gratitude to many I cannot individually acknowledge in this concise list.

Abstract

This thesis comprises two main parts. The details of the two parts are as follows:

The first part of the thesis deals with the monopole-dimer model. The dimer (resp. monomer-dimer) model deals with weighted enumeration of perfect matchings (resp. matchings). The monopole-dimer model is a signed variant of the monomer-dimer model which has determinantal structure. A more general model called the *loop-vertex model* has also been defined for an oriented graph and the partition function in this case can also be written as a determinant. However, this model depends on the orientation of the graph. The monopole-dimer model interprets the loop-vertex model independent of the orientation for planar graphs with Pfaffian orientation. The first part of the thesis focuses on the extension of the monopole-dimer model for planar graphs (*Math. Phys. Anal. Geom.*, 2015) to Cartesian products thereof. We show that the partition function of this model can be expressed as a determinant of a generalised signed adjacency matrix. We then show that the partition function is independent of the orientations of the planar graphs so long as they are Pfaffian. When these planar graphs are bipartite, we show that the computation of the partition function becomes especially simple. We then give an explicit product formula for the partition function of three-dimensional grid graphs à la Kasteleyn and Temperley–Fischer, which turns out to be fourth power of a polynomial when all grid lengths are even. Further, we generalise this product formula to higher dimensions, again obtaining an explicit product formula. We also discuss about the asymptotic formulas for the free energy and monopole densities.

Lu and Wu (*Physics Letters A*, 1999) evaluated the partition function of the dimer model on two-dimensional grids embedded on a Möbius strip and a Klein bottle. We first prove a product formula for the partition function of the monopole-dimer model for the higher dimensional grid graphs with cylindrical and toroidal boundary conditions. We then consider the monopole-dimer model on high-dimensional Möbius and Klein grids, and evaluate the partition function for three-dimensional Möbius and Klein grids. Further, we show that the formula does not generalise for the higher dimensions in

any natural way. Finally, we present a relation between the product formulas for three-dimensional grids with cylindrical and Möbius boundary conditions, generalising a result of Lu and Wu.

Let G be an undirected simple connected graph. We say a vertex u is eccentric to a vertex v in G if $d(u, v) = \max\{d(v, w) : w \in V(G)\}$. The eccentric graph of G , denoted $Ec(G)$, is a graph defined on the vertices of G in which two vertices are adjacent if one is eccentric to the other. In the second part of the thesis, we find the structure and the girth of the eccentric graph of trees, and see that the girth of the eccentric graph of a tree can either be zero, three, or four. Further, we study the structure of the eccentric graph of Cartesian product of graphs and prove that the girth of the eccentric graph of the Cartesian product of trees can only be zero, three, four or six. Furthermore, we provide a complete classification of when the eccentric girth assumes these values. We also give the structure of the eccentric graph of the grid graphs and Cartesian product of two cycles. Finally, we determine the conditions under which the eccentricity matrix of Cartesian product of trees becomes invertible.

Contents

1	Introduction	5
1.1	Brief Literature Review	5
1.2	Organisation of the thesis	8
2	Preliminaries	11
2.1	Basic terminology	11
2.2	The dimer model and the monopole-dimer model	12
2.3	The dimer model on grids embedded on different surfaces	16
2.4	Some useful linear algebraic identities	18
2.5	Concepts related to eccentricity	20
3	Monopole-dimer model on Cartesian products of plane graphs	23
3.1	Cycle decompositions	23
3.2	Extended monopole-dimer model	25
3.3	Cartesian products of plane bipartite graphs	28
4	Monopole-dimer model on grid graphs	35
4.1	Three-dimensional grid graphs	35
4.2	Higher-dimensional grid graphs	40
4.3	Asymptotic Behaviour	45
5	High-dimensional cylindrical and toroidal grid graphs	51
5.1	General cylindrical grids	51
6	Three-dimensional Möbius and Klein grid graphs	57
6.1	Three-dimensional Möbius grids	58
6.2	Three-dimensional Klein grids	63
7	Eccentric graph of trees	73
7.1	Structure of eccentric graph of a tree	73

7.2	Eccentric girth of a tree	76
8	Eccentric graph of Cartesian products	79
8.1	Cartesian product of graphs	79
8.2	Eccentric girth of Cartesian product of trees	82
8.3	Cartesian product of two path graphs	83
8.4	Cartesian product of two cycle graphs	85
8.5	Invertibility of eccentricity matrix of Cartesian product of trees	88

List of Papers and Preprints

This thesis is based on the following work.

- Anita Arora and Arvind Ayyer. The monopole-dimer model on Cartesian products of plane graphs. *Combinatorial Theory*, 3(3), 2023.
- Anita Arora and Rajiv Mishra. Eccentric graph of trees and their Cartesian products. *Discrete Mathematics*, 347(9):114062, 2024.
- Anita Arora. The monopole-dimer model on high-dimensional cylindrical, toroidal, Möbius and Klein grids. *arXiv:2406.05750*, 2024.

List of Notation

Notation	Description
$V(G)$	Set of vertices in the graph G
$E(G)$	Set of edges in the graph G
$\mathcal{M}(G)$	Set of all dimer coverings of the graph G
$\mathcal{L}(G)$	Set of loop-vertex configurations of the graph G
$\chi(c)$	The number of vertices in $V(G)$ enclosed by the cycle c
P_n	Path graph on n vertices
C_n	Cycle graph on n vertices
K_n	Complete graph on n vertices
$K_{n,m}$	Complete bipartite graph on $n + m$ vertices
$g(G)$	Girth of the graph G
$Ec(G)$	Eccentric graph of the graph G
\mathcal{E}_G	Eccentricity matrix of the graph G
$\text{Pf}(A)$	Pfaffian of a skew-symmetric matrix A
$\det A$	Determinant of the square matrix A .
$\mathcal{K}_G \equiv \mathcal{K}_{G,\mathcal{O}}$	Generalised adjacency matrix of the oriented graph (G, \mathcal{O})

Chapter 1

Introduction

The main objectives of this thesis are

1. to extend the monopole-dimer model from plane graphs to Cartesian product of plane graphs,
2. to explore some structural properties of the eccentric graph of a tree and Cartesian product of trees.

We start by giving a brief review of the related work in Section 1.1, followed by an outline of the thesis in Section 1.2.

1.1 Brief Literature Review

The *dimer model* originally arose as the study of the physical process of adsorption of diatomic molecules (like oxygen) on the surface of a solid. Abstractly it can be thought of as enumerating perfect matchings in an edge-weighted graph. For planar graphs, Kasteleyn [21] solved the problem completely by showing that the partition function defined in (2.2.1) can be written as a Pfaffian of a certain adjacency matrix built using a special class of orientations called Pfaffian orientations on the graph. An immediate corollary of Kasteleyn's result is that the Pfaffian is independent of the orientation. For the case of two-dimensional grid graphs $Q_{m,n}$, Kasteleyn [20] and Temperley–Fisher [13, 32] independently gave an explicit product formula. Fisher and Stephenson [14] also studied the correlation properties of the dimer model on two-dimensional grids. For example, when m and n are even, horizontal (resp. vertical) edges have weight a (resp. b), the partition function of the dimer model on $Q_{m,n}$ with free boundary condition can be written as

$$\prod_{i=1}^{m/2} \prod_{j=1}^{n/2} \left(4a^2 \cos^2 \frac{i\pi}{m+1} + 4b^2 \cos^2 \frac{j\pi}{n+1} \right). \quad (1.1.1)$$

We do not know of any simple recurrence for this formula. This formula is remarkable because although each factor is a degree-two polynomial in a and b with coefficients that may not be rational, the product turns out to be a polynomial with nonnegative integer coefficients. In particular, when $a = b = 1$, the result is an integer.

A similar product formula for the weighted enumeration of perfect matchings of the two-dimensional grid graph has been given by McCoy and Wu [29] for cylindrical and toroidal boundary conditions and by Lu and Wu [25] for Möbius and Klein boundary conditions. Kasteleyn [22] stated and Cimasoni and Reshetikhin [12] proved that the weighted enumeration of perfect matchings of a graph embeddable on a surface of genus g may be written as a linear combination of 4^g Pfaffians. Tesler [33] showed that the partition function of the dimer model on graphs embedded on non-orientable surfaces can be enumerated as a linear combination of some Pfaffians. Brankov and Priezzhev [9] gave explicit expressions for the free energy of the dimer model on finite two-dimensional grids embedded on a Möbius strip.

There have been attempts to generalise the dimer model while preserving this nice structure. The natural physical generalisation is the *monomer-dimer model*, which represents adsorption of a gas cloud consisting of both monoatomic and diatomic molecules. The abstract version here is the (weighted) enumeration of all matchings of a graph. The weights are interpreted as energies and are positive real numbers. This is known to be a computationally difficult problem [18] and the partition function here does not have such a clean formula. However, when there is a single monomer on the boundary of a plane graph, the partition function can indeed be written as a Pfaffian [36]. A lower bound for the partition function of the monomer-dimer model for d -dimensional grid graphs has been obtained by Hammersley–Menon [16] by generalising the method of Kasteleyn and Temperley–Fisher [32].

In another direction, a signed version of the monomer-dimer model called the *monopole-dimer model* has been introduced [6] for planar graphs. Configurations of the monopole-dimer model can be thought of as superpositions of two monomer-dimer configurations having monomers (called monopoles there) at the same locations. Thus, one ends up with even loops and isolated vertices. What makes the monopole-dimer model less physical is that configurations have a signed weight and they cannot be interpreted as energies anymore. On the other hand, the partition function here can be expressed as a determinant. Moreover, it is a perfect square for a $2m \times 2n$ grid graph. A combinatorial interpretation of the square root is given in [7].

In [6], a more general model called the *loop-vertex model* has also been defined for a general graph together with an orientation. The partition function in this case can also be written as a determinant. However, this model depends on the orientation. One of

the main motivations for this work is to find natural families of non-planar graphs where the partition function is independent of the orientation, just as in the monopole-dimer model. The second motivation comes from the intuition that the monopole-dimer model is an ‘integrable variant’ of the more physical monomer-dimer model. If this is correct, asymptotic properties of both models should be similar. This has been explained in [6] for the two-dimensional grid. We expect this to hold for high dimensional grids also. This is not easy to see because of the signs in monopole-dimer weights. We hope this work will be a starting point towards establishing this relationship between the two models. We note in passing that higher dimensional dimer models have started attracting attention; see [11, 17] for example.

The notion of eccentricity matrix was first introduced by Randić as the D_{max} -matrix in 2013 [30] and subsequently, Wang, Lu, Belardo and Randić renamed it as the eccentricity matrix in 2018 [34]. The eccentricity matrix of a graph is also called as anti-adjacency matrix in the following sense. The eccentricity matrix is obtained from the distance matrix by preserving only the largest distances in each row and column; on the other hand, the adjacency matrix is obtained from the distance matrix by preserving only the smallest non-zero distances in each row and column. Unlike the adjacency matrix and the distance matrix, the eccentricity matrix of a connected graph need not be irreducible. The eccentricity matrix of a complete bipartite graph is reducible and the eccentricity matrix of a tree is irreducible [34, 27].

Spectra of the eccentricity matrix for some graphs are studied by Mahato, Gurusamy, Kannan and Arockiaraj in [27] and by Wang, Lu, Belardo and Randić in [34], the lower and upper bounds for the \mathcal{E} -spectral radius of graphs are also discussed in [34]. Wang, Lu, Brunetti, Lu and Huang studied the non-isomorphic co-spectral graphs with respect to the eccentricity matrix [35]. The eccentricity matrix has interesting applications in the field of chemical graph theory [30, 31]. In another direction, some eccentricity-based indices have also been studied. Xu, Das and Maden [38] have obtained bounds on the non-self-centrality number (NSC number) of a graph G . The bounds for the difference of the eccentric connectivity index (ECI) and the connective eccentricity index (CEI) of a tree have been studied and the corresponding extremal trees have also been classified [37].

A necessary and sufficient condition for the eccentric graph of G to be isomorphic to G or the complement of G is given by Akiyama, Ando and Avis [2]. Kaspar, Gayathri, Kulandaivel, Shobhanadevi gave the complete structure of the eccentric graph for some well-known graphs like paths and cycles [19]. Many interesting properties of the eccentricity matrix of a tree have been established so far. For instance, Mahato, Gurusamy, Kannan, and Arockiaraj showed that the eccentricity matrix of a tree is invertible only if the tree is a star [26]. Additionally, Mahato and Kannan showed that the diameter

of the tree is odd if and only if the eigenvalues of its eccentricity matrix are symmetric about the origin [28].

1.2 Organisation of the thesis

The work in this thesis is motivated by the work in [6, 25, 26, 27, 28]. In particular, Ayyer [6] defines the two main models the monopole-dimer model for the planar graphs and the loop-vertex model for general oriented graphs. He showed that the monopole-dimer model interprets the loop-vertex model independent of the Pfaffian orientation for planar graphs. This raises the natural question of finding more families where the orientation independency can be observed. Lu and Wu [25] worked on the dimer model for the two-dimensional grid graphs embedded on different non-orientable surfaces, suggesting the scope of research for the higher-dimensional grids. Mahato, Gurusamy, Kannan and Arockiaraj [26, 27, 28] studied many intriguing properties about the eccentric graph of a tree which motivated us to examine the complete structure of the aforementioned.

In Chapter 2, we discuss the background theory, essential preliminaries and the notations crucial for this thesis. In Section 2.2 we formulate the models and in Section 2.3, we will look at the partition function of the dimer model on two-dimensional grids embedded on different surfaces. In Section 2.4, we see some unitary similarity transforms from linear algebra relevant to our work and finally in Section 2.5, we define quantities needed to talk about the eccentricity and eccentric graph.

To address the first question, we formulate the monopole-dimer model for Cartesian products of plane graphs in Chapter 3. A key ingredient in the formulation is the construction of special directed cycle decompositions of certain projections, which are themselves plane graphs with parallel edges. We show in Theorem 3.9 that the partition function of the (extended) monopole-dimer model is a determinant of a generalised adjacency matrix built using Pfaffian orientations. As in the dimer model, we see immediately in Corollary 3.10 that the determinant is independent of the orientation. In Section 3.3, we focus attention on the monopole-dimer model on Cartesian product of bipartite plane graphs. Here, we will show in Theorem 3.14 that we can allow arbitrary cycle decompositions of the projections mentioned above. This seems to be a new observation of independent interest.

In Chapter 4, we focus on the special family of grid graphs in high dimensions. We give an explicit product formula for the partition function of the monopole-dimer model on three-dimensional grid graphs in Theorem 4.1 generalising the formula (1.1.1). One peculiar feature of this partition function is that it is a fourth power of a polynomial

when all side lengths are even. Just as for the partition function of the monopole-dimer model for two-dimensional grids, it would be interesting to obtain a combinatorial interpretation of the fourth root. We then briefly discuss the higher dimensional case in Section 4.2 and give a similar explicit product formula in Theorem 4.4. We also discuss its asymptotic behaviour in Section 4.3.

In Chapter 5, we define high-dimensional cylindrical and toroidal grid graphs. We generalise the product formulas for the partition function of the dimer model on two-dimensional grids embedded on a cylinder and a torus for the monopole-dimer model on the d -dimensional cylindrical and toroidal grid graphs. We also give the product formula for the monopole-dimer model on the three-dimensional Möbius and Klein grids in Theorem 6.4 and Theorem 6.11. We show that the formulas do not hold for higher dimensions by providing counterexamples in Example 6.7 and Example 6.12. Further, we establish a relationship between three-dimensional grids with cylindrical and Möbius boundary conditions in Corollary 6.8, generalising a result of Lu and Wu [25].

In Chapter 7, we discuss about the eccentric graph of a tree. We give a complete structure of the eccentric graph of a general tree in Section 7.1 and prove that the eccentricity of a vertex is either the smallest or largest among its neighbors in the eccentric graph in Proposition 7.5. In Section 7.2, we prove that the eccentric girth of a tree can either be zero, three or four. We also discuss when these values are attained.

In Chapter 8, we present some structural properties of the eccentric graph of Cartesian product of graphs and classify all the possible values of the eccentric girth for Cartesian product of trees. We discuss the structure of the eccentric graph of Cartesian product of two path graphs and two cycle graphs in Sections 8.3 and 8.4. We also discuss about their girth. Lastly, in Section 8.5, generalising the result in [26, Theorem 2.1], we analyze and classify the conditions under which the eccentricity matrix of Cartesian product of trees becomes invertible.

Chapter 2

Preliminaries

In this chapter, we set up the notations and state the known results. We start by defining the well-known dimer model in Section 2.2 and see results for the partition function of dimer model on grids embedded on different surfaces in Section 2.3.

2.1 Basic terminology

We begin by recalling basic terminology from graph theory. A (*simple*) *graph* is an ordered pair $G = (V(G), E(G))$, where $V(G)$ is the set of *vertices* of G and $E(G)$ is a collection of two-element subsets of $V(G)$, known as *edges*. When we allow multiple edges between a pair of vertices (also called *parallel edges*), we will call such objects *multigraphs*. We will never allow self loops. We will work with undirected graphs and we will always assume that the graphs are finite and naturally vertex-labeled from $\{1, 2, \dots, |V(G)|\}$. A simple graph is therefore a graph with no parallel edges. The *degree* of a vertex is the number of edges incident to it and an *even* (multi)graph G is one in which all the vertices have even degree. A vertex of degree 1 is called a *leaf* or a *pendant* vertex. A *walk* in a graph G is a sequence $(v_0, e_1, v_1, \dots, v_{t-1}, e_t, v_t)$ of alternating vertices v_0, \dots, v_t and edges e_1, \dots, e_t of G , such that v_{i-1} and v_i are the endpoints of e_i for $1 \leq i \leq t$. v_0 and v_t are called the *initial* and *final* vertices respectively. A *path* in G is a walk whose vertices and edges both are distinct. A *cycle* in G is a path whose initial and final vertices are identical. The *size* of a path or a cycle is the number of edges in it. These definitions apply also to multigraphs. A *tree* is a connected graph with no cycles.

A *path graph* is a simple graph with vertices $\{1, \dots, n\}$ and two vertices are adjacent if and only if they are consecutive. A *cycle graph* is obtained from the path graph by adding an extra edge from vertex 1 to vertex n . Throughout the text, we will denote the path graph and the cycle graph on n vertices as P_n and C_n , respectively. A *star graph*

S_n on $(n + 1)$ vertices is a graph with n vertices of degree 1 and one vertex, called the *center*, of degree n . A *double star* $S_{s,t}$ is a graph obtained by adding an edge between the central vertices of two stars S_s and S_t . Let K_t denotes the complete graph on t vertices.

Recall that a *planar* graph is a graph which can be embedded in the plane, i.e. it can be drawn in such a way that no edges will cross each other. Such an embedding of a planar graph is referred as a *plane graph* and it divides the whole plane into regions, each of which is called a *face*. For a plane graph G and a cycle c in G , the vertices *enclosed by* c are the vertices lying strictly in the interior of c . We will consider only those embeddings of the graph for which parallel edges do not enclose any vertex. An *orientation* on a graph G is an assignment of arrows to its edges. A graph G with an orientation \mathcal{O} is called an *oriented graph* and is denoted (G, \mathcal{O}) . An orientation on a labeled graph obtained by orienting its edges from lower to higher labeled vertex is called a *canonical orientation*.

Definition 2.1. Let G_1 and G_2 be two simple connected graphs. The *Cartesian product* of G_1 and G_2 denoted as $G_1 \square G_2$ is a graph with vertex set $V(G_1) \times V(G_2)$, where two vertices (u_1, u_2) and (v_1, v_2) are adjacent if and only if either $u_1 = v_1$ and $u_2 \sim_{G_2} v_2$ or $u_1 \sim_{G_1} v_1$ and $u_2 = v_2$.

The above definition generalises to the *Cartesian product of k graphs* G_1, \dots, G_k , denoted $G_1 \square \dots \square G_k$. We write Q_{n_1, \dots, n_d} for the d -dimensional grid graph which is Cartesian product $P_{n_1} \square \dots \square P_{n_d}$.

2.2 The dimer model and the monopole-dimer model

All our models will be defined on simple graphs. We will encounter graphs with parallel edges only in certain decompositions.

Definition 2.2. An orientation on a plane graph G is said to be *Pfaffian* if it satisfies the property that each bounded face has an odd number of clockwise oriented edges. A Pfaffian orientation is said to possess the *clockwise-odd property*.

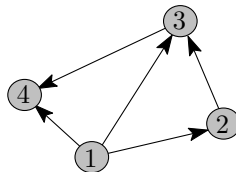


Figure 2.1: An oriented graph on 4 vertices.

For example, the orientation in Figure 2.1 is a Pfaffian orientation. Kasteleyn has shown that every plane graph has a Pfaffian orientation [21]. Recall that an edge e is said to *cover* a vertex v if v is a vertex in e . A *dimer covering* or *perfect matching* is a collection of edges in the graph G such that each vertex is covered in exactly one edge. The set of all dimer coverings of G will be denoted as $\mathcal{M}(G)$. Let G be an edge-weighted graph on $2n$ vertices with real positive weight w_e for $e \in E(G)$ (thought of as the energy of e). Then the *dimer model* is the collection of all dimer coverings where the weight of each dimer covering $M \in \mathcal{M}(G)$ is given by $w(M) = \prod_{e \in M} w_e$. The *partition function* of the dimer model on G is then defined as

$$Z_G := \sum_{M \in \mathcal{M}(G)} w(M), \quad (2.2.1)$$

which is basically the weighted enumeration of perfect matchings in G . To state Kasteleyn's celebrated result, recall that a matrix $A = (a_{i,j})$ is skew-symmetric if $a_{i,j} = -a_{j,i}$ for every i, j , and the *Pfaffian* of $2n \times 2n$ skew-symmetric matrix A is given by

$$\text{Pf}(A) = \frac{1}{2^n n!} \sum_{\sigma \in S_{2n}} \text{sgn}(\sigma) A_{\sigma_1, \sigma_2} A_{\sigma_3, \sigma_4} \cdots A_{\sigma_{2n-1}, \sigma_{2n}},$$

and Cayley's theorem [10] says that for such a matrix, $\det A = \text{Pf}(A)^2$.

Theorem 2.3 (Kasteleyn [21]). *If G is a plane graph with Pfaffian orientation \mathcal{O} , then the partition function of the dimer model on G is given by $Z_G = |\text{Pf}(K_G)|$, where K_G is a signed adjacency matrix defined by*

$$(K_G)_{u,v} = \begin{cases} w_e & u \rightarrow v \text{ in } \mathcal{O}, \\ -w_e & v \rightarrow u \text{ in } \mathcal{O}, \\ 0 & \text{otherwise.} \end{cases}$$

The partition function of the dimer model on the two-dimensional grid graphs $Q_{2m,2n}$ where horizontal (resp. vertical) edges have weight a (resp. b) is given by (1.1.1).

Throughout this article, we will refer to cycles in configurations on graphs as *loops*. We will always understand these loops to be directed. Let us now recall the generalization of the dimer model known as the loop-vertex model [6]. Let G be a simple weighted graph on n vertices with an orientation \mathcal{O} , vertex-weights $x(v)$ for $v \in V(G)$ and edge-weights $a_{v,v'} = a_{v',v}$ for $(v, v') \in E(G)$. A *loop-vertex configuration* C of G is a subgraph of G consisting of

- directed loops of even length (with length at least four),

- doubled edges (which can be thought of as loops of length two), and
- isolated vertices,

with the condition that each vertex of G is either an isolated vertex or is covered in exactly one loop. The set of all loop-vertex configurations of G will be denoted as $\mathcal{L}(G)$. Figure 2.2 shows a graph and two loop-vertex configurations on it.

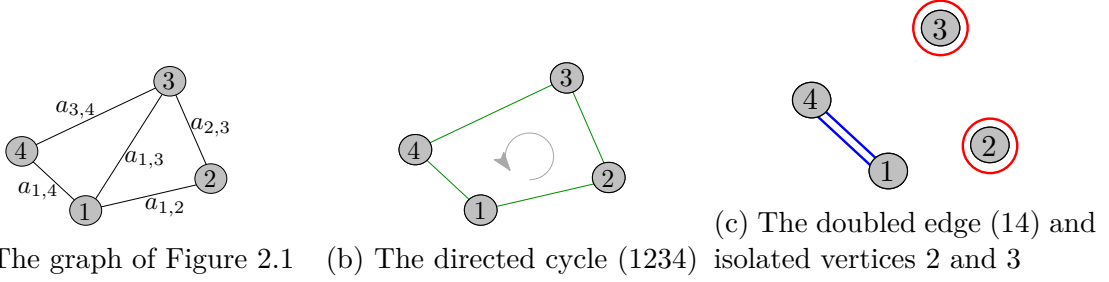


Figure 2.2: The graph of Figure 2.1 with edge weights marked in Figure 2.2a, and two loop-vertex configurations on it in Figure 2.2b and Figure 2.2c.

Let $\ell = (v_0, v_1, \dots, v_{2k-1}, v_{2k} = v_0)$ be a directed even loop for $k \geq 1$ in (G, \mathcal{O}) . The *weight* of the loop ℓ is given by

$$w(\ell) := - \prod_{i=0}^{2k-1} \text{sgn}(v_i, v_{i+1}) a_{v_i, v_{i+1}}, \quad (2.2.2)$$

where,

$$\text{sgn}(v, v') := \begin{cases} 1 & v \rightarrow v' \text{ in } \mathcal{O}, \\ -1 & v' \rightarrow v \text{ in } \mathcal{O}. \end{cases} \quad (2.2.3)$$

Note that the weight of a doubled edge (v_i, v_j) is always $+a_{v_i, v_j}^2$.

Then the *loop-vertex model* on the pair (G, \mathcal{O}) is the collection $\mathcal{L}(G)$ with the weight of a configuration, $C = (\ell_1, \dots, \ell_j; v_1, \dots, v_k)$ consisting of loops ℓ_1, \dots, ℓ_j and isolated vertices v_1, \dots, v_k , given by

$$w(C) = \prod_{i=1}^j w(\ell_i) \prod_{i=1}^k x(v_i). \quad (2.2.4)$$

The (*signed*) *partition function* of the loop-vertex model is defined as

$$\mathcal{Z}_{G, \mathcal{O}} := \sum_{C \in \mathcal{L}(G)} w(C).$$

The term partition function here comes directly from statistical physics and has no relation with integer partitions.

Example 2.4. Let G be a weighted graph on four vertices with vertex weights x for all the vertices and edge weights as shown in Figure 2.2a. Then the weights of the configuration shown in Figures 2.2b and 2.2c are $a_{1,2}a_{2,3}a_{3,4}a_{1,4}$ and $x^2a_{1,4}^2$. The partition function of the loop-vertex model on the graph in Figure 2.2a with the canonical orientation is

$$\mathcal{Z}_{G,\mathcal{O}} = x^4 + a_{1,2}^2x^2 + a_{1,3}^2x^2 + a_{1,4}^2x^2 + a_{2,3}^2x^2 + a_{3,4}^2x^2 + a_{1,2}^2a_{3,4}^2 + a_{1,4}^2a_{2,3}^2 + 2a_{1,2}a_{2,3}a_{3,4}a_{1,4}.$$

The last term has coefficient 2 as the cycle (1234) has two directions.

Definition 2.5. Let G be a graph with orientation \mathcal{O} , then the *generalised adjacency matrix* of (G, \mathcal{O}) is defined as

$$\mathcal{K}_{G,\mathcal{O}}(v, v') = \begin{cases} x(v) & v = v', \\ a_{v,v'} & v \rightarrow v' \text{ in } \mathcal{O}, \\ -a_{v,v'} & v' \rightarrow v \text{ in } \mathcal{O}, \\ 0 & (v, v') \notin E(G). \end{cases} \quad (2.2.5)$$

We use \mathcal{K}_G instead of $\mathcal{K}_{G,\mathcal{O}}$ whenever the underlying orientation is clear.

Theorem 2.6 ([6, Theorem 2.5]). *The partition function of the loop-vertex model on (G, \mathcal{O}) is*

$$\mathcal{Z}_{G,\mathcal{O}} = \det \mathcal{K}_G,$$

where \mathcal{K}_G is a generalised adjacency matrix of (G, \mathcal{O}) .

Example 2.7. The generalised adjacency matrix for the graph G in Example 2.4 with the canonical orientation is

$$\mathcal{K}_G = \begin{pmatrix} x & a_{1,2} & a_{1,3} & a_{1,4} \\ -a_{1,2} & x & a_{2,3} & 0 \\ -a_{1,3} & -a_{2,3} & x & a_{3,4} \\ -a_{1,4} & 0 & -a_{3,4} & x \end{pmatrix},$$

and

$$\det \mathcal{K}_G = x^4 + a_{1,2}^2x^2 + a_{1,3}^2x^2 + a_{1,4}^2x^2 + a_{2,3}^2x^2 + a_{3,4}^2x^2 + a_{1,2}^2a_{3,4}^2 + a_{1,4}^2a_{2,3}^2 + 2a_{1,2}a_{2,3}a_{3,4}a_{1,4},$$

which is exactly $\mathcal{Z}_{G,\mathcal{O}}$ from Example 2.4.

If G is a simple plane graph and \mathcal{O} is a Pfaffian orientation on it, then the loop-vertex model is called the *monopole-dimer model*. In that case, it has been shown [6, Theorem

3.3] that the weight of a loop $\ell = (v_0, v_1, \dots, v_{2k-1}, v_{2k} = v_0)$ can be written independent of the Pfaffian orientation as stated in the following result.

Theorem 2.8 ([6, Equation 3.1]). *Let G be a simple vertex- and edge-weighted plane graph and \mathcal{O} is a Pfaffian orientation on G . Then the weight of a loop $\ell = (v_0, v_1, \dots, v_{2k-1}, v_{2k} = v_0)$ in (2.2.2) can be written as*

$$w(\ell) = (-1)^{\text{number of vertices enclosed by } \ell} \prod_{j=0}^{2k-1} a_{v_j, v_{j+1}}. \quad (2.2.6)$$

Then Theorem 2.6 can be used to show the following result.

Corollary 2.9. *The determinant of the generalised adjacency matrix of a plane graph with a Pfaffian orientation is independent of the orientation.*

The monopole-dimer model reduces to the so-called double-dimer model [23, 24] when vertex weights are zero for all the vertices in the graph.

2.3 The dimer model on grids embedded on different surfaces

McCoy and Wu obtained a product formula for the partition function of two-dimensional grid graphs embedded on a cylinder and a torus similar to the one by Kasteleyn and Temperley-Fisher's formula in (1.1.1) for the two-dimensional grid graphs with free boundary.

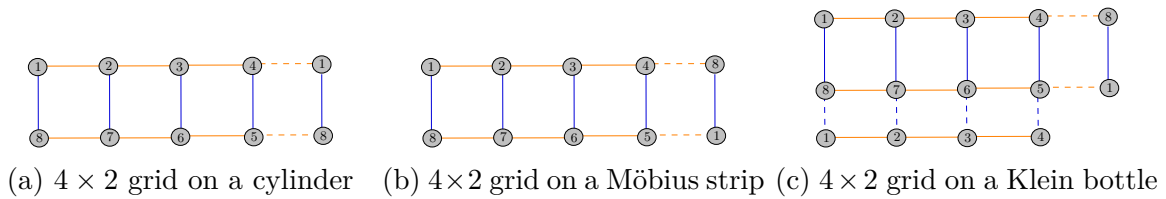


Figure 2.3: Two-dimensional grid with different boundary conditions

Theorem 2.10 ([29, Equation (6.33), (6.53)]). *The partition function of the dimer model on the two-dimensional grid graph $Q_{2m, 2n}$ where horizontal (resp. vertical) edges have weight a (resp. b) with cylindrical and toroidal boundary conditions is given by*

$$Z_{Q_{2m, 2n}}^{Cyl} = \prod_{i=1}^m \prod_{j=1}^n \left(4a^2 \sin^2 \frac{(2i-1)\pi}{2m} + 4b^2 \cos^2 \frac{j\pi}{2n+1} \right), \quad (2.3.1)$$

and

$$Z_{Q_{2m,2n}}^{Tor} = \prod_{i=1}^m \prod_{j=1}^n \left(4a^2 \sin^2 \frac{(2i-1)\pi}{2m} + 4b^2 \sin^2 \frac{(2j-1)\pi}{2n} \right), \quad (2.3.2)$$

respectively.

Lu and Wu have obtained the similar closed-form expressions for the partition function of the dimer model on $2m \times 2n$ grids embedded on non-orientable surfaces like Möbius strip and Klein bottle. Figure 2.3 shows a two-dimensional grid embedded on different surfaces.

Theorem 2.11 ([25, Equation (18), (19)]). *Let $Q_{2m,2n} = P_{2m} \square P_{2n}$ denote the two-dimensional grid graph with horizontal (resp. vertical) edges having weight a (resp. b). The partition function of the dimer model on $Q_{2m,2n}$ embedded on a Möbius strip and on a Klein bottle is given by*

$$Z_{Q_{2m,2n}}^{Möb} = \prod_{i=1}^m \prod_{j=1}^n \left(4a^2 \sin^2 \frac{(4i-1)\pi}{4m} + 4b^2 \cos^2 \frac{j\pi}{2n+1} \right), \quad (2.3.3)$$

and

$$Z_{Q_{2m,2n}}^{Klein} = \prod_{i=1}^m \prod_{j=1}^n \left(4a^2 \sin^2 \frac{(4i-1)\pi}{4m} + 4b^2 \sin^2 \frac{(2j-1)\pi}{2n} \right), \quad (2.3.4)$$

respectively.

In Chapters 5 and 6, we will generalise Theorem 2.10 and Theorem 2.11 for a more general model called the (extended) monopole-dimer model (defined in Chapter 3). This attempt parallels the approach used to find the partition function of the monopole-dimer model on higher dimensional grids with free boundary conditions in Chapter 4.

Now, let us define the labelling we use in this thesis. Recall that P_n denotes the path graph on n vertices and Q_{n_1, \dots, n_d} is the d -dimensional grid graph which can be regarded as Cartesian product of P_{n_1}, \dots, P_{n_d} denoted as $P_{n_1} \square \dots \square P_{n_d}$. We will associate the labelling L_d (defined inductively), with Q as follows: For $d = 1$, label L_1 is

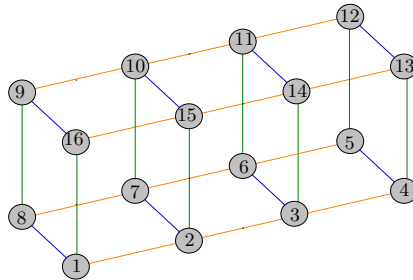


Figure 2.4: The boustrophedon labelling on $P_4 \square P_2 \square P_2$.

$1, 2, \dots, n_1$. For $d > 1$, Q consists of n_d copies of the $(d-1)$ -dimensional grids. Successive copies (with successive last coordinate $1, 2, \dots, n_d$) are labelled consecutively as $L_{d-1}, L'_{d-1}, L_{d-1}, L'_{d-1}, \dots$ where L'_{d-1} represents the labelling of $(d-1)$ -dimensional grid in reverse order of L_{d-1} . In particular, the vertex (p, q, r) in $Q_{2n_1, 2n_2, 2n_3}$ has label

$$\begin{cases} 8tn_1n_2 + 4sn_1 + p & q = 2s + 1, r = 2t + 1, \\ 8tn_1n_2 + 4sn_1 - p + 1 & q = 2s, r = 2t + 1, \\ 8tn_1n_2 - 4sn_1 - p + 1 & q = 2s + 1, r = 2t, \\ 8tn_1n_2 - 4sn_1 + p & q = 2s, r = 2t, \end{cases} \quad (2.3.5)$$

where $p \in [2n_1], q \in [2n_2]$ and $r \in [2n_3]$. Figure 2.4 shows this labelling on the graph $P_4 \square P_2 \square P_2$. Any snake-like labelling like the one above is called a *boustrophedon labelling*.

2.4 Some useful linear algebraic identities

In this section, we recall some unitary similarity transforms that will be useful for computing determinants in Chapters 4 to 6, along with their action on different matrices. We will use \sim to denote the equivalence relation of similarity on matrices and ι for $\sqrt{-1}$. Let $T_k(-s, z, s)$ denote the $k \times k$ tridiagonal Toeplitz matrix with diagonal entries z , subdiagonal entries $-s$ and superdiagonal entries s and J_k denote the $k \times k$ antidiagonal matrix with all antidiagonal entries equal to 1. We will use the following notation for an $n \times n$ diagonal and antidiagonal matrix

$$\text{diag}(x_1, \dots, x_n) = \begin{pmatrix} x_1 & & \\ & \ddots & \\ & & x_n \end{pmatrix},$$

$$\text{adiag}(x_1, \dots, x_n) = \begin{pmatrix} & & x_1 \\ & \ddots & \\ x_n & & \end{pmatrix}.$$

Recall the definition of the *Kronecker product* of two matrices.

Definition 2.12. Let $A = (a_{i,j})$ be an $m \times n$ matrix and $B = (b_{i,j})$ be a $p \times q$ matrix,

then the *Kronecker product*, $A \otimes B$, is an $mp \times nq$ block matrix defined as

$$\begin{pmatrix} a_{11}B & \cdots & a_{1n}B \\ \vdots & \ddots & \vdots \\ a_{m1}B & \cdots & a_{mn}B \end{pmatrix}.$$

The Kronecker product of two matrices is non-commutative in general. If A and B are square matrices of order n and p , respectively, then

$$\det A \otimes B = (\det A)^p (\det B)^n.$$

Lemma 2.13 ([13, Section 4]). *Let u_k be the standard unitary similarity transformation whose entries are given by*

$$(u_k)_{p,q} = \sqrt{\frac{2}{k+1}} \iota^p \sin\left(\frac{pq\pi}{k+1}\right). \quad (2.4.1)$$

Then, u_k transforms the Toeplitz matrix, $T_k(-s, z, s)$, into the diagonal matrix

$$D_k = \text{diag}\left(z + 2\iota s \cos \frac{\pi}{k+1}, \dots, z + 2\iota s \cos \frac{k\pi}{k+1}\right),$$

and

$$(u_k)^{-1} J_k u_k = \iota^{k-1} \begin{pmatrix} & & & (-1)^{k-1} \\ & & & (-1)^{k-2} \\ & & \ddots & \\ & & & \\ (-1)^0 & & & \end{pmatrix}. \quad (2.4.2)$$

Lemma 2.14 ([29, Section 6]). *Let V_n be the unitary similarity transform defined as*

$$V_n = \frac{1}{\sqrt{n}} \begin{pmatrix} 1 & \cdots & 1 \\ e^{\iota\theta_1} & \cdots & e^{\iota\theta_n} \\ \vdots & & \vdots \\ e^{(n-1)\iota\theta_1} & \cdots & e^{(n-1)\iota\theta_n} \end{pmatrix} \text{ for } \theta_j = \frac{2j-1}{n}\pi. \quad (2.4.3)$$

Then,

$$\begin{aligned} V_n^{-1} (T_n(-a, x, a) + a \text{adiag}(1, 0, \dots, 0, -1)) V_n \\ = \text{diag}\left(x + 2\iota a \sin \frac{\pi}{n}, \dots, x + 2\iota a \sin \frac{(2n-1)\pi}{n}\right), \end{aligned}$$

and

$$V_n^{-1} J_n V_n = \text{adiag} \left(-e^{i\frac{\pi}{n}}, \dots, -e^{i\frac{(2n-1)\pi}{n}} \right).$$

2.5 Concepts related to eccentricity

Let G be a simple undirected graph on n vertices with m edges. If two vertices $v, w \in V(G)$ are adjacent, we will write $v \sim_G w$. The *neighbourhood* of a vertex v in G is defined as $N_G(v) = \{w \in V(G) : v \sim_G w\}$. If the graph G is connected, the *distance* $d_G(v, w)$, between two vertices v and w is the length of the shortest path in G connecting them. The *distance matrix* of a connected graph G , denoted D_G , is the $n \times n$ matrix indexed by $V(G)$ whose (v, w) 'th-entry is equal to $d_G(v, w)$.

The *eccentricity*, $e_G(v)$, of a vertex $v \in V(G)$ is defined as

$$e_G(v) = \max\{d_G(u, v) : u \in V(G)\},$$

we will use $e(v)$ instead of $e_G(v)$ whenever there is no confusion about the underlying graph. If $d_G(u, v) = e(v)$, then we will say u is *eccentric* to v and a shortest path between u and v is called an *eccentric path* (starting from v). The *diameter* of G , $\text{diam}(G)$, is the maximum of eccentricities of the vertices in G . A *diametrical path* is a longest path among all eccentric paths in the graph G .

The *eccentricity matrix* of a connected graph G , denoted by \mathcal{E}_G , is constructed from the distance matrix D_G , retaining the largest distances in each row and each column, while other elements of the distance matrix are set to zero. In other words,

$$(\mathcal{E}_G)_{ij} = \begin{cases} d_G(u_i, u_j) & \text{if } d_G(u_i, u_j) = \min\{e(u_i), e(u_j)\}, \\ 0 & \text{otherwise.} \end{cases}$$

Example 2.15. The distance and eccentricity matrix of the path graph P_5 are

$$\mathcal{D}_{P_5} = \begin{pmatrix} 0 & 1 & 2 & 3 & 4 \\ 1 & 0 & 1 & 2 & 3 \\ 2 & 1 & 0 & 1 & 2 \\ 3 & 2 & 1 & 0 & 1 \\ 4 & 3 & 2 & 1 & 0 \end{pmatrix} \quad \text{and} \quad \mathcal{E}_{P_5} = \begin{pmatrix} 0 & 0 & 2 & 3 & 4 \\ 0 & 0 & 0 & 0 & 3 \\ 2 & 0 & 0 & 0 & 2 \\ 3 & 0 & 0 & 0 & 0 \\ 4 & 3 & 2 & 0 & 0 \end{pmatrix}.$$

Definition 2.16 ([2, Section 1]). The *eccentric graph*, denoted $Ec(G)$, of a connected graph G is the simple graph with the vertex set $V(G)$ and uv is an edge in $Ec(G)$ if either v is eccentric to u or u is eccentric to v . In that case, we call u and v are adjacent

in $Ec(G)$ and denote it as $u \sim_{Ec(G)} v$.

Note that the adjacency matrix of the eccentric graph $Ec(G)$ is obtained by replacing the non-zero entries in the eccentricity matrix \mathcal{E}_G , by 1.

Proposition 2.17 ([19, Proposition 1]). *Let P_n be the path graph on n vertices. Then,*

$$Ec(P_n) = \begin{cases} K_n, & \text{if } n \leq 3, \\ S_{\frac{n-2}{2}, \frac{n-2}{2}}, & \text{if } n > 3 \text{ is even,} \\ H_{\frac{n-3}{2}} & \text{if } n > 3 \text{ is odd,} \end{cases}$$

where H_t is a graph obtained by adding t pendant vertices to any two of the vertices of a triangle (see Figure 2.5).

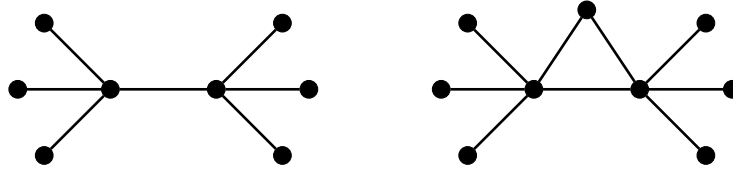


Figure 2.5: Eccentric graphs of the path graphs P_8 and P_9 ($S_{3,3}$ and H_3).

Proposition 2.18 ([19, Proposition 2]). *Let C_n be the cycle graph on n vertices. Then,*

$$Ec(C_n) = \begin{cases} \frac{n}{2}K_2 & \text{if } n \text{ is even,} \\ C_n & \text{if } n \text{ is odd.} \end{cases} \quad (2.5.1)$$

Also, $Ec(K_n) = K_n$ and $Ec(K_{s,t}) = K_s \cup K_t$ for $s, t > 1$.

Recall the *girth* of a graph G is the length of the shortest cycle present in G . If a graph G has no cycles, we will say that G has girth 0. We will call the girth of the eccentric graph as *eccentric girth* and denote it as $g(Ec(G))$. Girth is the dual concept to edge connectivity (minimum number of edges that must be removed to disconnect a graph), in the sense that the girth of a planar graph is the edge connectivity of its dual graph, and vice versa. Calculating the girth of a graph is an important task in graph theory, as it helps us understand the graph's structure and properties. We talk about the eccentric girth of trees and Cartesian product of trees in Chapters 7 and 8.

Chapter 3

Monopole-dimer model on Cartesian products of plane graphs

We now extend the definition of the monopole-dimer model to Cartesian products of plane graphs. Let G_1, \dots, G_k be k simple graphs and $G_1 \square \dots \square G_k$ be their Cartesian product. We will denote edges in $G_1 \square \dots \square G_k$ of the form $((u_1, \dots, u_i, \dots, u_k), (u_1, \dots, u'_i, \dots, u_k))$ as G_i -edges. Clearly, a path graph is plane. It is clear from the definition that Cartesian product of k path graphs is a cuboid in \mathbb{Z}^k , also known as a *grid graph*. Figure 3.1 shows Cartesian product $P_4 \square P_3$. We will use the notation $[n]$ for the set $\{1, \dots, n\}$.

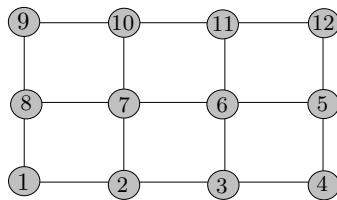


Figure 3.1: Cartesian product $P_4 \square P_3$ with its boustrophedon labelling; see Section 2.3.

3.1 Cycle decompositions

An *edge-disjoint multiset of cycles* in a multigraph G is a family of cycles $\mathcal{D} = \{d_1, \dots, d_k\}$ such that no edge belongs in more than one cycle. In particular, a *cycle decomposition* of a multigraph G is an edge-disjoint multiset of cycles \mathcal{D} of G such that $\bigcup_{d \in \mathcal{D}} E(d) = E(G)$. Veblen's theorem [8, Theorem 2.7] says that a multigraph admits a cycle decomposition if and only if it is even. We say that a cycle decomposition is *directed* if all of its cycles are directed. For a plane graph G and a cycle c in G , denote *the number of vertices in*

$V(G)$ enclosed by c as $\chi(c)$. For example, the number of vertices enclosed by the cycle $(3,4,5)$ is 1 for the graph shown in Figure 3.2a.

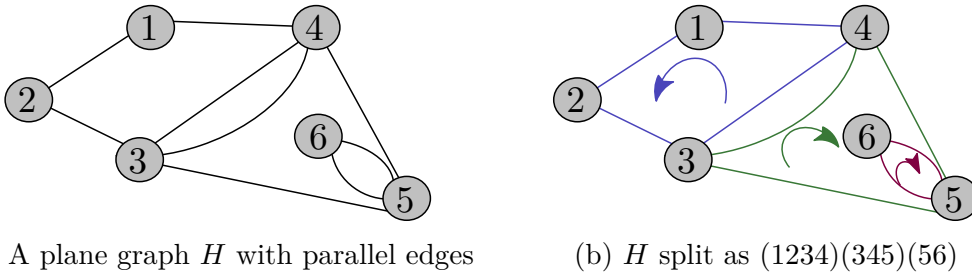
Definition 3.1. We say that the *sign* of an edge-disjoint multiset of directed cycles $\mathcal{D} = \{d_1, \dots, d_k\}$ of an even plane multigraph G is given by

$$\text{sgn}(\mathcal{D}) := \prod_{i=1}^k \begin{cases} (-1)^{\chi(d_i)} & \text{if } d_i \text{ has odd size and is directed clockwise,} \\ (-1)^{\chi(d_i)+1} & \text{if either } d_i \text{ has even size, or has odd size} \\ & \text{and is directed anticlockwise.} \end{cases} \quad (3.1.1)$$

Note that this formula also defines the sign of a directed cycle decomposition.

Example 3.2. For the even plane graph H shown in Figure 3.2a, the sign of its directed cycle decomposition $\{(1, 2, 3, 4), (3, 4, 5), (5, 6)\}$ shown in Figure 3.2b is

$$(-1)^{0+1} \times (-1)^1 \times (-1)^{0+1} = -1.$$



(a) A plane graph H with parallel edges

(b) H split as $(1234)(345)(56)$

Figure 3.2: (a) A plane graph on 6 vertices and (b) a directed cycle decomposition of it.

Recall that an *outerplanar (multi)graph* is a planar (multi)graph that has a planar drawing for which all vertices belong to the outer face of the drawing. Such a planar drawing is called an *outerplane (multi)graph*.

Corollary 3.3. The sign of an edge-disjoint multiset of directed cycles $\mathcal{D} = \{d_1, \dots, d_k\}$ of an even outerplane multigraph G is given by

$$\text{sgn}(\mathcal{D}) := (-1)^{\# \text{ of even cycles in } \mathcal{D} + \# \text{ of anticlockwise directed odd cycles in } \mathcal{D}} \quad (3.1.2)$$

A *trail* in a multigraph G is a walk whose vertices can be repeated but edges are distinct. In particular, trails are allowed to self intersect at vertices. A *closed trail* is one whose initial and terminal vertices are the same. Therefore, a closed trail can be decomposed into an edge-disjoint multiset of cycles. A *directed closed trail* is a closed trail with a definite direction of traversal.

Definition 3.4. Let T be a directed closed trail in a multigraph G . We say that a directed cycle decomposition \mathcal{D} of T is *compatible* with T if the direction of cycles in \mathcal{D} is inherited from the direction of T .

Lemma 3.5. *Let T be a closed directed trail in a plane multigraph G with Pfaffian orientation \mathcal{O} . Then all cycle decompositions of T compatible with it have the same sign.*

Proof. The idea of this proof is similar to that of [6, Theorem 3.3]. Let $\mathcal{D} = \{d_1, \dots, d_k\}$ be a directed cycle decomposition of T compatible with it. Then the number of edges of T oriented in the opposite direction to T is given by

$$\sum_{j=1}^k \left(\text{number of edges oriented in opposite direction of } d_j \right). \quad (3.1.3)$$

For $j \in [k]$, let E_j and F_j be the number of edges and faces enclosed by d_j respectively. Since \mathcal{O} is Pfaffian, the number of clockwise oriented edges on the boundary of any bounded face f is odd (say O_f). Thus the number of clockwise oriented edges of d_j is

$$\sum_{\substack{f \text{ is a face in } G \\ \text{enclosed by } d_j}} O_f - E_j,$$

because each edge enclosed by d_j contributes to exactly two faces, one clockwise and one anticlockwise. Since O_f is odd for any bounded face f , the above quantity has the same parity as $F_j - E_j$. Now, using the Euler characteristic on the plane graph enclosed by d_j , the number of clockwise oriented edges of d_j and the number of vertices enclosed by d_j , which we called $\chi(d_j)$, have opposite parity. Thus the quantity in (3.1.3) is equal to $\text{sgn}(\mathcal{D})$ given in (3.1.1). \square

3.2 Extended monopole-dimer model

Definition 3.6. The *oriented Cartesian product* of naturally labeled oriented graphs $(G_1, \mathcal{O}_1), \dots, (G_k, \mathcal{O}_k)$ is the graph $G_1 \square \dots \square G_k$ with orientation \mathcal{O} given as follows. For each $i \in [k]$, if $u_i \rightarrow u'_i$ in \mathcal{O}_i , then \mathcal{O} gives orientation $(u_1, \dots, u_i, \dots, u_k) \rightarrow (u_1, \dots, u'_i, \dots, u_k)$ if $u_{i+1} + u_{i+2} + \dots + u_k + (k - i) \equiv 0 \pmod{2}$ and $(u_1, \dots, u'_i, \dots, u_k) \rightarrow (u_1, \dots, u_i, \dots, u_k)$ otherwise.

If we assign the canonical orientation to the graph in Figure 3.1, it can be thought of as an oriented Cartesian product of paths P_4 and P_3 which are labeled consecutively from one leaf to another.

Definition 3.7. The i -*projection* of a subgraph S of the Cartesian product $G_1 \square \cdots \square G_k$ is the multigraph obtained by contracting all but G_i -edges of S and is denoted \tilde{S}_i .

Let G_1, \dots, G_k be k plane simple naturally labeled graphs and P be their Cartesian product. Let $\ell = (w_0, w_1, \dots, w_{2s-1}, w_{2s} = w_0)$ be a directed even loop in P , and \mathcal{D}_i be a cycle decomposition compatible with the i -projection $\tilde{\ell}_i$. For $i \in [k]$, let $\hat{G}^{(i)}$ be the graph $G_1 \square \cdots \square G_{i-1} \square G_{i+1} \square \cdots \square G_k$. For $\hat{v} = (v_1, \dots, v_{i-1}, v_{i+1}, \dots, v_k) \in V(\hat{G}^{(i)})$, let $G_i(\hat{v})$ be the copy of G_i in P corresponding to \hat{v} and let $e_i(\hat{v})$ be the number of edges lying both in ℓ and $G_i(\hat{v})$. Now let

$$e_i = \sum_{\substack{\hat{v} \in V(\hat{G}^{(i)}) \\ v_{i+1} + \cdots + v_k + (k-i) \equiv 1 \pmod{2}}} e_i(\hat{v}).$$

Then the *sign* of ℓ is defined by

$$\text{sgn}(\ell) := - \prod_{i=1}^{k-1} (-1)^{e_i} \prod_{j=1}^k \text{sgn}(\mathcal{D}_j). \quad (3.2.1)$$

Note that the sign of ℓ is well-defined by Lemma 3.5. Now suppose that P has been given vertex weights $x(w)$ for $w \in V(P)$ and edge weights a_e for $e \in E(P)$. Then the *weight of the loop ℓ* is defined as

$$w(\ell) := \text{sgn}(\ell) \prod_{e \in E(\ell)} a_e. \quad (3.2.2)$$

Note that the orientation of a graph G is not relevant for the definition of the loop-vertex configuration (defined in Section 2.2) on G . We will call a loop-vertex configuration an *(extended) monopole-dimer configuration* when the underlying graph G is a Cartesian product of simple plane graphs.

Definition 3.8. The *(extended) monopole-dimer model* on the weighted Cartesian product $P = G_1 \square \cdots \square G_k$ is the collection \mathcal{L} of monopole-dimer configurations on P where the weight of each configuration $C = (\ell_1, \dots, \ell_m; v_1, \dots, v_n)$ given by

$$w(C) = \prod_{i=1}^m w(\ell_i) \prod_{i=1}^n x(v_i).$$

The *(signed) partition function* of the monopole-dimer model on Cartesian product P is

$$\mathcal{Z}_P := \sum_{C \in \mathcal{L}} w(C).$$

From the above definition, it is clear that \mathcal{Z}_P is independent of the orientations on G_1, \dots, G_k . The following result is a generalisation of Theorem 2.6 when G is plane and \mathcal{O} is Pfaffian. Recall that \mathcal{K}_P is the generalised adjacency matrix defined in (2.2.5) for (P, \mathcal{O}) .

Theorem 3.9. *Let G_1, \dots, G_k be k simple plane naturally labeled graphs with Pfaffian orientations $\mathcal{O}_1, \dots, \mathcal{O}_k$ respectively. The (signed) partition function of the monopole-dimer model for the weighted oriented Cartesian product (P, \mathcal{O}) of G_1, \dots, G_k is given by*

$$\mathcal{Z}_P = \det \mathcal{K}_P. \quad (3.2.3)$$

The proof strategy is similar to that of Theorem 2.6.

Proof. Since \mathcal{K}_P is the sum of a diagonal matrix and an antisymmetric matrix, the only terms contributing to $\det \mathcal{K}_P$ correspond to permutations which are product of even cycles and singletons, and hence are in bijective correspondence with monopole-dimer configurations on P . Thus, we only need to show that sign coming from an even cyclic permutation $(v_0, v_1, \dots, v_{2s-1}, v_{2s} = v_0)$ coincides with the sign of the corresponding directed loop $\ell = (v_0, v_1, \dots, v_{2s-1}, v_{2s} = v_0)$. That is, we have to prove that

$$(-1)^{\#\text{edges pointing in opposite direction of } \ell \text{ (under } \mathcal{O})+1} = \text{sgn } \ell.$$

Let r be the number of edges pointing in opposite direction of ℓ under \mathcal{O} . Note that the contribution to r comes from k type of edges, G_1 -edges, G_2 -edges, \dots , G_k -edges in ℓ . Since ℓ is a directed cycle, the i -th projection $\tilde{\ell}_i$, of ℓ is a directed trail in \tilde{P}_i (which is just G_i with multiple edges). Let $\mathcal{D}_i = \{d_{i,1}, d_{i,2}, \dots, d_{i,m_i}\}$ be a directed cycle decomposition compatible with $\tilde{\ell}_i$ according to Definition 3.4. Denote the number of edges in $d_{i,j}$, for $j \in [m_i]$, oriented under \mathcal{O} in the direction opposite to it as $\varepsilon^{i,j}$.

Recall the notation $\chi(c)$ and e_i from earlier in this section. For $i \in [k-1]$, the edges contributing to e_i have been reversed while defining \mathcal{O} and thus the contribution of G_i -edges to r is

$$\begin{aligned} \sum_{j=1}^{m_i} \varepsilon^{i,j} &\equiv e_i \\ &+ \sum_{j=1}^{m_i} (\text{number of edges in } d_{i,j} \text{ oriented under } \mathcal{O}_i \text{ in the direction opposite to it}) \end{aligned} \quad (\text{mod } 2).$$

By the proof of Lemma 3.5, it follows that the number of clockwise oriented edges of $d_{i,j}$ under \mathcal{O}_i and $\chi(d_{i,j})$ have opposite parity. Therefore,

$$\sum_{j=1}^{m_i} \varepsilon^{i,j} \equiv e_i + \sum_{j=1}^{m_i} \begin{cases} \chi(d_{i,j}) & \text{if } d_{i,j} \text{ has odd size and is directed clockwise,} \\ \chi(d_{i,j}) + 1 & \text{if either } d_{i,j} \text{ has even size, or has odd size} \\ & \text{and is directed anticlockwise.} \end{cases} \pmod{2}.$$

Now, by Definition 3.1, G_i -edges of ℓ contribute $(-1)^{e_i} \operatorname{sgn} \mathcal{D}_i$ to $(-1)^r$. Similarly, the contribution of G_k -edges to $(-1)^r$ is $\operatorname{sgn} \mathcal{D}_k$ as we have not altered the directions coming from \mathcal{O}_k in any copy of G_k . Thus,

$$(-1)^r = \prod_{i=1}^{k-1} (-1)^{e_i} \operatorname{sgn} \mathcal{D}_i \times \operatorname{sgn} \mathcal{D}_k = \prod_{i=1}^{k-1} (-1)^{e_i} \prod_{s=1}^k \operatorname{sgn} \mathcal{D}_s,$$

resulting in $(-1)^{r+1} = \operatorname{sgn} \ell$. Hence, we get the (signed) partition function of the (extended) monopole-dimer model for the oriented Cartesian product as a determinant. \square

Recall that the partition function of the monopole-dimer model is defined for (unoriented) Cartesian product of graphs in Definition 3.8. The next result can thus be seen as an analogue of Corollary 2.9.

Corollary 3.10. *Let G_1, \dots, G_k be k simple plane naturally labeled graphs with Pfaffian orientations $\mathcal{O}_1, \dots, \mathcal{O}_k$ respectively. Then the determinant of the generalised adjacency matrix \mathcal{K}_P of the oriented Cartesian product, (P, \mathcal{O}) , of $(G_1, \mathcal{O}_1), \dots, (G_k, \mathcal{O}_k)$ is independent of the Pfaffian orientations $\mathcal{O}_1, \dots, \mathcal{O}_k$.*

3.3 Cartesian products of plane bipartite graphs

Recall that a *bipartite (multi)graph* is a graph G whose vertex set can be partitioned into two subsets X and Y such that each edge of G has one end in X and other end in Y . Recall that an even multigraph (defined in section 2.1) is one in which all vertices have even degree. Bipartite graphs only have cycles of even length. Since the direction of even cycles does not affect the sign in Definition 3.1, we can write the *sign* of an edge-disjoint multiset of cycles $\mathcal{D} = \{d_1, \dots, d_k\}$ in an even bipartite plane multigraph G as

$$\operatorname{sgn}(\mathcal{D}) := \prod_{i=1}^k (-1)^{\chi(d_i)+1}.$$

Note that the above formula also applies to a cycle decomposition of an even bipartite

plane multigraph. We will show that the sign of a cycle decomposition remains the same for all cycle decompositions of a plane bipartite even multigraph. For that we first define some moves on two cycles in a decomposition.

Let G be an even plane bipartite multigraph and (c_1, \dots, c_t) be an edge-disjoint multiset of cycles in G . Then we define the following moves transforming one multiset of cycles into another. For each move, we also calculate the change in the sign of this multiset of cycles.

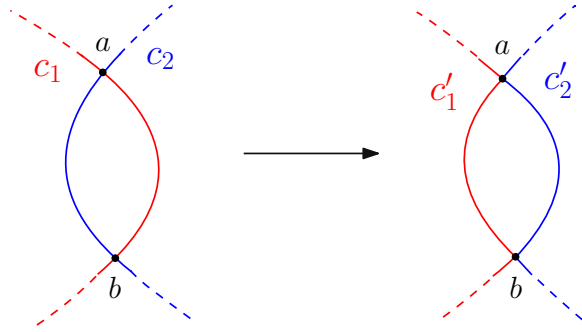


Figure 3.3: The M_1 -move from Item 1. Here, the dotted blue and red lines indicate that they are allowed to intersect each other.

1. The M_1 -move changes cycles c_1, c_2 into cycles c'_1, c'_2 as shown in Figure 3.3. Let v (resp. v') be the number of internal vertices lying on the blue (resp. red) solid path from a to b along c_2 (resp. c_1) in the left side of Figure 3.3. Let u be the number of vertices enclosed by the cycle formed by these two paths. Then

$$\begin{aligned} \chi(c'_1) + \chi(c'_2) &= \chi(c_1) - u - v + \chi(c_2) - u - v' \\ &\equiv \chi(c_1) + \chi(c_2) \pmod{2} \\ &\equiv (\chi(c_1) + 1) + (\chi(c_2) + 1) \pmod{2}, \end{aligned}$$

where we have used the fact that $v + v' \equiv 0$ (as G is bipartite) in the second line. Thus, performing the M_1 -move in this multiset of cycles preserves its sign.

2. Let c_1, c_2 intersect as shown on the left side of Figure 3.4. Without loss of generality, the left arc of c_1 strictly between a and b does not intersect c_2 , and the right arc of c_1 strictly between a and b intersects the left arc of c_2 strictly between a and b only at the t points shown. The M_2 -move changes cycles c_1, c_2 into $(t + 2)$ cycles $c'_1, c'_2, \dots, c'_{t+2}$ as shown in the right side of Figure 3.4. Then, by considering

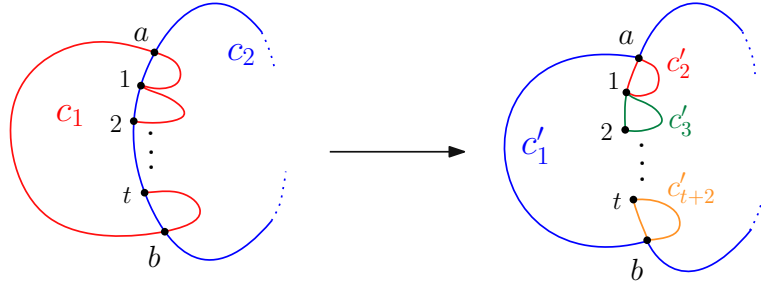


Figure 3.4: The M_2 -move from Item 2. The dotted arc of c_2 on the right indicates that it can intersect with the part of c_1 from a to b on the right side.

internal vertices in all regions, the sign of the latter multiset is given by

$$\begin{aligned} \sum_{i=1}^{t+2} (\chi(c'_i) + 1) &= \chi(c'_1) + \sum_{i=2}^{t+2} \chi(c'_i) + (t+2) \\ &= \left(\chi(c_1) + \chi(c_2) + t - \sum_{i=2}^{t+2} \chi(c'_i) \right) + \sum_{i=2}^{t+2} \chi(c'_i) + t + 2 \\ &\equiv (\chi(c_1) + 1) + (\chi(c_2) + 1) \pmod{2}. \end{aligned}$$

Thus, the M_2 -move also preserves the sign of the multiset of cycles.

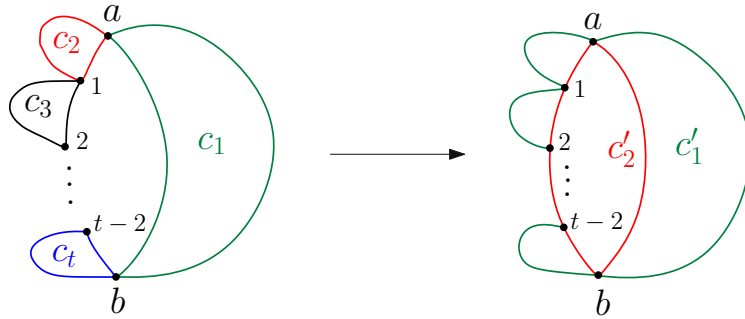


Figure 3.5: The M_3 -move from Item 3.

3. For $t \geq 2$, suppose c_1, \dots, c_t are cycles in the multigraph G such that they form a closed chain as shown on the left side in Figure 3.5. Note that these cycles do not intersect at points other than those shown in the figure. The M_3 -move converts these t cycles into two cycles namely c'_1, c'_2 as shown in the right side of Figure 3.5. Then the sign of the latter multiset of cycles is

$$\begin{aligned} \sum_{i=1}^2 (\chi(c'_i) + 1) &\equiv \chi(c'_1) - \chi(c'_2) \pmod{2}, \\ &\equiv \sum_{i=1}^t \chi(c_i) + (\text{size of } c'_2) - t \pmod{2}, \end{aligned}$$

because c'_1 encloses all the vertices except $a, b, 1, \dots, (t-2)$ lying on c'_2 . Since G is bipartite, it can only have cycles of even size. Thus

$$\begin{aligned} \sum_{i=1}^2 (\chi(c'_i) + 1) &\equiv \sum_{i=1}^t \chi(c_i) + t \pmod{2} \\ &\equiv \sum_{i=1}^t (\chi(c_i) + 1) \pmod{2}. \end{aligned}$$

Again, the sign of the multiset is preserved under the M_3 -move.

We have thus shown that performing any sequence of moves of the form Items 1 to 3 will not affect the sign of a multiset of cycles.

Recall that a *bridge* or *cut edge* in a multigraph G is an edge whose deletion increases the number of connected components in G . Let G be a connected even plane multigraph. Then G cannot have a bridge [8, Exercise 3.2.3] and hence the boundary of the outer face (being a closed trail) can be decomposed into cycles c_1, \dots, c_k such that $|V(c_i) \cap V(c_j)| \leq 1$ for all $i, j \in [k]$.

Definition 3.11. Let G be a connected even plane multigraph and C be the boundary of the outer face consisting of cycles c_1, \dots, c_k . Then an *outer cycle decomposition* of G is a cycle decomposition of G containing c_1, \dots, c_k and the latter will be called *boundary cycles*.

Example 3.12. Any cycle decomposition containing the cycle $(1, 2, 3, 4, 5, 6, 7, 8)$ is an outer cycle decomposition for the graph in Figure 3.6. For example, $\{(1, 2, 3, 4, 5, 6, 7, 8), (2, 4, 6, 8)\}$ is an outer cycle decomposition but $\{(1, 2, 8), (2, 3, 4), (4, 5, 6), (6, 7, 8)\}$ is not.

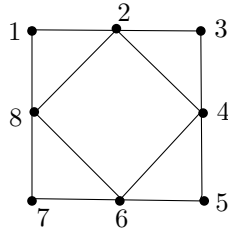


Figure 3.6: A planar graph on 8 vertices

The next result is a crucial step towards the main result of this section.

Lemma 3.13. *Let G be a connected bipartite even plane multigraph. Then for any cycle decomposition \mathcal{D} of G , there exists an outer cycle decomposition \mathcal{D}' of G with same sign.*

Proof. Suppose c_1, \dots, c_k are the boundary cycles. If $k > 1$, we can work separately with each subgraph of G lying inside the cycle c_j for each $j \in [k]$. Thus, without loss of generality, we can assume that there is just a single cycle c (say). If \mathcal{D} contains c , there is nothing to prove. So assume \mathcal{D} does not contain c . Then there exist at least two cycles in \mathcal{D} which will intersect c in some edge(s). There are two possibilities now depending on whether the cycles above intersect each other more than once or not.

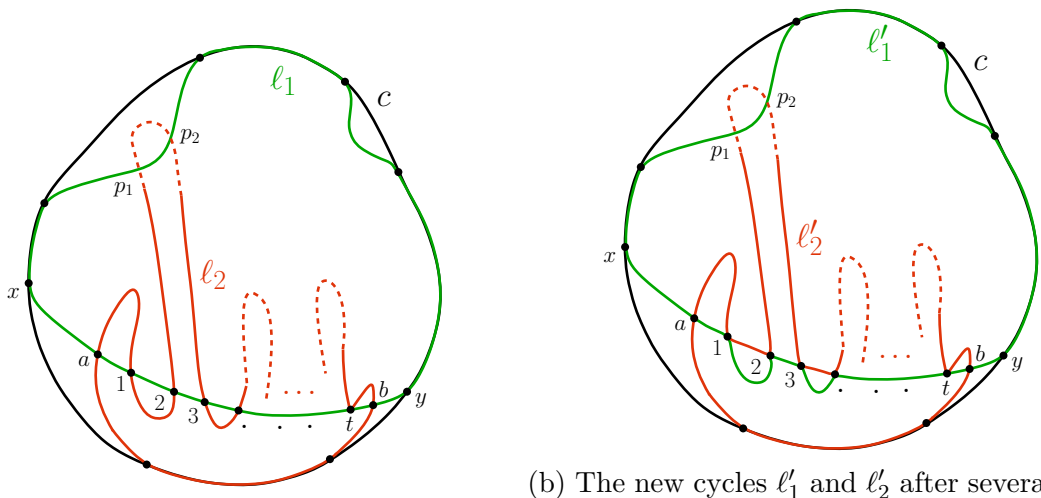
1. If there are two cycles among these, say ℓ_1 and ℓ_2 , which intersect each other in more than one point, say a and b , then ℓ_1, ℓ_2 will look as in Figure 3.7a. Let the bottom arc of ℓ_1 joining x to y intersect ℓ_2 in t additional points as shown. First perform the necessary number of M_1 -moves to reach the stage in Figure 3.7b. At this point, the top part of the ℓ_2 cycle between a and b lies on the same side of the bottom part of the ℓ_1 cycle. Now, perform an M_2 -move to increase the number of edges of c covered by ℓ_1 as depicted in Figure 3.7c. Since these moves preserve the sign, the cycle decomposition containing $(t + 2)$ transformed cycles in place of two original cycles will have the same sign.
2. If no two cycles of \mathcal{D} which have a common edge with c intersect each other in more than one point, then we have a certain number, say $t \geq 3$, of cycles intersecting c . Focus on one of the cycles, ℓ_1 say. It will intersect another cycle at a vertex of c . Call it ℓ_2 . Now following ℓ_1 in the interior, find the first of these t cycles and call it ℓ_t . The situation will look as in left of Figure 3.8. Now perform an M_3 -move to increase the number of edges of c covered by ℓ_1 and arrive at the right of Figure 3.8. The resulting cycle decomposition will have the same sign.

Apply these cases inductively. Notice that we might need to alternate between these two. In each case, the number of edges in the intersection of ℓ_1 and c increases. As the number of edges in c is finite, the process of performing these moves will eventually stop and we will end up with a cycle decomposition containing c with the sign same as that of \mathcal{D} . □

Now we will see a result analogous to Lemma 3.5 in the case of bipartite graphs.

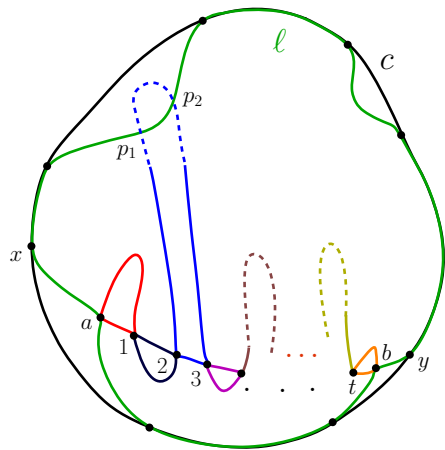
Theorem 3.14. *Let G be a connected bipartite even plane multigraph. Then all cycle decompositions \mathcal{D} of G will have same sign.*

Proof. Since G is even and connected, the boundary of the outer face of G can be decomposed into cycles. For simplicity, we suppose the boundary is a single cycle c . If not, the argument below extends in an obvious way to each component of the boundary.



(a) The original cycles l_1 and l_2 .

(b) The new cycles l'_1 and l'_2 after several M_1 -moves.



(c) The final cycles after an M_2 -move. Note that there are a total of $t + 2$ cycles now.

Figure 3.7: Two cycles l_1 and l_2 intersecting the boundary cycle c , and intersecting each other in more than one point in Figure 3.7a. In Figure 3.7c, the cycle l intersects c in more edges than l_1 .

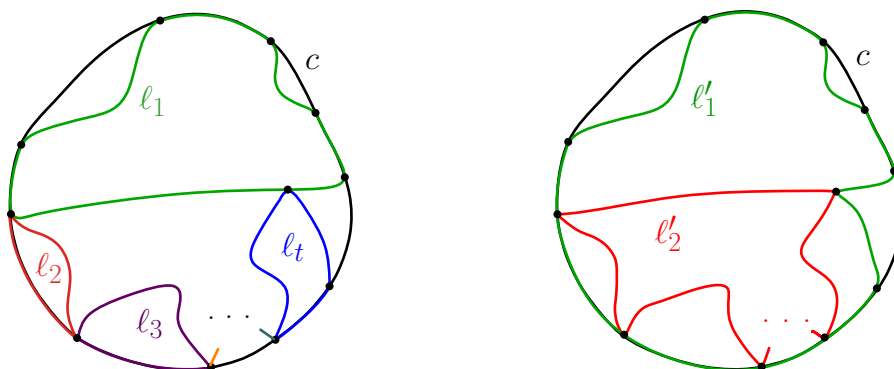


Figure 3.8: A cycle decomposition where the cycles intersecting the boundary cycle are shown before and after an M_3 -move.

Let \mathcal{D} be a cycle decomposition of G . Using Lemma 3.13, we obtain another cycle decomposition \mathcal{D}_1 containing c which has the same sign as \mathcal{D} . Let G_1 be obtained from G by removing all the edges of c and the resulting isolated vertices. Note that although G_1 can be disconnected, the regions enclosed by its connected components $G_{1,1}, G_{1,2}, \dots, G_{1,t}$ will not intersect. Now, $\mathcal{D}_1 \setminus \{c\}$ is a cycle decomposition of G_1 . Again using Lemma 3.13 on G_1 , we obtain a cycle decomposition \mathcal{D}_2 of G containing c and $d_{1,1}, d_{1,2}, \dots, d_{1,t}$, the boundary cycles of $G_{1,1}, G_{1,2}, \dots, G_{1,t}$ respectively, such that $\text{sgn } \mathcal{D}_1 = \text{sgn } \mathcal{D}_2$. Now remove $d_{1,1}, d_{1,2}, \dots, d_{1,t}$ from G_1 to obtain G_2 and continue this process. Since G is finite, this process must stop. In fact, it will stop at the cycle decomposition obtained by successively including outer boundaries of G_1, G_2 and so on. \square

Recall the i -projection, the sign of a directed loop and the notation e_i defined in Definition 3.7, (3.2.1) and Chapter 3 respectively. By the fact that bipartite graphs only have even cycles and by Theorem 3.14, we have the following result.

Corollary 3.15. *Let G_1, \dots, G_k be plane simple naturally labeled bipartite graphs and P be their Cartesian product. Let $\ell = (w_0, w_1, \dots, w_{2s-1}, w_{2s} = w_0)$ be a directed even loop in P and \mathcal{D}_i be an arbitrary cycle decomposition of the i -projection $\tilde{\ell}_i$ for $i \in [k]$. Then*

$$\text{sgn}(\ell) = - \prod_{i=1}^{k-1} (-1)^{e_i} \prod_{j=1}^k \text{sgn}(\mathcal{D}_j),$$

and is well-defined. In particular, there is no restriction on the choice of cycle decomposition of any i -projection in the monopole-dimer model for Cartesian product of bipartite graphs.

Chapter 4

Monopole-dimer model on grid graphs

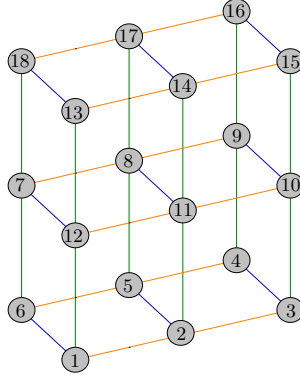
We now focus on the family of grid graphs in higher dimensions. We compute the partition function of the monopole-dimer model on three-dimensional and higher-dimensional grid graphs in Theorem 4.1 and Theorem 4.4, respectively.

4.1 Three-dimensional grid graphs

Assign the natural labelling increasing from one leaf to another to P_n , and denote its oriented variant with the canonical orientation as (P_n, \mathcal{O}_n) . Consider the two-dimensional grid graph $Q_{\ell,m} = P_\ell \square P_m = \{(p, q) \mid p \in [\ell], q \in [m]\}$ whose vertex (p, q) has label $2s\ell + p$ if $q = 2s + 1$ and $2s\ell - p + 1$ if $q = 2s$. Observe that it is a *boustrophedon labelling* (see Section 2.3). With the canonical orientation, denote this graph as $(P_\ell \square P_m, \mathcal{O}_{\ell,m})$. For the purposes of our next result, we will think of Cartesian product of $P_\ell \square P_m$ with P_n as embedded in \mathbb{Z}^3 where the coordinate axes x, y, z are aligned parallel to the edges in P_ℓ, P_m and P_n respectively.

Theorem 4.1 ([4, Theorem 5.1]). *Let (G, \mathcal{O}) be the oriented Cartesian product of $(P_\ell \square P_m, \mathcal{O}_{\ell,m})$ with (P_n, \mathcal{O}_n) . Let vertex weights be x for all vertices of G , and edge weights be a, b, c for the edges along the three coordinate axes. Then the partition function of the monopole-dimer model on G is given by*

$$\mathcal{Z}_G \equiv \mathcal{Z}_{\ell,m,n} = \prod_{j=1}^{\lfloor n/2 \rfloor} \prod_{s=1}^{\lfloor m/2 \rfloor} \prod_{k=1}^{\lfloor \ell/2 \rfloor} \left(x^2 + 4a^2 \cos^2 \frac{\pi k}{\ell + 1} + 4b^2 \cos^2 \frac{\pi s}{m + 1} + 4c^2 \cos^2 \frac{\pi j}{n + 1} \right)^4$$

Figure 4.1: The boustrophedon labelling on $P_3 \square P_2 \square P_3$.

$$\times \begin{cases} 1 & \ell, n, m \in 2\mathbb{N}, \\ T_{n,m}^2(b, c; x) & \ell \notin 2\mathbb{N}, m, n \in 2\mathbb{N}, \\ T_{n,\ell}^2(a, c; x) & \ell, n \in 2\mathbb{N}, m \notin 2\mathbb{N}, \\ T_{n,m}^2(b, c; x) T_{n,\ell}^2(a, c; x) S_n(c; x) & \ell, m \notin 2\mathbb{N}, n \in 2\mathbb{N}, \\ T_{m,\ell}^2(a, b; x) & \ell, m \in 2\mathbb{N}, n \notin 2\mathbb{N}, \\ T_{n,m}^2(b, c; x) T_{m,\ell}^2(a, b; x) S_m(b; x) & \ell, n \notin 2\mathbb{N}, m \in 2\mathbb{N}, \\ T_{n,\ell}^2(a, c; x) T_{m,\ell}^2(a, b; x) S_\ell(a; x) & \ell \in 2\mathbb{N}, m, n \notin 2\mathbb{N}, \\ x T_{n,m}^2(b, c; x) T_{n,\ell}^2(a, c; x) T_{m,\ell}^2(a, b; x) S_n(c; x) S_m(b; x) S_\ell(a; x) & \ell, m, n \notin 2\mathbb{N}, \end{cases}$$

where

$$S_n(c; x) = \prod_{k=1}^{\lfloor n/2 \rfloor} \left(x^2 + 4c^2 \cos^2 \frac{\pi k}{n+1} \right),$$

and

$$T_{n,\ell}(a, b; x) = \prod_{j=1}^{\lfloor n/2 \rfloor} \prod_{k=1}^{\lfloor \ell/2 \rfloor} \left(x^2 + 4a^2 \cos^2 \frac{\pi k}{\ell+1} + 4b^2 \cos^2 \frac{\pi j}{n+1} \right).$$

Remark 4.2. The boustrophedon labelling that induces the orientation \mathcal{O} over the graph G is given in (2.3.5) for an even ℓ, m and n . Figure 4.1 shows this labelling on the graph $P_3 \square P_2 \square P_3$.

Proof. The signed adjacency matrix for the graph (G, \mathcal{O}) with the above labelling can be written as

$$\mathcal{K}_{\ell,m,n} = I_n \otimes I_m \otimes T_\ell(-a, x, a) + I_n \otimes T_m(-b, 0, b) \otimes J_\ell + T_n(-c, 0, c) \otimes J_m \otimes J_\ell, \quad (4.1.1)$$

where $T_k(-s, z, s)$ and J_k be as defined in Section 2.4. Let u_k be the standard unitary similarity transformation given by the matrix u_k defined in (2.4.1). Then, using the

unitary transform $u_n \otimes u_m \otimes u_\ell$ and Lemma 2.13, we find that

$$\begin{aligned} \mathcal{K}_{\ell,m,n} \sim & I_n \otimes I_m \otimes \text{diag}\left(x + 2\iota a \cos \frac{\pi}{\ell+1}, \dots, x + 2\iota a \cos \frac{\ell\pi}{\ell+1}\right) \\ & + I_n \otimes 2\iota b \text{diag}\left(\cos \frac{\pi}{m+1}, \dots, \cos \frac{m\pi}{m+1}\right) \otimes \iota^{\ell-1} \begin{pmatrix} & & & (-1)^{\ell-1} \\ & & & \\ & & \ddots & \\ & & & \\ (-1)^0 & & & \end{pmatrix} \\ & + 2\iota c \text{diag}\left(\cos \frac{\pi}{n+1}, \dots, \cos \frac{n\pi}{n+1}\right) \\ & \otimes \iota^{m-1} \begin{pmatrix} & & & (-1)^{m-1} \\ & & & \\ & & \ddots & \\ & & & \\ (-1)^0 & & & \end{pmatrix} \otimes \iota^{\ell-1} \begin{pmatrix} & & & (-1)^{\ell-1} \\ & & & \\ & & \ddots & \\ & & & \\ (-1)^0 & & & \end{pmatrix}. \end{aligned}$$

Note that each term in the above sum is a block diagonal matrix as the first matrix in each tensor factor is diagonal. Therefore, $\mathcal{K}_{\ell,m,n}$ is similar to an $n \times n$ block diagonal matrix with the block F_j for $j \in [n]$ given by

$$\begin{aligned} F_j = & I_m \otimes \text{diag}\left(x + 2\iota a \cos \frac{\pi}{\ell+1}, \dots, x + 2\iota a \cos \frac{\ell\pi}{\ell+1}\right) \\ & + \begin{pmatrix} 2\iota b \cos \frac{\pi}{m+1} & & & (-1)^{m-1} 2\iota^m c \cos \frac{j\pi}{n+1} \\ & \ddots & \ddots & \\ & & \ddots & \\ & & & \\ (-1)^0 2\iota^m c \cos \frac{j\pi}{n+1} & & & 2\iota b \cos \frac{m\pi}{m+1} \end{pmatrix} \otimes \iota^{\ell-1} \begin{pmatrix} & & & (-1)^{\ell-1} \\ & & & \\ & & \ddots & \\ & & & \\ (-1)^0 & & & \end{pmatrix}. \end{aligned}$$

Define

$$\lambda_{s,j}^{m,n} = \sqrt{4b^2 \cos^2 \frac{s\pi}{m+1} + 4c^2 \cos^2 \frac{j\pi}{n+1}}, \quad s \in [m], j \in [n],$$

and let

$$D_j = \begin{cases} \text{diag}\left(\iota\lambda_{1,j}^{m,n}, -\iota\lambda_{1,j}^{m,n}, \iota\lambda_{2,j}^{m,n}, -\iota\lambda_{2,j}^{m,n}, \dots, \iota\lambda_{\frac{m}{2},j}^{m,n}, -\iota\lambda_{\frac{m}{2},j}^{m,n}\right) & m \text{ even,} \\ \text{diag}\left(\iota\lambda_{1,j}^{m,n}, -\iota\lambda_{1,j}^{m,n}, \iota\lambda_{2,j}^{m,n}, -\iota\lambda_{2,j}^{m,n}, \dots, \iota\lambda_{\lfloor \frac{m}{2} \rfloor, j}^{m,n}, -\iota\lambda_{\lfloor \frac{m}{2} \rfloor, j}^{m,n}, \iota\lambda_{\frac{m+1}{2}, j}^{m,n}\right) & m \text{ odd.} \end{cases}$$

The matrix

$$\begin{pmatrix} 2\iota b \cos \frac{\pi}{m+1} & & & (-1)^{m-1} 2\iota^m c \cos \frac{j\pi}{n+1} \\ & \ddots & \ddots & \\ & & \ddots & \\ (-1)^0 2\iota^m c \cos \frac{j\pi}{n+1} & & & 2\iota b \cos \frac{m\pi}{m+1} \end{pmatrix},$$

when diagonalized, becomes equal to D_j . Thus, F_j becomes similar to

$$I_m \otimes \text{diag} \left(x + 2\iota a \cos \frac{\pi}{\ell+1}, \dots, x + 2\iota a \cos \frac{\ell\pi}{\ell+1} \right) + D_j \otimes \iota^{\ell-1} \begin{pmatrix} & & & (-1)^{\ell-1} \\ & & \ddots & \\ & & & \\ (-1)^0 & & & \end{pmatrix}. \quad (4.1.2)$$

Again, as the first matrix in both tensor products of (4.1.2) is diagonal, each block F_j is similar to a block diagonal matrix given by

$$F_j \sim \begin{cases} \text{diag} \left(F_{1,j}^+, F_{1,j}^-, \dots, F_{\frac{m}{2},j}^+, F_{\frac{m}{2},j}^- \right) & m \text{ even,} \\ \text{diag} \left(F_{1,j}^+, F_{1,j}^-, \dots, F_{\frac{m-1}{2},j}^+, F_{\frac{m-1}{2},j}^-, F_{\frac{m+1}{2},j}^+ \right) & m \text{ odd,} \end{cases}$$

where

$$\begin{aligned} F_{s,j}^\pm &= \text{diag} \left(x + 2\iota a \cos \frac{\pi}{\ell+1}, \dots, x + 2\iota a \cos \frac{\ell\pi}{\ell+1} \right) \pm \iota^\ell \lambda_{s,j}^{m,n} \begin{pmatrix} & & & (-1)^{\ell-1} \\ & & \ddots & \\ & & & \\ (-1)^0 & & & \end{pmatrix} \\ &= \begin{pmatrix} x + 2\iota a \cos \frac{\pi}{\ell+1} & & & \pm (-1)^{\ell-1} \iota^\ell \lambda_{s,j}^{m,n} \\ & \ddots & \ddots & \\ & & \ddots & \\ \pm (-1)^0 \iota^\ell \lambda_{s,j}^{m,n} & & & x + 2\iota a \cos \frac{\ell\pi}{\ell+1} \end{pmatrix}. \end{aligned}$$

Now defining

$$Y_{k,s,j}^\pm = \begin{pmatrix} x + 2\iota a \cos \frac{k\pi}{\ell+1} & \pm (-1)^{\ell-k} \iota^\ell \lambda_{s,j}^{m,n} \\ \pm (-1)^{k-1} \iota^\ell \lambda_{s,j}^{m,n} & x - 2\iota a \cos \frac{k\pi}{\ell+1} \end{pmatrix}, \quad 1 \leq s \leq \lfloor (m+1)/2 \rfloor,$$

and performing simultaneous row and column interchanges on $F_{s,j}^\pm$, we can write

$$F_{s,j}^\pm \sim \begin{cases} \text{diag} (Y_{1,s,j}^\pm, Y_{2,s,j}^\pm, \dots, Y_{\lfloor \frac{\ell}{2} \rfloor, s,j}^\pm) & \ell \text{ even,} \\ \text{diag} (Y_{1,s,j}^\pm, Y_{2,s,j}^\pm, \dots, Y_{\lfloor \frac{\ell}{2} \rfloor, s,j}^\pm, x \pm \iota \lambda_{s,j}^{m,n}) & \ell \text{ odd.} \end{cases}$$

Note that

$$\det Y_{k,s,j}^+ = \det Y_{k,s,j}^- = x^2 + 4a^2 \cos^2 \frac{k\pi}{\ell+1} + 4b^2 \cos^2 \frac{s\pi}{m+1} + 4c^2 \cos^2 \frac{j\pi}{n+1},$$

which implies that

$$\det F_{s,j}^+ \det F_{s,j}^- = \prod_{k=1}^{\lfloor \ell/2 \rfloor} (\det Y_{k,s,j}^+ \det Y_{k,s,j}^-) \times \begin{cases} 1 & \ell \text{ even,} \\ x^2 + (\lambda_{s,j}^{m,n})^2 & \ell \text{ odd.} \end{cases}$$

Then we get,

$$\det F_j = \prod_{s=1}^{\lfloor m/2 \rfloor} (\det F_{s,j}^+ \det F_{s,j}^-) \times \begin{cases} 1 & m \text{ even,} \\ \det F_{\frac{m+1}{2},j}^+ & m \text{ odd.} \end{cases}$$

Hence,

$$\det F_j = \prod_{s=1}^{\lfloor m/2 \rfloor} \prod_{k=1}^{\lfloor \ell/2 \rfloor} \left(x^2 + 4a^2 \cos^2 \frac{k\pi}{\ell+1} + 4b^2 \cos^2 \frac{s\pi}{m+1} + 4c^2 \cos^2 \frac{j\pi}{n+1} \right)^2 \times \begin{cases} 1 & \ell, m \in 2\mathbb{N}, \\ \prod_{s=1}^{\lfloor m/2 \rfloor} (x^2 + (\lambda_{s,j}^{m,n})^2) & \ell \notin 2\mathbb{N}, m \in 2\mathbb{N}, \\ \prod_{k=1}^{\lfloor \ell/2 \rfloor} \left(x^2 + 4a^2 \cos^2 \frac{k\pi}{\ell+1} + 4c^2 \cos^2 \frac{j\pi}{n+1} \right) & \ell \in 2\mathbb{N}, m \notin 2\mathbb{N}, \\ \prod_{k=1}^{\lfloor \ell/2 \rfloor} \left(x^2 + 4a^2 \cos^2 \frac{k\pi}{\ell+1} + 4c^2 \cos^2 \frac{j\pi}{n+1} \right) & \\ \times \left(x + 2\iota c \cos \frac{j\pi}{n+1} \right) \prod_{s=1}^{\lfloor m/2 \rfloor} (x^2 + (\lambda_{s,j}^{m,n})^2) & \ell, m \notin 2\mathbb{N}. \end{cases}$$

Since, $\det \mathcal{K}_{\ell,m,n} = \prod_{j=1}^n \det F_j$ and $\det F_j = \det F_{n-j+1}$ we obtain the result. \square

We now make a few remarks about this result. First, the orientation on G is Pfaffian over all standard planes and G is non-planar when at least two of ℓ, m, n are greater than 2. Second, although it is not obvious from Theorem 4.1, $\mathcal{Z}_{\ell,m,n}$ is always a polynomial in x, a, b, c with nonnegative integer coefficients. Third, $\mathcal{Z}_{\ell,m,n}$ is the fourth power of a polynomial when ℓ, m and n are all even and the square of a polynomial when exactly two of ℓ, m and n are even. Fourth, the formula in Theorem 4.1 coincides with the already

known partition function [6] of the monopole-dimer model for the two-dimensional grid graph when either of ℓ, m, n are equal to 1. Finally, although it is not obvious from the construction, the formula is symmetric in all three directions. That is to say, it is symmetric under any permutation interchanging $(a, \ell), (b, m)$ and (c, n) .

We now prove that our monopole-dimer model on Cartesian products satisfies an associativity property at least for path graphs.

Proposition 4.3. *The partition function of the monopole-dimer model on the oriented Cartesian product of $(P_\ell \square P_m, \mathcal{O}_{\ell,m})$ with (P_n, \mathcal{O}_n) is the same as the partition function of the monopole-dimer model on the oriented Cartesian product of $(P_\ell, \mathcal{O}_\ell)$ with $(P_m \square P_n, \mathcal{O}_{m,n})$.*

Proof. The orientation on both the products is induced from the same boustrophedon labelling given in Remark 4.2. Moreover, the partition function of the monopole-dimer model is the same as the partition function of the loop-vertex model on $P_\ell \square P_m \square P_n$ with the canonical orientation induced from boustrophedon labelling. \square

4.2 Higher-dimensional grid graphs

We now generalise the results from Section 4.1 to higher dimensional grid graphs. Let us consider d path graphs $P_{m_1}, P_{m_2}, \dots, P_{m_d}$, ℓ of which are odd. Without loss of generality, we assume that the first ℓ of these are odd, that is m_1, \dots, m_ℓ are odd.

Theorem 4.4 ([4, Theorem 6.1]). *Let (G, \mathcal{O}) be the oriented Cartesian product of the graphs $(P_{m_1} \square P_{m_2}, \mathcal{O}_{m_1, m_2}), (P_{m_3}, \mathcal{O}_{m_3}), \dots, (P_{m_d}, \mathcal{O}_{m_d})$, where m_1, \dots, m_ℓ are odd. Let vertex weights be x for all vertices of G and edge weights be a_i for the P_{m_i} -edges. Then the partition function of the monopole-dimer model on G is given by*

$$\mathcal{Z}_G \equiv \mathcal{Z}_{m_1, \dots, m_d} = \prod_{S \subseteq [\ell]} (T_S)^{2^{d-1-\#S}}, \quad (4.2.1)$$

where for $S = [d] \setminus \{p_1, \dots, p_r\}$,

$$T_S = \prod_{i_{p_1}=1}^{\lfloor \frac{m_{p_1}}{2} \rfloor} \cdots \prod_{i_{p_r}=1}^{\lfloor \frac{m_{p_r}}{2} \rfloor} \left(x^2 + \sum_{q=1}^r 4a_s^2 \cos^2 \frac{i_{p_q} \pi}{m_{p_q} + 1} \right),$$

and when $\ell = d$, the empty product in $T_{[d]}$ must be interpreted as x^2 .

Note that if $\ell = d$ then the term in (4.2.1) corresponding to $S = [d]$ is just x which is expected since each configuration will have at least one monomer. The proof strat-

egy is similar to that of [16, Section 4]. Using ideas similar to the proof of Proposition 4.3, it can be shown that for $s \in [d - 1]$, the formula above coincides with the partition function of the monopole-dimer model on the oriented Cartesian product $P_{m_1} \square P_{m_2} \square \cdots \square P_{m_{s-1}} \square (P_{m_s} \square P_{m_{s+1}}) \square P_{m_{s+2}} \square \cdots \square P_{m_d}$. We first demonstrate the strategy of proof in an example below.

Example 4.5. Consider the 4-dimensional oriented hypercube, Q_4 , built as an oriented Cartesian product of 4 copies of (P_2, \mathcal{O}_2) as in Definition 3.6. Then the generalised adjacency matrix is

$$\begin{aligned} \mathcal{K}_G &= I_2 \otimes I_2 \otimes I_2 \otimes T_2(-a_1, x, a_1) + I_2 \otimes I_2 \otimes T_2(-a_2, 0, a_2) \otimes J_2 \\ &\quad + I_2 \otimes T_2(-a_3, 0, a_3) \otimes J_2 \otimes J_2 + T_2(-a_4, 0, a_4) \otimes J_2 \otimes J_2 \otimes J_2. \end{aligned}$$

Let u_k be as defined in Lemma 2.13, then using the unitary transform $u_2 \otimes u_2 \otimes u_2 \otimes u_2$, we see that

$$\begin{aligned} \mathcal{K}_G &\sim I_2 \otimes I_2 \otimes I_2 \otimes \begin{pmatrix} x + \iota a_1 & 0 \\ 0 & x - \iota a_1 \end{pmatrix} + I_2 \otimes I_2 \otimes \begin{pmatrix} \iota a_2 & 0 \\ 0 & -\iota a_2 \end{pmatrix} \otimes \iota \begin{pmatrix} 0 & -1 \\ 1 & 0 \end{pmatrix} \\ &\quad + I_2 \otimes \begin{pmatrix} \iota a_3 & 0 \\ 0 & -\iota a_3 \end{pmatrix} \otimes \iota \begin{pmatrix} 0 & -1 \\ 1 & 0 \end{pmatrix} \otimes \iota \begin{pmatrix} 0 & -1 \\ 1 & 0 \end{pmatrix} \\ &\quad + \begin{pmatrix} \iota a_4 & 0 \\ 0 & -\iota a_4 \end{pmatrix} \otimes \iota \begin{pmatrix} 0 & -1 \\ 1 & 0 \end{pmatrix} \otimes \iota \begin{pmatrix} 0 & -1 \\ 1 & 0 \end{pmatrix} \otimes \iota \begin{pmatrix} 0 & -1 \\ 1 & 0 \end{pmatrix}. \end{aligned}$$

Define, for $1 \leq i_4 \leq 2$,

$$\begin{aligned} F_{i_4} &= I_2 \otimes I_2 \otimes \begin{pmatrix} x + \iota a_1 & 0 \\ 0 & x - \iota a_1 \end{pmatrix} + I_2 \otimes \begin{pmatrix} \iota a_2 & 0 \\ 0 & -\iota a_2 \end{pmatrix} \otimes \iota \begin{pmatrix} 0 & -1 \\ 1 & 0 \end{pmatrix} \\ &\quad + \begin{pmatrix} \iota a_3 & (-1)^{i_4-1} a_4 \\ (-1)^{i_4} a_4 & -\iota a_3 \end{pmatrix} \otimes \iota \begin{pmatrix} 0 & -1 \\ 1 & 0 \end{pmatrix} \otimes \iota \begin{pmatrix} 0 & -1 \\ 1 & 0 \end{pmatrix}, \end{aligned}$$

and note that $\det \mathcal{K}_G = \det F_1 \det F_2$. Now

$$\begin{aligned} F_1 &\sim F_2 \sim I_2 \otimes I_2 \otimes \begin{pmatrix} x + \iota a_1 & 0 \\ 0 & x - \iota a_1 \end{pmatrix} + I_2 \otimes \begin{pmatrix} \iota a_2 & 0 \\ 0 & -\iota a_2 \end{pmatrix} \otimes \iota \begin{pmatrix} 0 & -1 \\ 1 & 0 \end{pmatrix} \\ &\quad + \begin{pmatrix} \iota \sqrt{a_3^2 + a_4^2} & 0 \\ 0 & -\iota \sqrt{a_3^2 + a_4^2} \end{pmatrix} \otimes \iota \begin{pmatrix} 0 & -1 \\ 1 & 0 \end{pmatrix} \otimes \iota \begin{pmatrix} 0 & -1 \\ 1 & 0 \end{pmatrix}, \end{aligned}$$

and thus both F_1 and F_2 have same the determinant. Hence $\det \mathcal{K}_G = \det F_1^2$. Iterating

the same procedure two more times, we get

$$\det \mathcal{K}_G = \det \begin{pmatrix} x + \iota a_1 & \sqrt{a_2^2 + a_3^2 + a_4^2} \\ -\sqrt{a_2^2 + a_3^2 + a_4^2} & x - \iota a_1 \end{pmatrix}^8.$$

Thus, the partition function of the monopole-dimer model on Q_4 is given by

$$\mathcal{Z}_{Q_4} = (x^2 + a_1^2 + a_2^2 + a_3^2 + a_4^2)^8.$$

Proof of Theorem 4.4. Using Theorem 3.9, the partition function is the determinant of the generalised adjacency matrix, \mathcal{K}_G , of (G, \mathcal{O}) with the boustrophedon labelling, as discussed in Remark 4.2. It will be convenient for us to index the components in the tensor factors in decreasing order. Let

$$M_j^d = \begin{cases} I_{m_d} \otimes \cdots \otimes I_{m_2} \otimes T_{m_1}(-a_1, x, a_1) & j = 1 \\ I_{m_d} \otimes \cdots \otimes I_{m_{j+1}} \otimes T_{m_j}(-a_j, 0, a_j) \otimes J_{m_{j-1}} \otimes \cdots \otimes J_{m_1} & 2 \leq j \leq d, \end{cases}$$

where $T_k(-s, z, s)$ and J_k are defined in the proof of Theorem 4.1. Then \mathcal{K}_G can be written as

$$\mathcal{K}_G = M_1^d + \cdots + M_d^d. \quad (4.2.2)$$

For $j \in [d]$, define the $m_j \times m_j$ diagonal matrix

$$D_j = \text{diag} \left(2\iota a_j \cos \frac{\pi}{m_j + 1}, \dots, 2\iota a_j \cos \frac{m_j \pi}{m_j + 1} \right)$$

and antidiagonal matrix

$$J'_j = \iota^{m_j-1} \begin{pmatrix} & & & (-1)^{m_j-1} \\ & & & \\ & & \ddots & \\ & & & \\ (-1)^0 & & & \end{pmatrix}.$$

Let

$$K_j^d = \begin{cases} I_{m_d} \otimes \cdots \otimes I_{m_2} \otimes (xI_{m_1} + D_1) & j = 1 \\ I_{m_d} \otimes \cdots \otimes I_{m_{j+1}} \otimes D_j \otimes J'_{j-1} \otimes \cdots \otimes J'_1 & 2 \leq j \leq d. \end{cases}$$

Let u_k be as defined in Lemma 2.13. Then, using the unitary transform $u_{m_d} \otimes \cdots \otimes u_{m_1}$,

we see that $\mathcal{K}_G \sim K_1^d + \cdots + K_d^d$. Let

$$\lambda_{i_d, i_{d-1}, \dots, i_p} = \sqrt{\sum_{s=p}^d 4a_s^2 \cos^2 \frac{i_s \pi}{m_s + 1}}, 1 \leq p \leq d.$$

Since the first matrix in each tensor product K_j^d is diagonal, \mathcal{K}_G is similar to an $m_d \times m_d$ block diagonal matrix with the block F_{i_d} , $i_d \in [m_d]$, given by

$$F_{i_d} = K_1^{d-1} + \cdots + K_{d-2}^{d-1} + \left(D_{d-1} + 2\iota a_d \cos \frac{i_d \pi}{m_d + 1} J'_{d-1} \right) \otimes J'_{d-2} \otimes \cdots \otimes J'_1.$$

Diagonalizing the matrix

$$D_{d-1} + 2\iota a_d \cos \frac{i_d \pi}{m_d + 1} J'_{d-1}$$

leads to the matrix

$$\begin{cases} \text{diag}(\iota \lambda_{i_d, 1}, -\iota \lambda_{i_d, 1}, \iota \lambda_{i_d, 2}, -\iota \lambda_{i_d, 2}, \dots, \iota \lambda_{i_d, \lfloor \frac{m_d-1}{2} \rfloor}, -\iota \lambda_{i_d, \lfloor \frac{m_d-1}{2} \rfloor}) & m_{d-1} \text{ even,} \\ \text{diag}(\iota \lambda_{i_d, 1}, -\iota \lambda_{i_d, 1}, \dots, \iota \lambda_{i_d, \lfloor \frac{m_d-1}{2} \rfloor}, -\iota \lambda_{i_d, \lfloor \frac{m_d-1}{2} \rfloor}, 2a_k \iota \cos \frac{i_d \pi}{m_d+1}) & m_{d-1} \text{ odd.} \end{cases}$$

Set $F_{i_d}^+ = F_{i_d}$, $F_{i_d}^- = F_{m_d-i_d+1}$ for $1 \leq i_d \leq \lfloor \frac{m_d}{2} \rfloor$, and observe that $F_{i_d}^+ \sim F_{i_d}^-$. Since the determinant of a matrix is invariant under similarity transformation, the partition function can now be calculated as

$$\mathcal{Z}_G = \prod_{i_d=1}^{\lfloor \frac{m_d}{2} \rfloor} (\det F_{i_d}^+)^2 \times \begin{cases} 1 & m_d \text{ even,} \\ \det F_{\frac{m_d+1}{2}} & m_d \text{ odd.} \end{cases} \quad (4.2.3)$$

Let us first assume $\ell < d$, i.e. m_d is even. Repeating the above idea, $F_{i_d}^+$ is similar to an $m_{d-1} \times m_{d-1}$ block diagonal matrix with blocks $F_{i_d, i_{d-1}}^\pm$ for $1 \leq i_{d-1} \leq \lfloor \frac{m_{d-1}}{2} \rfloor$ and continue this process. Inductively, we obtain

$$\mathcal{Z}_G = \prod_{i_d=1}^{\frac{m_d}{2}} \cdots \prod_{i_{\ell+1}=1}^{\frac{m_{\ell+1}}{2}} (\det F_{i_d, i_{d-1}, \dots, i_{\ell+1}}^+ \det F_{i_d, i_{d-1}, \dots, i_{\ell+1}}^-)^{2^{d-\ell-1}}, \quad (4.2.4)$$

with

$$F_{i_d, i_{d-1}, \dots, i_{\ell+1}}^\pm = K_1^\ell + \cdots + K_{\ell-1}^\ell + \left(D_\ell \pm \iota \lambda_{i_d, \dots, i_{\ell+1}} J'_\ell \right) \otimes J'_{\ell-1} \otimes \cdots \otimes J'_1.$$

Again diagonalizing, the matrix

$$D_\ell \pm \iota \lambda_{i_d, \dots, i_{\ell+1}} J'_\ell$$

is similar to

$$\text{diag}\left(\iota\lambda_{i_d, \dots, i_{\ell+1}, 1}, -\iota\lambda_{i_d, \dots, i_{\ell+1}, 1}, \dots, \iota\lambda_{i_d, \dots, i_{\ell+1}, \lfloor \frac{m_\ell}{2} \rfloor}, -\iota\lambda_{i_d, \dots, i_{\ell+1}, \lfloor \frac{m_\ell}{2} \rfloor}, \pm\iota\lambda_{i_d, \dots, i_{\ell+1}, \frac{m_\ell+1}{2}}\right).$$

Therefore,

$$\det F_{i_d, i_{d-1}, \dots, i_{\ell+1}}^+ = \det F_{i_d, \dots, i_{\ell+1}, \frac{m_\ell+1}{2}}^+ \prod_{i_\ell=1}^{\lfloor m_\ell/2 \rfloor} (\det F_{i_d, \dots, i_{\ell+1}, i_\ell}^+ \det F_{i_d, \dots, i_{\ell+1}, i_\ell}^-), \quad (4.2.5)$$

and

$$\det F_{i_d, i_{d-1}, \dots, i_{\ell+1}}^- = \det F_{i_d, \dots, i_{\ell+1}, \frac{m_\ell+1}{2}}^- \prod_{i_\ell=1}^{\lfloor m_\ell/2 \rfloor} (\det F_{i_d, \dots, i_{\ell+1}, i_\ell}^+ \det F_{i_d, \dots, i_{\ell+1}, i_\ell}^-), \quad (4.2.6)$$

where

$$F_{i_d, i_{d-1}, \dots, i_\ell}^\pm = K_1^{\ell-1} + \dots + K_{\ell-2}^{\ell-1} + \left(D_{\ell-1} \pm \iota\lambda_{i_d, \dots, i_\ell} J'_{\ell-1}\right) \otimes J'_{\ell-2} \otimes \dots \otimes J'_1.$$

Substituting (4.2.5) and (4.2.6) in (4.2.4) gives

$$\begin{aligned} \mathcal{Z}_G &= \prod_{i_d=1}^{\frac{m_d}{2}} \cdots \prod_{i_\ell=1}^{\frac{m_\ell}{2}} (\det F_{i_d, i_{d-1}, \dots, i_\ell}^+ \det F_{i_d, i_{d-1}, \dots, i_\ell}^-)^{2^{d-\ell}} \\ &\quad \prod_{i_d=1}^{\frac{m_d}{2}} \cdots \prod_{i_{\ell+1}=1}^{\frac{m_{\ell+1}}{2}} \left(\det F_{i_d, \dots, i_{\ell+1}, \frac{m_\ell+1}{2}}^+ \det F_{i_d, \dots, i_{\ell+1}, \frac{m_\ell+1}{2}}^- \right)^{2^{d-\ell-1}} \end{aligned}$$

By repeated application of this procedure, we will get

$$\mathcal{Z}_G = \prod_{i_d=1}^{\frac{m_d}{2}} \cdots \prod_{i_1=1}^{\lfloor \frac{m_1}{2} \rfloor} (\det F_{i_d, \dots, i_1}^+ \det F_{i_d, \dots, i_1}^-)^{2^{d-1}} \prod_{\substack{S \subset [\ell] \\ |S|=1}} T_S^{2^{d-2}} \prod_{\substack{S \subset [\ell] \\ |S|=2}} T_S^{2^{d-3}} \cdots \prod_{\substack{S \subset [\ell] \\ |S|=\ell}} T_S^{2^{d-\ell-1}},$$

where F_{i_d, \dots, i_1}^\pm is the 1×1 matrix

$$\left(\pm\iota \sqrt{x^2 + \sum_{s=1}^d 4a_s^2 \cos^2 \frac{i_s \pi}{m_s + 1}} \right).$$

Thus, we finally arrive at

$$\mathcal{Z}_G = \prod_{i_d=1}^{\frac{m_d}{2}} \cdots \prod_{i_1=1}^{\lfloor \frac{m_1}{2} \rfloor} \left(x^2 + \sum_{s=1}^d 4a_s^2 \cos^2 \frac{i_s \pi}{m_s + 1} \right)^{2^{d-1}} \prod_{\substack{S \subseteq [\ell] \\ |S|=1}} T_S^{2^{d-2}} \prod_{\substack{S \subseteq [\ell] \\ |S|=2}} T_S^{2^{d-3}} \cdots \prod_{\substack{S \subseteq [\ell] \\ |S|=\ell}} T_S^{2^{d-\ell-1}}. \quad (4.2.7)$$

The last case is when $\ell = d$. Then the right hand side of (4.2.7) will have an additional factor of $\det F_{\frac{m_d+1}{2}}$, and the latter is the generalised adjacency matrix for the oriented Cartesian product $(P_{m_1} \square P_{m_2}, \mathcal{O}_{m_1, m_2}) \square (P_{m_3}, \mathcal{O}_{m_3}) \square \cdots \square (P_{m_{d-1}}, \mathcal{O}_{m_{d-1}})$. Thus,

$$\det F_{\frac{m_d+1}{2}} = \prod_{S \subseteq [d-1]} (T_S)^{2^{d-2-\#S}} = \prod_{\substack{\emptyset \subsetneq S \subseteq [d] \\ d \in S}} (T_S)^{2^{d-1-\#S}},$$

by induction. Substituting this in (4.2.3) completes the proof. \square

As for the three-dimensional case, it is not obvious from the formula (4.2.1) for $\mathcal{Z}_{m_1, \dots, m_d}$ that it is a polynomial with nonnegative integer coefficients. The formula is also symmetric under any permutation of $(a_1, m_1), \dots, (a_k, m_d)$. Finally, (4.2.1) tells that the partition function of the monopole-dimer model for even grid lengths is the $2^{(d-1)}$ 'th power of a polynomial. Again a combinatorial interpretation of the underlying polynomial would be interesting.

Let us now present an example of a well-studied family of graphs.

Example 4.6. Consider the d -dimensional oriented hypercube, Q_d , built as an oriented Cartesian product of d copies of (P_2, \mathcal{O}_2) as in Definition 3.6. Then the partition function of the monopole-dimer model on Q_d is given by

$$\mathcal{Z}_{Q_d} = (x^2 + a_1^2 + \cdots + a_d^2)^{2^{d-1}}.$$

While this formula is amazingly simple, it is a result of a lot of cancellation of terms. Finding a combinatorial interpretation of this formula would certainly be very interesting. An interpretation in the two-dimensional case has been given in [7].

4.3 Asymptotic Behaviour

It is natural to ask how fast the partition function of these monopole-dimer models on grid graphs grows as the size increases. We are also interested in understanding the ‘probability’ of seeing a monopole at a given vertex or a dimer at a given edge. The reason these are not strict probabilities is that we are working with signed measures.

As a warm-up, we begin with three-dimensional grids. We then move on to the general d -dimensional grids in the next section, where the formulas are not as explicit. We will follow the strategy in [6, Section 5].

Define the *free energy* as

$$\Phi_3(a, b, c, x) := \lim_{\ell, m, n \rightarrow \infty} \frac{1}{8\ell mn} \ln \mathcal{Z}_{2\ell, 2m, 2n}.$$

Using the product formula in Theorem 4.1,

$$\begin{aligned} \Phi_3(a, b, c, x) &= \lim_{\ell, m, n \rightarrow \infty} \frac{1}{8\ell mn} \\ &\times \sum_{j=0}^n \sum_{s=0}^m \sum_{k=0}^{\ell} \ln \left(x^2 + 4a^2 \cos^2 \frac{\pi k}{2\ell + 1} + 4b^2 \cos^2 \frac{\pi s}{2m + 1} + 4c^2 \cos^2 \frac{\pi j}{2n + 1} \right)^4. \end{aligned}$$

Note that the right hand side can be expressed as a Riemann sum. Therefore,

$$\Phi_3(a, b, c, x) = \frac{4}{\pi^3} \int_0^{\pi/2} \int_0^{\pi/2} \int_0^{\pi/2} \ln(x^2 + 4a^2 \cos^2 \theta + 4b^2 \cos^2 \phi + 4c^2 \cos^2 \psi) d\theta d\phi d\psi.$$

Hence, the *density* of a -type edges and of monopoles will be

$$\begin{aligned} \rho_{3,a} &:= a \frac{\partial}{\partial a} \Phi_3 = \frac{4}{\pi^3} \int_0^{\pi/2} \int_0^{\pi/2} \int_0^{\pi/2} \frac{8a^2 \cos^2 \theta}{(x^2 + 4a^2 \cos^2 \theta + 4b^2 \cos^2 \phi + 4c^2 \cos^2 \psi)} d\theta d\phi d\psi, \\ \rho_{3,x} &:= x \frac{\partial}{\partial x} \Phi_3 = \frac{4}{\pi^3} \int_0^{\pi/2} \int_0^{\pi/2} \int_0^{\pi/2} \frac{2x^2}{(x^2 + 4a^2 \cos^2 \theta + 4b^2 \cos^2 \phi + 4c^2 \cos^2 \psi)} d\theta d\phi d\psi, \end{aligned}$$

respectively. Similarly, the density of b - and c -type dimers can be defined and one can check that $\rho_{3,a} + \rho_{3,b} + \rho_{3,c} + \rho_{3,x} = 1$ as expected.

Recall the *elliptic integral of the first kind*,

$$F(\phi, k) = \int_0^{\phi} \frac{d\alpha}{\sqrt{1 - k^2 \sin^2 \alpha}},$$

and the *elliptic integral of the second kind*,

$$E(\phi, k) = \int_0^{\phi} \sqrt{1 - k^2 \sin^2 \alpha} d\alpha.$$

The *complete elliptic integral of the first kind* is $K(k) = F(\pi/2, k)$ and the *complete*

elliptic integral of the second kind is $E(k) = E(\pi/2, k)$. Then, the Jacobi zeta function is

$$Z(\phi, k) = E(\phi, k) - \frac{E(k)}{K(k)}F(\phi, k).$$

See Gradshteyn and Rizhik [15] for basic properties of elliptic integrals.

Now performing similar calculations as in [6] using

$$\epsilon_3 = \tan^{-1} \left(\frac{\sqrt{x^2 + 4c^2 \cos^2 \psi + 4b^2}}{2a} \right)$$

and

$$q_3 = \frac{4ab}{\sqrt{(x^2 + 4c^2 \cos^2 \psi + 4a^2)(x^2 + 4c^2 \cos^2 \psi + 4b^2)}},$$

we get,

$$\rho_{3,a} = 1 - \frac{2}{\pi} \int_0^{\pi/2} \Lambda_0(\epsilon_3, \sin^{-1} q_3) d\psi, \quad (4.3.1)$$

$$\rho_{3,x} = \frac{x^2}{\pi^2 ab} \int_0^{\pi/2} q_3 K(q_3) d\psi, \quad (4.3.2)$$

where $\Lambda_0(\theta, y)$ is the Heuman lambda function [1, Formula 17.4.39] defined as

$$\Lambda_0(\theta, y) = \frac{F(\phi, \cos y)}{K(\cos y)} + \frac{2}{\pi} K(\sin y) Z(\phi, \cos y).$$

Let us now calculate the monopole density for the three dimensional case when all the vertex and edge weights are 1. Using (4.3.2), we get

$$\rho_{3,x} = \frac{1}{\pi^2} \int_0^{\pi/2} \frac{4}{5 + 4 \cos^2 \psi} K\left(\frac{4}{5 + 4 \cos^2 \psi}\right) d\psi \approx 0.1705.$$

We now move on to the asymptotic behaviour for the case of d -dimensional grid graphs where all side lengths are even, vertex weights are x and edges along the j 'th direction have weight a_j . The free energy is given by

$$\Phi_d(a_1, \dots, a_d, x) := \lim_{m_1, \dots, m_d \rightarrow \infty} \frac{1}{2^d m_1 \dots m_d} \ln \mathcal{Z}_{2m_1, \dots, 2m_d}.$$

The product formula in Theorem 4.4 together with the Riemann sum implies that

$$\Phi_d(a_1, \dots, a_d, x) = \frac{2^{d-1}}{\pi^d} \int_0^{\pi/2} \cdots \int_0^{\pi/2} \ln \left(x^2 + \sum_{s=1}^d 4a_s^2 \cos^2 \theta_s \right) d\theta_1 \cdots d\theta_d.$$

Again defining the densities of monopoles and s -type edges for $s \in [d]$ as

$$\rho_{d,x} := x \frac{\partial}{\partial x} \Phi_d, \quad \rho_{d,a_s} := a_s \frac{\partial}{\partial a_s} \Phi_d,$$

one can again get that $\rho_{d,x} + \sum_{s=1}^d \rho_{d,a_s} = 1$. Following the strategy in [6], we define

$$\epsilon_d = \tan^{-1} \left(\frac{\sqrt{x^2 + 4a_2^2 + \sum_{s=3}^d 4a_s^2 \cos^2 \theta_s}}{2a_1} \right),$$

$$q_d = \frac{4a_1 a_2}{\sqrt{(x^2 + 4a_1^2 + \sum_{s=3}^d 4a_s^2 \cos^2 \theta_s)(x^2 + 4a_2^2 + \sum_{s=3}^d 4a_s^2 \cos^2 \theta_s)}},$$

and we get

$$\rho_{d,a_1} = 1 - \frac{2^{d-2}}{\pi^{d-2}} \int_0^{\pi/2} \cdots \int_0^{\pi/2} \Lambda_0(\epsilon_d, \sin^{-1} q_d) d\theta_3 \cdots d\theta_d,$$

$$\rho_{d,x} = \frac{2^{d-3} x^2}{\pi^{d-1} a_1 a_2} \int_0^{\pi/2} \cdots \int_0^{\pi/2} q_d K(q_d) d\theta_3 \cdots d\theta_d.$$

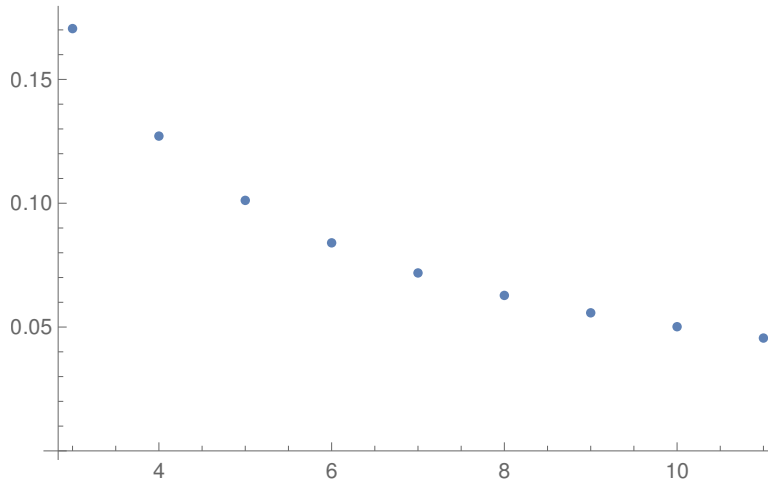


Figure 4.2: Monopole densities $\rho_{d,x}$ for limiting grid graphs in dimensions d ranging from 3 to 11 when all the vertex and edge weights are 1.

Figure 4.2 shows the numerically evaluated monopole density $\rho_{d,x}$ for the first few dimensions when all the vertex and edge weights are 1. Observe that $\rho_{d,x}$ seems to decrease monotonically as dimension increases. It would be interesting to determine the limit of $\rho_{d,x}$ as d tends to infinity, if it exists. In particular, it is not clear whether this limit is 0 or not.

Chapter 5

High-dimensional cylindrical and toroidal grid graphs

First, recall that P_n denotes the path graph on n vertices and Q_{n_1, n_2, n_3} is the three-dimensional grid graph. Throughout the chapter, we will assign $Q_{2n_1, 2n_2, 2n_3}$ the boustrophedon labelling defined in (2.3.5). Figure 2.4 shows this labelling on the graph $Q_{4, 2, 2}$. We will denote the following $n \times n$ antidiagonal matrices as

$$\begin{aligned} B_n^{Cyl} &= \text{adiag}(1, 0, \dots, 0, -1), \\ B_n^{Möb} &= \text{adiag}(1, 0, \dots, 0, 1). \end{aligned}$$

Let us now delve into the discussion regarding the partition function of the monopole-dimer model on higher dimensional grids with cylindrical and toroidal boundary conditions.

5.1 General cylindrical grids

Definition 5.1. We define an ℓ -cylindrical grid denoted Q_{n_1, \dots, n_d}^ℓ as the graph $C_{n_1} \square \dots \square C_{n_\ell} \square P_{n_{\ell+1}} \square \dots \square P_{n_d}$. For $\ell = 1$ ($\ell = d$), we call it a *cylindrical (toroidal) grid* and use the notation $Q_{n_1, \dots, n_d}^{Cyl}$ ($Q_{n_1, \dots, n_d}^{Tor}$).

We sometimes refer to Q_{n_1, \dots, n_d}^ℓ as the d -dimensional grid Q_{n_1, \dots, n_d} with cylindrical, toroidal and mixed boundary conditions depending on whether ℓ is 1, d or in between, respectively. Note that Q_{n_1, \dots, n_d}^ℓ with canonical orientation induced from Boustrophedon labelling can be regarded as the oriented Cartesian product of $C_{n_1}, \dots, C_{n_\ell}, P_{n_{\ell+1}}, \dots, P_{n_d}$. Thus, the loop-vertex model on an ℓ -cylindrical grid is nothing but the monopole-dimer model.

Theorem 5.2 ([3, Theorem 3.2]). *Let G be the d -dimensional cylindrical grid $Q_{2m_1, \dots, 2m_d}^{Cyl}$ with boustrophedon labelling. Let (G, \mathcal{O}) be obtained from G by orienting the edges from lower-labelled vertex to higher-labelled vertex. Let the vertex weights be x for all vertices of G , and edge weights be a_1, \dots, a_d for the edges along the different coordinate axes. Then the partition function of the monopole-dimer model on G is given by*

$$\mathcal{Z}_{2m_1, \dots, 2m_d}^{Cyl} \equiv \mathcal{Z}_G^{Cyl} = \prod_{i_1=1}^{m_1} \cdots \prod_{i_d=1}^{m_d} \left(x^2 + 4a_1^2 \sin^2 \frac{(2i_1 - 1)\pi}{2m_1} + \sum_{q=2}^d 4a_q^2 \cos^2 \frac{i_q \pi}{2m_q + 1} \right)^{2^{d-1}}.$$

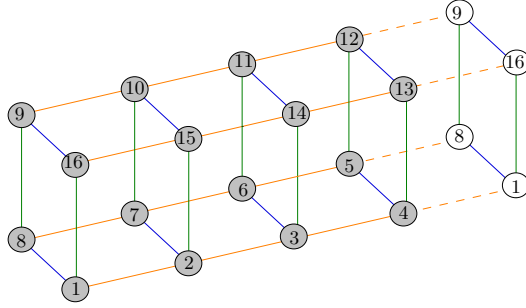


Figure 5.1: The boustrophedon labelling on the cylindrical grid $Q_{4,2,2}^{Cyl}$.

Figure 5.1 shows a three-dimensional grid graph with boustrophedon labelling and cylindrical boundary conditions. Using [4, Corollary 3.9], \mathcal{Z}_G^{Cyl} remains independent of the various Pfaffian orientations on $C_{2n_1}, P_{2n_2}, \dots, P_{2n_d}$. Before presenting the proof, we exemplify the proof strategy below.

Example 5.3. Consider G to be the three-dimensional cylindrical grid $Q_{4,2,2}^{Cyl}$ with the boustrophedon labelling as shown in Figure 5.1. Orient G in the canonical way. Then the generalised adjacency matrix is

$$\begin{aligned} \mathcal{K}_G &= I_2 \otimes I_2 \otimes T_4(-a_1, x, a_1) + I_2 \otimes T_2(-a_2, 0, a_2) \otimes J_4 + T_2(-a_3, 0, a_3) \otimes J_2 \otimes J_4 \\ &\quad + a_1 I_2 \otimes I_2 \otimes B_4^{Cyl}. \end{aligned}$$

Let u_2 be the unitary matrix,

$$u_2 = \sqrt{\frac{2}{3}} \begin{pmatrix} \iota \sin \frac{\pi}{3} & \iota \sin \frac{2\pi}{3} \\ -\sin \frac{2\pi}{3} & -\sin \frac{4\pi}{3} \end{pmatrix}.$$

Then using the unitary transform $u_2 \otimes u_2 \otimes I_4$ and by Lemma 2.13

$$\begin{aligned} \mathcal{K}_G \sim I_2 \otimes I_2 \otimes \begin{pmatrix} x & a_1 & 0 & a_1 \\ -a_1 & x & a_1 & 0 \\ 0 & -a_1 & x & a_1 \\ -a_1 & 0 & -a_1 & x \end{pmatrix} + I_2 \otimes \text{diag}(\iota a_2, -\iota a_2) \otimes J_4 \\ + \text{diag}(\iota a_3, -\iota a_3) \otimes \iota \text{adiag}(-1, 1) \otimes J_4. \end{aligned}$$

Define, for $i_3 = 1, 2$,

$$F_{i_3} = I_2 \otimes \begin{pmatrix} x & a_1 & 0 & a_1 \\ -a_1 & x & a_1 & 0 \\ 0 & -a_1 & x & a_1 \\ -a_1 & 0 & -a_1 & x \end{pmatrix} + \begin{pmatrix} \iota a_2 & (-1)^{i_3-1} a_3 \\ (-1)^{i_3} a_3 & -\iota a_2 \end{pmatrix} \otimes J_4,$$

and $\det \mathcal{K}_G = \det F_1 \det F_2$. Now

$$F_1 \sim F_2 \sim I_2 \otimes \begin{pmatrix} x & a_1 & 0 & a_1 \\ -a_1 & x & a_1 & 0 \\ 0 & -a_1 & x & a_1 \\ -a_1 & 0 & -a_1 & x \end{pmatrix} + \begin{pmatrix} \iota \sqrt{a_2^2 + a_3^2} & 0 \\ 0 & -\iota \sqrt{a_2^2 + a_3^2} \end{pmatrix} \otimes J_4,$$

and thus both F_1 and F_2 have same the determinant. Hence $\det \mathcal{K}_G = \det F_1^2$. Iterating the same procedure one more time, we get,

$$\mathcal{Z}_G^{Cyl} = \left(\det F_{1,1}^+ \det F_{1,1}^- \right)^2,$$

where

$$F_{1,1}^\pm = \begin{pmatrix} x & a_1 & 0 & a_1 \\ -a_1 & x & a_1 & 0 \\ 0 & -a_1 & x & a_1 \\ -a_1 & 0 & -a_1 & x \end{pmatrix} \pm \iota \sqrt{a_2^2 + a_3^2} J_4.$$

Let V_4 be the unitary similarity transform defined in (2.4.3) for $n = 4$, then by Lemma 2.14

$$V_4^* F_{1,1}^\pm V_4 = \begin{pmatrix} x + 2\iota a_1 \sin \frac{\pi}{4} & 0 & 0 & \mp \iota e^{\frac{\pi}{4}\iota} \sqrt{a_2^2 + a_3^2} \\ 0 & x + 2\iota a_1 \sin \frac{3\pi}{4} & \mp \iota e^{\frac{3\pi}{4}\iota} \sqrt{a_2^2 + a_3^2} & 0 \\ 0 & \mp \iota e^{\frac{5\pi}{4}\iota} \sqrt{a_2^2 + a_3^2} & x + 2\iota a_1 \sin \frac{5\pi}{4} & 0 \\ \mp \iota e^{\frac{7\pi}{4}\iota} \sqrt{a_2^2 + a_3^2} & 0 & 0 & x + 2\iota a_1 \sin \frac{7\pi}{4} \end{pmatrix}.$$

Thus, the partition function of the monopole-dimer model on G is given by

$$\mathcal{Z}_G = (x^2 + 2a_1^2 + a_2^2 + a_3^2)^8.$$

Proof of Theorem 5.2. Define

$$M_j^d = \begin{cases} I_{2m_d} \otimes \cdots \otimes I_{2m_2} \otimes T_{2m_1}(-a_1, x, a_1) & j = 1 \\ I_{2m_d} \otimes \cdots \otimes I_{2m_{j+1}} \otimes T_{2m_j}(-a_j, 0, a_j) \otimes J_{2m_{j-1}} \otimes \cdots \otimes J_{2m_1} & 2 \leq j \leq d. \end{cases}$$

Using Theorem 2.6, the partition function of the monopole-dimer model on (G, \mathcal{O}) is the determinant of the generalised adjacency matrix, \mathcal{K}_G , of (G, \mathcal{O}) and the generalised adjacency matrix, \mathcal{K}_G with the boustrophedon labelling can be written as

$$\mathcal{K}_G = M_1^d + \cdots + M_d^d + a_1 I_{2m_d} \otimes \cdots \otimes I_{2m_2} \otimes B_{2m_1}^{Cyl}. \quad (5.1.1)$$

For $j \in [d] \setminus \{1\}$, define the $2m_j \times 2m_j$ diagonal and antidiagonal matrices

$$D_j = \text{diag} \left(2\iota a_j \cos \frac{\pi}{2m_j + 1}, \dots, 2\iota a_j \cos \frac{2m_j \pi}{2m_j + 1} \right), \quad (5.1.2)$$

$$J'_j = \iota^{2m_j-1} \text{adiag}(-1, 1, \dots, -1, 1), \quad (5.1.3)$$

and let

$$K_j^d = I_{2m_d} \otimes \cdots \otimes I_{2m_{j+1}} \otimes D_j \otimes J'_{j-1} \otimes \cdots \otimes J'_2 \otimes J_{2m_1},$$

$$\lambda_{i_d, i_{d-1}, \dots, i_p} = \sqrt{\sum_{s=p}^d 4a_s^2 \cos^2 \frac{i_s \pi}{2m_s + 1}}, \quad 1 < p \leq d.$$

Let u_k be the similarity transformation defined in Lemma 2.13. Then using the unitary transform $u_{2m_d} \otimes \cdots \otimes u_{2m_2} \otimes I_{2m_1}$, we see that

$$\mathcal{K}_G \sim I_{2m_d} \otimes \cdots \otimes I_{2m_2} \otimes \left(T_{2m_1}(-a_1, x, a_1) + a_1 B_{2m_1}^{Cyl} \right) + K_2^d + \cdots + K_d^d. \quad (5.1.4)$$

Since the first matrix of each tensor product in (5.1.4) is diagonal, \mathcal{K}_G is similar to an $2m_d \times 2m_d$ block diagonal matrix with the block F_{i_d} , $i_d \in [2m_d]$, given by

$$F_{i_d} = I_{2m_{d-1}} \otimes \cdots \otimes I_{2m_2} \otimes \left(T_{2m_1}(-a_1, x, a_1) + a_1 B_{2m_1}^{Cyl} \right) + K_2^{d-1} + \cdots + K_{d-2}^{d-1}$$

$$+ \left(D_{d-1} + 2\iota a_d \cos \frac{i_d \pi}{2m_d + 1} J'_{d-1} \right) \otimes J'_{d-2} \otimes \cdots \otimes J_{2m_1}.$$

Diagonalizing the cruciform matrix (a matrix whose nonzero entries lie only on the diagonal and the antidiagonal)

$$D_{d-1} + 2\iota a_d \cos \frac{i_d \pi}{2m_d + 1} J'_{d-1}$$

leads to the matrix

$$\text{diag}(\iota \lambda_{i_d,1}, -\iota \lambda_{i_d,1}, \iota \lambda_{i_d,2}, -\iota \lambda_{i_d,2}, \dots, \iota \lambda_{i_d,m_{d-1}}, -\iota \lambda_{i_d,m_{d-1}}).$$

Set $F_{i_d}^+ = F_{i_d}$, $F_{i_d}^- = F_{2m_d-i_d+1}$ for $1 \leq i_d \leq m_d$, and observe that $F_{i_d}^+ \sim F_{i_d}^-$. Since the determinant of a matrix is invariant under similarity transformation, the partition function can now be calculated as

$$\mathcal{Z}_G^{Cyl} = \prod_{i_d=1}^{m_d} (\det F_{i_d}^+)^2. \quad (5.1.5)$$

Continuing with the above approach, $F_{i_d}^+$ is similar to an $2m_{d-1} \times 2m_{d-1}$ block diagonal matrix with blocks $F_{i_d, i_{d-1}}^\pm$ ($1 \leq i_{d-1} \leq m_{d-1}$), resulting

$$\mathcal{Z}_G^{Cyl} = \prod_{i_d=1}^{m_d} \prod_{i_{d-1}=1}^{m_{d-1}} (\det F_{i_d, i_{d-1}}^+)^4. \quad (5.1.6)$$

Inductively,

$$\mathcal{Z}_G^{Cyl} = \prod_{i_d=1}^{m_d} \cdots \prod_{i_2=1}^{m_2} (\det F_{i_d, \dots, i_2}^+ \det F_{i_d, \dots, i_2}^-)^{2^{d-2}}, \quad (5.1.7)$$

where

$$F_{i_d, \dots, i_2}^\pm = \left(T_{2m_1}(-a_1, x, a_1) + a_1 B_{2m_1}^{Cyl} \right) \pm \iota \lambda_{i_d, \dots, i_2} J_{2m_1}.$$

Let V_k be the unitary similarity transform defined in (2.4.3). Then by Lemma 2.14,

$$V_{2m_1}^* F_{i_d, \dots, i_2}^\pm V_{2m_1} = \begin{pmatrix} x + 2\iota a_1 \sin \frac{\pi}{2m_1} & & & \mp \iota e^{\frac{\pi}{2m_1} \iota} \lambda_{i_d, \dots, i_2} \\ & \ddots & \ddots & \\ & & \ddots & \ddots \\ \mp \iota e^{\frac{(4m_1-1)\pi}{2m_1} \iota} \lambda_{i_d, \dots, i_2} & & & x + 2\iota a_1 \sin \frac{(4m_1-1)\pi}{2m_1} \end{pmatrix},$$

resulting,

$$\det F_{i_d, \dots, i_2}^\pm = \prod_{i_1=1}^{m_1} \left(x^2 + 4a_1^2 \sin^2 \frac{(2i_1-1)\pi}{2m_1} + \sum_{s=2}^d 4a_s^2 \cos^2 \frac{i_s \pi}{2m_s + 1} \right).$$

Substituting this in (5.1.7), concludes the proof. \square

We can see an ℓ -cylindrical grid graph as obtained from a d -dimensional grid graph by imposing cylindrical boundary conditions in the first ℓ directions and keeping the rest free. A similar proof technique can be used to prove the following general theorem.

Theorem 5.4 ([3, Theorem 3.4]). *Let G be the ℓ -cylindrical grid graph $Q_{2m_1, \dots, 2m_d}^\ell$ with boustrophedon labelling in d dimension. Let (G, \mathcal{O}) be obtained from G by orienting the edges from a lower-labelled vertex to a higher-labelled vertex. Let the vertex weights be x for all vertices of G , and edge weights be a_1, \dots, a_d for the edges along the different coordinate axes. Then the partition function of the monopole-dimer model on G is given by*

$$\mathcal{Z}_{2m_1, \dots, 2m_d}^{Mix} = \prod_{i_1=1}^{m_1} \cdots \prod_{i_d=1}^{m_d} \left(x^2 + \sum_{s=1}^{\ell} 4a_s^2 \sin^2 \frac{(2i_s - 1)\pi}{2m_s} + \sum_{t=\ell+1}^d 4a_t^2 \cos^2 \frac{i_t \pi}{2m_t + 1} \right)^{2^{d-1}}.$$

Let us now consider d -dimensional grids with toroidal boundary conditions which are obtained by imposing cylindrical boundary conditions in all directions of a d -dimensional grid.

Corollary 5.5 ([3, Theorem 3.5]). *Let G be the toroidal grid graph $Q_{2m_1, \dots, 2m_d}^{Tor}$ with boustrophedon labelling in d dimension. Let (G, \mathcal{O}) be obtained from G by orienting the edges from a lower-labelled vertex to a higher-labelled vertex. Let the vertex weights be x for all vertices of G , and edge weights be a_1, \dots, a_d for the edges along the different coordinate axes. Then the partition function of the monopole-dimer model on G is given by*

$$\mathcal{Z}_{2m_1, \dots, 2m_d}^{Tor} = \prod_{i_1=1}^{m_1} \cdots \prod_{i_d=1}^{m_d} \left(x^2 + \sum_{s=1}^d 4a_s^2 \sin^2 \frac{(2i_s - 1)\pi}{2m_s} \right)^{2^{d-1}}.$$

Now, we will focus on higher dimensional Möbius and Klein grid graphs.

Chapter 6

Three-dimensional Möbius and Klein grid graphs

In this chapter, we will extend the product formula (2.3.3) and (2.3.4) for three-dimensional grids and show that the formula does not extend to higher dimensions in the obvious way. We start by presenting the following lemma. We will use the notation \bar{A} and A^* to denote the conjugate and conjugate transpose of the matrix A , respectively.

Lemma 6.1. *Let A and B be two square matrices of order n such that A is invertible, $\bar{B}A^* = \bar{A}\bar{B}$, and $B^t = B$. Then, the determinant of the block matrix*

$$\det \begin{pmatrix} A & B \\ -\bar{B} & \bar{A} \end{pmatrix} = \det (AA^* + BB^*).$$

Proof. When D is invertible, it is well known that

$$\begin{aligned} \det \begin{pmatrix} A & B \\ C & D \end{pmatrix} &= \det (A - BD^{-1}C) \det D \\ &= \det (A - BD^{-1}C) \det D^t, \\ &= \det (AD^t - BD^{-1}CD^t). \end{aligned}$$

Here, we have $D = \bar{A}$ and $C = -\bar{B}$, therefore

$$\begin{aligned} \det \begin{pmatrix} A & B \\ -\bar{B} & \bar{A} \end{pmatrix} &= \det (A\bar{A}^t + B\bar{A}^{-1}\bar{B}A^*) \\ &= \det (A\bar{A}^t + B\bar{A}^{-1}\bar{A}B^*) \\ &= \det (AA^* + BB^*). \end{aligned}$$

□

6.1 Three-dimensional Möbius grids

Let us begin by defining what we mean by the term “high-dimensional Möbius grid”.

Definition 6.2. Let Q_{n_1, \dots, n_d} be the d -dimensional grid graph, we add an edge between the vertices $(1, k_2, \dots, k_d)$ and $(n_1, n_2 - k_2 + 1, \dots, n_d - k_d + 1)$ for all $1 \leq k_i \leq n_i$ ($2 \leq i \leq d$) to obtain Q_{n_1, \dots, n_d} with *Möbius boundary condition* along the first direction. We call these edges as *dashed edges* and the remaining as *solid edges*. We call this new graph as d -dimensional *Möbius grid graph* and denote it as $Q_{n_1, \dots, n_d}^{\text{Möb}}$.

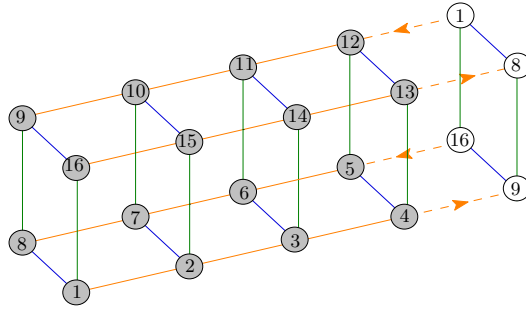
Let $G = Q_{n_1, \dots, n_d}^{\text{Möb}}$ be the d -dimensional Möbius grid graph with boustrophedon labelling. Orient the solid edges from lower-labelled vertex to higher-labelled vertex, orient the dashed edge at 1 outward and the remaining dashed edges such that each two-dimensional square satisfies the clockwise-odd property. Let us denote the resulting oriented graph as (G, \mathcal{O}) . We will always orient the edges coming from the Möbius boundary condition as described above. Figure 6.1 shows such an orientation over the Möbius grid graph $Q_{4,2,2}^{\text{Möb}}$.

Definition 6.3. We define the *monopole-dimer model* on the d -dimensional Möbius grid graph G as the loop-vertex model on G with the above orientation \mathcal{O} . The *partition function* of the monopole-dimer model is then the partition function of the loop-vertex model.

Theorem 6.4 ([3, Theorem 4.4]). *Let G be the three-dimensional Möbius grid graph $Q_{2m_1, 2m_2, 2m_3}^{\text{Möb}}$ with boustrophedon labelling. Let the vertex weights be x for all vertices of G , and edge weights be a_1, a_2 and a_3 for the edges along the x -, y - and z - coordinate axes respectively. Then the partition function of the monopole-dimer model on G is given by*

$$\begin{aligned} & \mathcal{Z}_{2m_1, 2m_2, 2m_3}^{\text{Möb}} \\ &= \prod_{i_1=1}^{m_1} \prod_{i_2=1}^{m_2} \prod_{i_3=1}^{m_3} \left(x^2 + 4a_1^2 \sin^2 \frac{(4i_1 - 1)\pi}{4m_1} + 4a_2^2 \cos^2 \frac{i_2\pi}{2m_2 + 1} + 4a_3^2 \cos^2 \frac{i_3\pi}{2m_3 + 1} \right)^4. \end{aligned}$$

Remark 6.5. The product formula in Theorem 6.4 remains unchanged even if one starts by orienting the dashed edge at 1 inward and the remaining dashed edges such that each two-dimensional square satisfies the clockwise-odd property.

Figure 6.1: The three-dimensional Möbius grid graph $Q_{4,2,2}^{\text{Möb}}$.

Remark 6.6. Note that the oriented d -dimensional Möbius grid $Q_{2m_1, \dots, 2m_d}^{\text{Möb}}$ can be regarded as the oriented Cartesian product of $P_{2m_1}, \dots, P_{2m_d}$ (oriented from one leaf to another) together with some additional dashed edges oriented in the specified way. We believe that the partition function of the monopole-dimer model remains unchanged regardless of the orientation on the path graphs. That is the reason for naming it as the monopole-dimer model.

Proof. Let D_j and J'_j be as defined in (5.1.2) and (5.1.3). The generalised adjacency matrix \mathcal{K}_G of the oriented three-dimensional Möbius grid graph (G, \mathcal{O}) is

$$\begin{aligned} \mathcal{K}_G = & I_{2m_3} \otimes I_{2m_2} \otimes T_{2m_1}(-a_1, x, a_1) + I_{2m_3} \otimes T_{2m_2}(-a_2, 0, a_2) \otimes J_{2m_1} \\ & + T_{2m_3}(-a_3, 0, a_3) \otimes J_{2m_2} \otimes J_{2m_1} + a_1 \text{diag}(1, -1, \dots, 1, -1) \otimes \text{diag}(1, -1, \dots, 1, -1) \\ & \otimes B_{2m_1}^{\text{Möb}} \end{aligned}$$

Let u_k be the standard unitary similarity transformation defined in Lemma 2.13. Then using the unitary transform $u_{2m_3} \otimes u_{2m_2} \otimes I_{2m_1}$, it is clear that

$$\begin{aligned} \mathcal{K}_G \sim & I_{2m_3} \otimes I_{2m_2} \otimes T_{2m_1}(-a_1, x, a_1) + I_{2m_3} \otimes D_2 \otimes J_{2m_1} + D_3 \otimes J'_2 \otimes J_{2m_1} \\ & + a_1 \iota^{2m_3-1} \text{diag}(1, -1, \dots, 1, -1) \otimes J_{2m_2} \otimes B_{2m_1}^{\text{Möb}}. \quad (6.1.1) \end{aligned}$$

Given that the initial matrix of each tensor product is diagonal in (6.1.1), \mathcal{K}_G becomes similar to a $2m_3 \times 2m_3$ block diagonal matrix, with each block F_{i_3} , ($i_3 \in [2m_3]$), defined as

$$\begin{aligned} F_{i_3} = & I_{2m_2} \otimes T_{2m_1}(-a_1, x, a_1) + D_2 \otimes J_{2m_1} + 2\iota a_3 \cos \frac{i_3 \pi}{2m_3 + 1} J'_2 \otimes J_{2m_1} \\ & + a_1 (-1)^{i_3-1} \iota^{2m_3-1} J_{2m_2} \otimes B_{2m_1}^{\text{Möb}}. \quad (6.1.2) \end{aligned}$$

Therefore,

$$\det \mathcal{K}_G = \prod_{i_3=1}^{2m_3} \det F_{i_3}. \quad (6.1.3)$$

Applying some simultaneous row and column interchanges on the first matrix in each tensor of (6.1.2) results in

$$\begin{aligned} F_{i_3} &\sim I_{m_2} \otimes I_2 \otimes T_{2m_1}(-a_1, x, a_1) \\ &+ \text{diag}\left(2\iota a_2 \cos \frac{\pi}{2m_2+1}, \dots, 2\iota a_2 \cos \frac{m_2\pi}{2m_2+1}\right) \otimes \begin{pmatrix} 1 & 0 \\ 0 & -1 \end{pmatrix} \otimes J_{2m_1} \\ &+ 2\iota^{2m_2} a_3 \cos \frac{i_3\pi}{2m_3+1} \text{diag}(1, -1, 1, -1, \dots) \otimes \begin{pmatrix} 0 & -1 \\ 1 & 0 \end{pmatrix} \otimes J_{2m_1} \\ &+ a_1(-1)^{i_3-1} \iota^{2m_3-1} I_{m_2} \otimes J_2 \otimes B_{2m_1}^{\text{Möb}}. \end{aligned}$$

Consequently,

$$\begin{aligned} \det F_{i_3} &= \prod_{i_2=1}^{m_2} \det \left(I_2 \otimes T_{2m_1}(-a_1, x, a_1) + 2\iota a_2 \cos \frac{i_2\pi}{2m_2+1} \begin{pmatrix} 1 & 0 \\ 0 & -1 \end{pmatrix} \otimes J_{2m_1} \right. \\ &\quad \left. + 2(-1)^{i_2-1} \iota^{2m_2} a_3 \cos \frac{i_3\pi}{2m_3+1} \begin{pmatrix} 0 & -1 \\ 1 & 0 \end{pmatrix} \otimes J_{2m_1} \right. \\ &\quad \left. + a_1(-1)^{i_3-1} \iota^{2m_3-1} J_2 \otimes B_{2m_1}^{\text{Möb}} \right). \end{aligned}$$

Using the unitary transform

$$\frac{1}{\sqrt{2}} \begin{pmatrix} -1 & 1 \\ 1 & 1 \end{pmatrix} \otimes I_{2m_1},$$

the determinant of F_{i_3} can be expressed as the following product:

$$\begin{aligned} \det F_{i_3} &= \prod_{i_2=1}^{m_2} \det \left(I_2 \otimes T_{2m_1}(-a_1, x, a_1) + 2\iota a_2 \cos \frac{i_2\pi}{2m_2+1} \begin{pmatrix} 0 & -1 \\ -1 & 0 \end{pmatrix} \otimes J_{2m_1} \right. \\ &\quad \left. + 2(-1)^{i_2-1} \iota^{2m_2} a_3 \cos \frac{i_3\pi}{2m_3+1} \begin{pmatrix} 0 & 1 \\ -1 & 0 \end{pmatrix} \otimes J_{2m_1} \right. \\ &\quad \left. + a_1(-1)^{i_3-1} \iota^{2m_3-1} \begin{pmatrix} -1 & 0 \\ 0 & 1 \end{pmatrix} \otimes B_{2m_1}^{\text{Möb}} \right). \end{aligned}$$

Finally, notice that F_{i_3} is the product of determinants of 2×2 block matrices of the

following form

$$\begin{pmatrix} A & B \\ -\bar{B} & \bar{A} \end{pmatrix}$$

where

$$A = T_{2m_1}(-a_1, x, a_1) - a_1(-1)^{i_3-1} \iota^{2m_3-1} B_{2m_1}^{\text{Möb}}$$

and

$$B = \left(-2\iota a_2 \cos \frac{i_2\pi}{2m_2+1} + 2(-1)^{i_2-1} \iota^{2m_2} a_3 \cos \frac{i_3\pi}{2m_3+1} \right) J_{2m_1}.$$

Observe that

$$\begin{aligned} \bar{B}A^* &= \left(2\iota a_2 \cos \frac{i_2\pi}{2m_2+1} + 2(-1)^{i_2-1} \iota^{2m_2} a_3 \cos \frac{i_3\pi}{2m_3+1} \right) \\ &\quad \times J_{2m_1} \left(T_{2m_1}(a_1, x, -a_1) + a_1(-1)^{i_3-1} \iota^{2m_3-1} B_{2m_1}^{\text{Möb}} \right) \end{aligned}$$

Since, J_{2m_1} commutes with $B_{2m_1}^{\text{Möb}}$ and $J_{2m_1}T_{2m_1}(a_1, x, -a_1) = T_{2m_1}(-a_1, x, a_1)J_{2m_1}$

$$\begin{aligned} \bar{B}A^* &= \left(2\iota a_2 \cos \frac{i_2\pi}{2m_2+1} + 2(-1)^{i_2-1} \iota^{2m_2} a_3 \cos \frac{i_3\pi}{2m_3+1} \right) \\ &\quad \times \left(T_{2m_1}(-a_1, x, a_1)J_{2m_1} + a_1(-1)^{i_3-1} \iota^{2m_3-1} B_{2m_1}^{\text{Möb}} J_{2m_1} \right) \end{aligned}$$

After re-arranging the terms, we get

$$\begin{aligned} \bar{B}A^* &= \left(T_{2m_1}(-a_1, x, a_1) + a_1(-1)^{i_3-1} \iota^{2m_3-1} B_{2m_1}^{\text{Möb}} \right) \\ &\quad \times \left(2\iota a_2 \cos \frac{i_2\pi}{2m_2+1} + 2(-1)^{i_2-1} \iota^{2m_2} a_3 \cos \frac{i_3\pi}{2m_3+1} \right) J_{2m_1} \\ &= \bar{A}\bar{B}. \end{aligned}$$

Now, using Lemma 6.1, we get

$$\det \begin{pmatrix} A & B \\ -\bar{B} & \bar{A} \end{pmatrix} = \det(AA^* + BB^*). \quad (6.1.4)$$

Diagonalizing the matrix A yields the following:

$$A \sim \text{diag} \left(x + 2(-1)^{m_3+i_3-1} \iota a_1 \sin \frac{3\pi}{4m_1}, \dots, x + 2(-1)^{m_3+i_3-1} \iota a_1 \sin \frac{(4(2m_1)-1)\pi}{4m_1} \right),$$

and

$$AA^* \sim \text{diag} \left(x^2 + 4a_1^2 \sin^2 \frac{3\pi}{4m_1}, \dots, x^2 + 4a_1^2 \sin^2 \frac{(8m_1 - 1)\pi}{4m_1} \right). \quad (6.1.5)$$

Further, a quick calculation shows that

$$BB^* = \left(4a_2^2 \cos^2 \frac{i_2\pi}{2m_2 + 1} + 4a_3^2 \cos^2 \frac{i_3\pi}{2m_3 + 1} \right) I_{2m_1}. \quad (6.1.6)$$

Combining equations (6.1.4), (6.1.5), and (6.1.6) results

$$\det F_{i_3} = \prod_{i_2=1}^{m_2} \prod_{i_1=1}^{2m_1} \left(x^2 + 4a_1^2 \sin^2 \frac{(4i_1 - 1)\pi}{4m_1} + 4a_2^2 \cos^2 \frac{i_2\pi}{2m_2 + 1} + 4a_3^2 \cos^2 \frac{i_3\pi}{2m_3 + 1} \right).$$

Finally, (6.1.3) together with the following trigonometric identities

$$\sin \frac{(4(m_1 + i_1) - 1)\pi}{4m_1} = -\sin \frac{(4i_1 - 1)\pi}{4m_1}, \quad (6.1.7)$$

$$\cos \frac{(2m_3 - i_3 + 1)\pi}{2m_3 + 1} = -\cos \frac{i_3\pi}{2m_3 + 1} \quad (6.1.8)$$

concludes the proof. \square

We now provide an example showing that the formula does not generalise for higher dimensions.

Example 6.7. Let $G = Q_{2,2,2,2}^{\text{Möb}}$ be the four-dimensional Möbius grid as shown in Figure 6.2. The solid edges are oriented from lower labelled vertex to higher labelled vertex and dashed edges are oriented as described in the paragraph just below Definition 6.2. Let the vertex weight be 0 for all the vertices and edge weights be a_1, a_2, a_3 and a_4

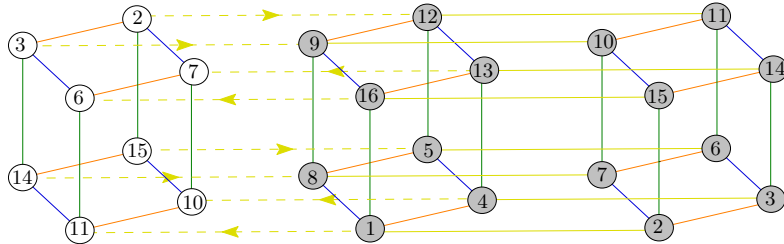


Figure 6.2: The four-dimensional cube with Möbius boundary conditions

for the edges along the different coordinate axes. Then, the partition function of the monopole-dimer model on G is

$$(4a_1^2 + a_2^2 + a_3^2 + a_4^2)^4 (a_2^2 + a_3^2 + a_4^2)^4$$

which is not an 8th power. This leads us to conclude that the product formula in (2.3.3) does not generalise to higher dimensions.

Using Theorem 5.2 and Theorem 6.4 together with the following identities,

$$\sin^2 \frac{(2(2i) - 1)\pi}{4n} = \sin^2 \frac{(2(2n - 2i + 1) - 1)\pi}{4n} = \sin^2 \frac{(4i - 1)\pi}{4n}, \quad \text{for } 1 \leq i \leq n,$$

we can deduce the generalized relationship between the partition function of the monopole-dimer model on the three-dimensional Möbius and cylindrical grid graphs, akin to the relationship between the partition function of the dimer model on two-dimensional grids embedded on a cylinder and a Möbius strip [25, (24)].

Corollary 6.8. *Let $\mathcal{Z}_{4n_1, 2n_2, 2n_3}^{Cyl}$ and $\mathcal{Z}_{2n_1, 2n_2, 2n_3}^{Möb}$ be the partition function of the monopole-dimer model on the oriented three-dimensional Möbius grid $Q_{4n_1, 2n_2, 2n_3}^{Möb}$ and cylindrical grid $Q_{2n_1, 2n_2, 2n_3}^{Cyl}$ with boustrophedon labelling, respectively. Then*

$$\mathcal{Z}_{4n_1, 2n_2, 2n_3}^{Cyl} = \left(\mathcal{Z}_{2n_1, 2n_2, 2n_3}^{Möb} \right)^2. \quad (6.1.9)$$

6.2 Three-dimensional Klein grids

A d -dimensional grid is considered to have *Klein boundary conditions* if it exhibits Möbius boundary conditions along the first direction and cylindrical boundary conditions along the remaining directions.

Definition 6.9. Let $P_{n_1} \square C_{n_2} \square \dots \square C_{n_d}$ be Cartesian product of $P_{n_1}, C_{n_2}, \dots, C_{n_d}$, we add an edge between the vertices $(1, k_2, \dots, k_d)$ and $(n_1, n_2 - k_2 + 1, \dots, n_d - k_d + 1)$ for all $1 \leq k_i \leq n_i$ ($2 \leq i \leq d$) to obtain a new graph called the d -dimensional *Klein grid graph* $Q_{n_1, \dots, n_d}^{Klein}$. We call these additional edges as *dashed edges* and the remaining as *solid edges*.

Let $G = Q_{n_1, \dots, n_d}^{Klein}$ be the d -dimensional Klein grid graph with boustrophedon labelling. Orient the solid edges from lower-labelled vertex to higher-labelled vertex, orient the dashed edge at 1 outward and the remaining dashed edges such that each two-dimensional square satisfies the clockwise-odd property. Let us denote the resulting oriented graph as (G, \mathcal{O}) . Note that $Q_{n_1, \dots, n_d}^{Möb}$ is a subgraph of $Q_{n_1, \dots, n_d}^{Klein}$. Figure 6.3 shows such an orientation over the Klein grid graph $Q_{4, 2, 2}^{Klein}$.

Definition 6.10. We define the *monopole-dimer model* on the d -dimensional Klein grid graph G as the loop-vertex model on G with the above orientation \mathcal{O} . *The partition*

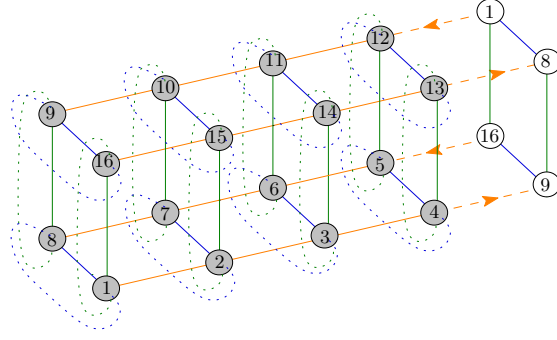


Figure 6.3: The three-dimensional Möbius grid graph $Q_{4,2,2}^{Klein}$.

function of the monopole-dimer model is then the partition function of the loop-vertex model.

Theorem 6.11 ([3, Theorem 5.3]). *Let $G = Q_{2m_1, 2m_2, 2m_3}^{Klein}$ be the three-dimensional Klein grid graph. Let vertex weights be x for all vertices of G , and edge weights be a_1, a_2 and a_3 for the edges along the x -, y - and z - coordinate axes respectively. Then the partition function of the monopole-dimer model on (G, \mathcal{O}) is given by*

$$\begin{aligned} & \mathcal{Z}_{2m_1, 2m_2, 2m_3}^{Klein} \\ &= \prod_{i_1=1}^{m_1} \prod_{i_2=1}^{m_2} \prod_{i_3=1}^{m_3} \left(x^2 + 4a_1^2 \sin^2 \frac{(4i_1 - 1)\pi}{4m_1} + 4a_2^2 \sin^2 \frac{(2i_2 - 1)\pi}{2m_2} + 4a_3^2 \sin^2 \frac{(2i_3 - 1)\pi}{2m_3} \right)^4. \end{aligned}$$

Proof. Again, let T_k, J_k, D_j and J'_j be as defined in the proof of Theorem 5.2. The generalised adjacency matrix, \mathcal{K}_G of the oriented three-dimensional grid graph with Klein boundary conditions, (G, \mathcal{O}) is

$$\begin{aligned} \mathcal{K}_G &= I_{2m_3} \otimes I_{2m_2} \otimes T_{2m_1}(-a_1, x, a_1) + a_1 \text{adiag}(1, -1, \dots, 1, -1) \otimes \text{diag}(1, -1, \dots, 1, -1) \\ & \quad \otimes B_{2m_1}^{\text{Möb}} \\ &+ I_{2m_3} \otimes \left(T_{2m_2}(-a_2, 0, a_2) + a_2 B_{2m_2}^{\text{Cyl}} \right) \otimes J_{2m_1} + \left(T_{2m_3}(-a_3, 0, a_3) + a_3 B_{2m_3}^{\text{Cyl}} \right) \otimes J_{2m_2} \otimes J_{2m_1}. \end{aligned}$$

Let V_k be the similarity transformation defined in Lemma 2.14. Then using the unitary transform $V_{2m_3} \otimes V_{2m_2} \otimes I_{2m_1}$, it is clear that

$$\mathcal{K}_G \sim I_{2m_3} \otimes I_{2m_2} \otimes T_{2m_1}(-a_1, x, a_1)$$

$$\begin{aligned}
& + a_1 \left(\begin{array}{c|c} e^{t \frac{\pi}{2m_3}} & \\ \hline & 0 \\ \hline 0 & \\ e^{t \frac{(4m_3-1)\pi}{2m_3}} & \end{array} \right) \otimes \left(\begin{array}{c|c} 0 & I_{m_2} \\ \hline I_{m_2} & 0 \end{array} \right) \otimes B_{2m_1}^{\text{Möb}} \\
& + I_{2m_3} \otimes \text{diag} \left(2\iota a_2 \sin \frac{(2 \cdot 1 - 1)\pi}{2m_2}, \dots, 2\iota a_2 \sin \frac{(2 \cdot 2m_2 - 1)\pi}{2m_2} \right) \otimes J_{2m_1} \\
& + \text{diag} \left(2\iota a_3 \sin \frac{(2 \cdot 1 - 1)\pi}{2m_3}, \dots, 2\iota a_3 \sin \frac{(2 \cdot 2m_3 - 1)\pi}{2m_3} \right) \\
& \otimes \text{adiag} \left(-e^{t \frac{\pi}{2m_2}}, \dots, -e^{t \frac{(2 \cdot 2m_2 - 1)\pi}{2m_2}} \right) \otimes J_{2m_1}.
\end{aligned}$$

Using the following identities

$$\begin{aligned}
e^{t \frac{(2(n+k)-1)\pi}{2n}} &= -e^{t \frac{(2k-1)\pi}{2n}}, \\
\sin \frac{(2(n+k)-1)\pi}{2n} &= -\sin \frac{(2k-1)\pi}{2n},
\end{aligned} \tag{6.2.1}$$

we get

$$\begin{aligned}
\mathcal{K}_G &\sim I_2 \otimes I_{m_3} \otimes I_{2m_2} \otimes T_{2m_1}(-a_1, x, a_1) \\
&+ a_1 \begin{pmatrix} 1 & 0 \\ 0 & -1 \end{pmatrix} \otimes \text{adiag} \left(e^{t \frac{\pi}{2m_3}}, \dots, e^{t \frac{(2m_3-1)\pi}{2m_3}} \right) \otimes \left(\begin{array}{c|c} 0 & I_{m_2} \\ \hline I_{m_2} & 0 \end{array} \right) \otimes B_{2m_1}^{\text{Möb}} \\
&+ I_2 \otimes I_{m_3} \otimes \text{diag} \left(2\iota a_2 \sin \frac{(2 \cdot 1 - 1)\pi}{2m_2}, \dots, 2\iota a_2 \sin \frac{(2 \cdot 2m_2 - 1)\pi}{2m_2} \right) \otimes J_{2m_1} \\
&+ \begin{pmatrix} 1 & 0 \\ 0 & -1 \end{pmatrix} \otimes \text{diag} \left(2\iota a_3 \sin \frac{(2 \cdot 1 - 1)\pi}{2m_3}, \dots, 2\iota a_3 \sin \frac{(2m_3 - 1)\pi}{2m_3} \right) \\
&\quad \otimes \text{adiag} \left(-e^{t \frac{\pi}{2m_2}}, \dots, -e^{t \frac{(2 \cdot 2m_2 - 1)\pi}{2m_2}} \right) \otimes J_{2m_1}.
\end{aligned}$$

Observing that

$$e^{t \frac{(2(n-k+1)-1)\pi}{2n}} = -e^{-t \frac{(2k-1)\pi}{2n}}, \tag{6.2.2}$$

$$\sin \frac{(2(n-k+1)-1)\pi}{2n} = \sin \frac{(2k-1)\pi}{2n}, \tag{6.2.3}$$

and applying some simultaneous row and column interchanges on the second matrix of

each tensor, turns it into a block diagonal matrix. In particular, if m_3 is even,

$$\begin{aligned}
\mathcal{K}_G &\sim I_2 \otimes I_{m_3} \otimes I_{2m_2} \otimes T_{2m_1}(-a_1, x, a_1) \\
&+ a_1 \begin{pmatrix} 1 & 0 \\ 0 & -1 \end{pmatrix} \otimes \left(\begin{array}{c|c} \begin{matrix} 0 & e^{i\frac{\pi}{2m_3}} \\ -e^{-i\frac{\pi}{2m_3}} & 0 \end{matrix} & 0 \\ \hline 0 & \begin{matrix} 0 & e^{i\frac{(2\cdot\frac{m_3}{2}-1)\pi}{2m_3}} \\ -e^{-i\frac{(2\cdot\frac{m_3}{2}-1)\pi}{2m_3}} & 0 \end{matrix} \end{array} \right) \otimes \left(\begin{array}{c|c} 0 & I_{m_2} \\ \hline I_{m_2} & 0 \end{array} \right) \otimes B_{2m_1}^{\text{Möb}} \\
&+ I_2 \otimes I_{m_3} \otimes \text{diag} \left(2\iota a_2 \sin \frac{(2 \cdot 1 - 1)\pi}{2m_2}, \dots, 2\iota a_2 \sin \frac{(2 \cdot 2m_2 - 1)\pi}{2m_2} \right) \otimes J_{2m_1} \\
&+ \begin{pmatrix} 1 & 0 \\ 0 & -1 \end{pmatrix} \otimes 2\iota a_3 \text{diag} \left(\sin \frac{\pi}{2m_3}, \sin \frac{\pi}{2m_3}, \dots, \sin \frac{(2 \cdot \frac{m_3}{2} - 1)\pi}{2m_3}, \sin \frac{(2 \cdot \frac{m_3}{2} - 1)\pi}{2m_3} \right) \\
&\quad \otimes \text{adiag} \left(-e^{i\frac{\pi}{2m_2}}, \dots, -e^{i\frac{(4m_2-1)\pi}{2m_2}} \right) \otimes J_{2m_1}. \quad (6.2.4)
\end{aligned}$$

Since the first matrix of each tensor product in (6.2.4) is diagonal and the second matrix is block diagonal, the determinant of the matrix \mathcal{K}_G can be written as the following product.

$$\begin{aligned}
\det(\mathcal{K}_G) &= \prod_{i_3=1}^{\lfloor \frac{m_3}{2} \rfloor} \det \left(I_2 \otimes I_2 \otimes I_{2m_2} \otimes T_{2m_1}(-a_1, x, a_1) \right. \\
&+ a_1 \begin{pmatrix} 1 & 0 \\ 0 & -1 \end{pmatrix} \otimes \left(\begin{array}{c|c} \begin{matrix} 0 & e^{i\frac{(2i_3-1)\pi}{2m_3}} \\ -e^{-i\frac{(2i_3-1)\pi}{2m_3}} & 0 \end{matrix} & 0 \\ \hline 0 & \begin{matrix} 0 & e^{i\frac{(2i_3-1)\pi}{2m_3}} \\ -e^{-i\frac{(2i_3-1)\pi}{2m_3}} & 0 \end{matrix} \end{array} \right) \otimes \left(\begin{array}{c|c} 0 & I_{m_2} \\ \hline I_{m_2} & 0 \end{array} \right) \otimes B_{2m_1}^{\text{Möb}} \\
&+ I_2 \otimes I_2 \otimes \text{diag} \left(2\iota a_2 \sin \frac{(2 \cdot 1 - 1)\pi}{2m_2}, \dots, 2\iota a_2 \sin \frac{(2 \cdot 2m_2 - 1)\pi}{2m_2} \right) \otimes J_{2m_1} \\
&+ \begin{pmatrix} 1 & 0 \\ 0 & -1 \end{pmatrix} \otimes 2\iota a_3 \begin{pmatrix} \sin \frac{(2i_3-1)\pi}{2m_3} & 0 \\ 0 & \sin \frac{(2i_3-1)\pi}{2m_3} \end{pmatrix} \otimes \text{adiag} \left(-e^{i\frac{\pi}{2m_2}}, \dots, -e^{i\frac{(4m_2-1)\pi}{2m_2}} \right) \\
&\quad \left. \otimes J_{2m_1} \right)
\end{aligned}$$

$$\times \begin{cases} 1 & \text{if } m_3 \text{ is even,} \\ \det \left(I_2 \otimes I_{2m_2} \otimes T_{2m_1}(-a_1, x, a_1) \right. \\ \left. + \iota a_1 \begin{pmatrix} 1 & 0 \\ 0 & -1 \end{pmatrix} \otimes \left(\begin{array}{c|c} 0 & I_{m_2} \\ \hline I_{m_2} & 0 \end{array} \right) \otimes B_{2m_1}^{\text{Möb}} \right. \\ \left. + I_2 \otimes \text{diag} \left(2\iota a_2 \sin \frac{(2 \cdot 1 - 1)\pi}{2m_2}, \dots, 2\iota a_2 \sin \frac{(2 \cdot 2m_2 - 1)\pi}{2m_2} \right) \otimes J_{2m_1} \right. \\ \left. + 2\iota a_3 \begin{pmatrix} 1 & 0 \\ 0 & -1 \end{pmatrix} \otimes \text{adiag} \left(-e^{\iota \frac{\pi}{2m_2}}, \dots, -e^{\iota \frac{(4m_2 - 1)\pi}{2m_2}} \right) \otimes J_{2m_1} \right) & \text{if } m_3 \text{ is odd.} \end{cases}$$

Further, $\text{adiag} \left(e^{\iota \frac{(2i_3 - 1)\pi}{2m_3}}, -e^{-\iota \frac{(2i_3 - 1)\pi}{2m_3}} \right)$ diagonalizes to $\text{diag}(\iota, -\iota)$. Therefore,

$$\begin{aligned} \det(\mathcal{K}_G) &= \prod_{i_3=1}^{\lfloor \frac{m_3}{2} \rfloor} \det \left(I_2 \otimes I_2 \otimes I_{2m_2} \otimes T_{2m_1}(-a_1, x, a_1) \right. \\ &\quad \left. + a_1 \begin{pmatrix} 1 & 0 \\ 0 & -1 \end{pmatrix} \otimes \begin{pmatrix} \iota & 0 \\ 0 & -\iota \end{pmatrix} \otimes \left(\begin{array}{c|c} 0 & I_{m_2} \\ \hline I_{m_2} & 0 \end{array} \right) \otimes B_{2m_1}^{\text{Möb}} \right. \\ &\quad \left. + I_2 \otimes I_2 \otimes \text{diag} \left(2\iota a_2 \sin \frac{(2 \cdot 1 - 1)\pi}{2m_2}, \dots, 2\iota a_2 \sin \frac{(2 \cdot 2m_2 - 1)\pi}{2m_2} \right) \otimes J_{2m_1} \right. \\ &\quad \left. + \begin{pmatrix} 1 & 0 \\ 0 & -1 \end{pmatrix} \otimes 2\iota a_3 \sin \frac{(2i_3 - 1)\pi}{2m_3} \begin{pmatrix} 1 & 0 \\ 0 & 1 \end{pmatrix} \otimes \text{adiag} \left(-e^{\iota \frac{\pi}{2m_2}}, \dots, -e^{\iota \frac{(4m_2 - 1)\pi}{2m_2}} \right) \otimes J_{2m_1} \right) \end{aligned}$$

$$\times \begin{cases} 1 & \text{if } m_3 \text{ is even,} \\ \det \left(I_2 \otimes I_{2m_2} \otimes T_{2m_1}(-a_1, x, a_1) + \iota a_1 \begin{pmatrix} 1 & 0 \\ 0 & -1 \end{pmatrix} \otimes \left(\begin{array}{c|c} 0 & I_{m_2} \\ \hline I_{m_2} & 0 \end{array} \right) \right. \\ \left. \otimes B_{2m_1}^{\text{Möb}} + I_2 \otimes 2\iota a_2 \text{diag} \left(\sin \frac{(2 \cdot 1 - 1)\pi}{2m_2}, \dots, \sin \frac{(2 \cdot 2m_2 - 1)\pi}{2m_2} \right) \otimes J_{2m_1} \right. \\ \left. + 2\iota a_3 \begin{pmatrix} 1 & 0 \\ 0 & -1 \end{pmatrix} \otimes \text{adiag} \left(-e^{\iota \frac{\pi}{2m_2}}, \dots, -e^{\iota \frac{(4m_2 - 1)\pi}{2m_2}} \right) \otimes J_{2m_1} \right) & \text{if } m_3 \text{ is odd.} \end{cases}$$

Now, since the initial two matrices of each tensor product are 2×2 diagonal matrices, it is enough to determine the determinant of the following matrices:

$$\begin{aligned}
F_{i_3}^{\alpha,\beta} (\text{ for } \alpha = \pm 1, \beta = \pm 1) &= I_{2m_2} \otimes T_{2m_1}(-a_1, x, a_1) + \iota\alpha a_1 \begin{pmatrix} 0 & I_{m_2} \\ I_{m_2} & 0 \end{pmatrix} \otimes B_{2m_1}^{\text{Möb}} \\
&+ 2\iota a_2 \text{diag} \left(\sin \frac{(2 \cdot 1 - 1)\pi}{2m_2}, \dots, \sin \frac{(2 \cdot 2m_2 - 1)\pi}{2m_2} \right) \otimes J_{2m_1} \\
&- 2\iota\beta a_3 \sin \frac{(2i_3 - 1)\pi}{2m_3} \text{adiag} \left(e^{\iota \frac{\pi}{2m_2}}, \dots, e^{\iota \frac{(4m_2 - 1)\pi}{2m_2}} \right) \otimes J_{2m_1}.
\end{aligned}$$

We can rewrite $F_{i_3}^{\alpha,\beta}$ with the help of the trigonometric identities in (6.2.1) as

$$\begin{aligned}
F_{i_3}^{\alpha,\beta} &= I_2 \otimes I_{m_2} \otimes T_{2m_1}(-a_1, x, a_1) + \iota\alpha a_1 \begin{pmatrix} 0 & 1 \\ 1 & 0 \end{pmatrix} \otimes I_{m_2} \otimes B_{2m_1}^{\text{Möb}} \\
&+ \begin{pmatrix} 1 & 0 \\ 0 & -1 \end{pmatrix} \otimes 2\iota a_2 \text{diag} \left(\sin \frac{(2 \cdot 1 - 1)\pi}{2m_2}, \dots, \sin \frac{(2 \cdot m_2 - 1)\pi}{2m_2} \right) \otimes J_{2m_1} \\
&- 2\iota\beta a_3 \sin \frac{(2i_3 - 1)\pi}{2m_3} \begin{pmatrix} 0 & 1 \\ -1 & 0 \end{pmatrix} \otimes \text{adiag} \left(e^{\iota \frac{\pi}{2m_2}}, \dots, e^{\iota \frac{(2m_2 - 1)\pi}{2m_2}} \right) \otimes J_{2m_1}.
\end{aligned}$$

Using the unitary transform

$$\frac{1}{\sqrt{2}} \begin{pmatrix} -1 & 1 \\ 1 & 1 \end{pmatrix} \otimes I_{m_2} \otimes I_{2m_1},$$

we obtain

$$\begin{aligned}
F_{i_3}^{\alpha,\beta} &\sim I_2 \otimes I_{m_2} \otimes T_{2m_1}(-a_1, x, a_1) + \iota\alpha a_1 \begin{pmatrix} -1 & 0 \\ 0 & 1 \end{pmatrix} \otimes I_{m_2} \otimes B_{2m_1}^{\text{Möb}} \\
&+ \begin{pmatrix} 0 & -1 \\ -1 & 0 \end{pmatrix} \otimes \text{diag} \left(2\iota a_2 \sin \frac{(2 \cdot 1 - 1)\pi}{2m_2}, \dots, 2\iota a_2 \sin \frac{(2 \cdot m_2 - 1)\pi}{2m_2} \right) \otimes J_{2m_1} \\
&- 2\iota\beta a_3 \sin \frac{(2i_3 - 1)\pi}{2m_3} \begin{pmatrix} 0 & -1 \\ 1 & 0 \end{pmatrix} \otimes \text{adiag} \left(e^{\iota \frac{\pi}{2m_2}}, \dots, e^{\iota \frac{(2m_2 - 1)\pi}{2m_2}} \right) \otimes J_{2m_1}.
\end{aligned}$$

Repeating the same procedure on the second matrix in each tensor if m_2 is even, results

in

$$\begin{aligned}
F_{i_3}^{\alpha,\beta} &\sim I_2 \otimes I_{m_2} \otimes T_{2m_1}(-a_1, x, a_1) + \iota\alpha a_1 \begin{pmatrix} -1 & 0 \\ 0 & 1 \end{pmatrix} \otimes I_{m_2} \otimes B_{2m_1}^{\text{Möb}} \\
&+ \begin{pmatrix} 0 & -1 \\ -1 & 0 \end{pmatrix} \otimes 2\iota a_2 \text{diag} \left(\sin \frac{\pi}{2m_2}, \sin \frac{\pi}{2m_2}, \dots, \sin \frac{(2 \cdot \frac{m_2}{2} - 1)\pi}{2m_2}, \sin \frac{(2 \cdot \frac{m_2}{2} - 1)\pi}{2m_2} \right) \\
&\hspace{20em} \otimes J_{2m_1} \\
&- 2\iota\beta a_3 \sin \frac{(2i_3 - 1)\pi}{2m_3} \begin{pmatrix} 0 & -1 \\ 1 & 0 \end{pmatrix} \otimes \text{diag}(\iota, -\iota, \dots, \iota, -\iota) \otimes J_{2m_1}.
\end{aligned}$$

Further, notice that $F_{i_3}^{\alpha,\beta}$ is the product of determinants of 2×2 block matrices of the following form

$$\begin{pmatrix} A & B \\ -\bar{B} & \bar{A} \end{pmatrix}$$

where

$$A = I_{m_2} \otimes T_{2m_1}(-a_1, x, a_1) - \iota\alpha a_1 I_{m_2} \otimes B_{2m_1}^{\text{Möb}},$$

and

$$\begin{aligned}
B &= \\
&- 2\iota a_2 \text{diag} \left(\sin \frac{\pi}{2m_2}, \sin \frac{\pi}{2m_2}, \dots, \sin \frac{(2 \cdot \frac{m_2}{2} - 1)\pi}{2m_2}, \sin \frac{(2 \cdot \frac{m_2}{2} - 1)\pi}{2m_2} \right) \otimes J_{2m_1} \\
&\quad + 2\iota\beta a_3 \sin \frac{(2i_3 - 1)\pi}{2m_3} \text{diag}(\iota, -\iota, \dots, \iota, -\iota) \otimes J_{2m_1}.
\end{aligned}$$

Using a similar argument as in the proof of Theorem 6.4, we can see that $\bar{B}A^* = \bar{A}\bar{B}$.

Now, using Lemma 6.1, we get

$$\det \begin{pmatrix} A & B \\ -\bar{B} & \bar{A} \end{pmatrix} = \det(AA^* + BB^*). \quad (6.2.5)$$

Diagonalizing the matrix A yields the following:

$$\begin{aligned}
A &= I_{m_2} \otimes \left(T_{2m_1}(-a_1, x, a_1) - \iota\alpha a_1 B_{2m_1}^{\text{Möb}} \right) \\
&\sim I_{m_2} \otimes \text{diag} \left(x - 2\iota\alpha a_1 \sin \frac{3\pi}{4m_1}, \dots, x - 2\iota\alpha a_1 \sin \frac{(4(2m_1) - 1)\pi}{4m_1} \right)
\end{aligned}$$

and

$$AA^* \sim I_{m_2} \otimes \text{diag} \left(x^2 + 4a_1^2 \sin^2 \frac{3\pi}{4m_1}, \dots, x^2 + 4a_1^2 \sin^2 \frac{(8m_1 - 1)\pi}{4m_1} \right). \quad (6.2.6)$$

Further, a quick calculation shows that

$$\begin{aligned} BB^* = & \left(\text{diag} \left(4a_2^2 \sin^2 \frac{\pi}{2m_2}, 4a_2^2 \sin^2 \frac{\pi}{2m_2}, \dots, 4a_2^2 \sin^2 \frac{(2 \cdot \frac{m_2}{2} - 1)\pi}{2m_2}, 4a_2^2 \sin^2 \frac{(2 \cdot \frac{m_2}{2} - 1)\pi}{2m_2} \right) \right. \\ & \left. + 4a_3^2 \sin^2 \frac{(2i_3 - 1)\pi}{2m_3} I_{m_2} \right) \otimes I_{2m_1}. \end{aligned} \quad (6.2.7)$$

Combining equations (6.2.5), (6.2.6), and (6.2.7) results in

$$\begin{aligned} \det F_{i_3}^{\alpha, \beta} &= \prod_{i_2=1}^{\lfloor \frac{m_2}{2} \rfloor} \prod_{i_1=1}^{2m_1} \left(x^2 + 4a_1^2 \sin^2 \frac{(4i_1 - 1)\pi}{4m_1} + 4a_2^2 \sin^2 \frac{(2i_2 - 1)\pi}{2m_2} + 4a_3^2 \sin^2 \frac{(2i_3 - 1)\pi}{2m_3} \right)^2 \\ &\times \begin{cases} 1 & m_2 \text{ is even,} \\ \prod_{i_1=1}^{2m_1} \left(x^2 + 4a_1^2 \sin^2 \frac{(4i_1 - 1)\pi}{4m_1} + 4a_2^2 \sin^2 \frac{((m_2 + 1) - 1)\pi}{2m_2} + 4a_3^2 \sin^2 \frac{(2i_3 - 1)\pi}{2m_3} \right) & m_2 \text{ is odd.} \end{cases} \end{aligned}$$

Hence,

$$\begin{aligned} \det(\mathcal{K}_G) &= \prod_{i_3=1}^{\lfloor \frac{m_3}{2} \rfloor} \prod_{i_2=1}^{m_2} \prod_{i_1=1}^{2m_1} \left(x^2 + 4a_1^2 \sin^2 \frac{(4i_1 - 1)\pi}{4m_1} + 4a_2^2 \sin^2 \frac{(2i_2 - 1)\pi}{2m_2} + 4a_3^2 \sin^2 \frac{(2i_3 - 1)\pi}{2m_3} \right)^4 \\ &\times \begin{cases} 1 & m_3 \text{ is even,} \\ \prod_{i_2=1}^{m_2} \prod_{i_1=1}^{2m_1} \left(x^2 + 4a_1^2 \sin^2 \frac{(4i_1 - 1)\pi}{4m_1} + 4a_2^2 \sin^2 \frac{(2i_2 - 1)\pi}{2m_2} + 4a_3^2 \sin^2 \frac{((m_3 + 1) - 1)\pi}{2m_3} \right)^2 & m_3 \text{ is odd,} \end{cases} \end{aligned}$$

which can be rewritten using the trigonometric identities (6.1.7) and (6.2.3) as

$$\det(\mathcal{K}_G) = \prod_{i_3=1}^{m_3} \prod_{i_2=1}^{m_2} \prod_{i_1=1}^{m_1} \left(x^2 + 4a_1^2 \sin^2 \frac{(4i_1 - 1)\pi}{4m_1} + 4a_2^2 \sin^2 \frac{(2i_2 - 1)\pi}{2m_2} + 4a_3^2 \sin^2 \frac{(2i_3 - 1)\pi}{2m_3} \right)^4.$$

□

We conclude the section by providing an example that shows that the formula in (2.3.4) can only be generalised to three dimensions and by raising a pertinent question of whether it is possible to define the non-orientable boundary conditions such that the product formulas for higher dimensions still hold while preserving the relationship in (6.1.9).

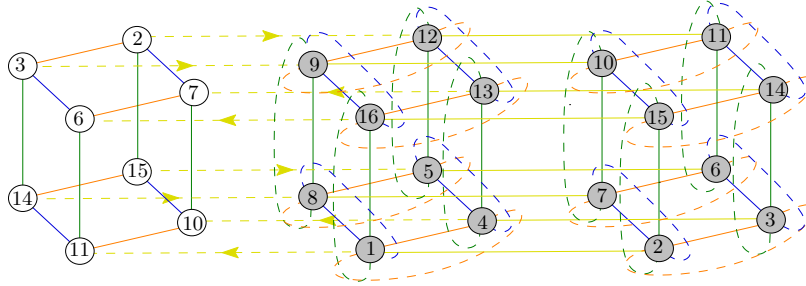


Figure 6.4: four-dimensional Klein grid graph, $Q_{2,2,2,2}^{\text{Klein}}$.

Example 6.12. Let $G = Q_{2,2,2,2}^{\text{Klein}}$ be the four-dimensional Klein grid graph as shown in Figure 6.4. Solid edges are oriented from a lower labelled vertex to a higher labelled vertex and dashed edges are oriented as described above. Let the vertex weight be 0 for all the vertices and edge weights be a_1, a_2, a_3 and a_4 for the edges along the different coordinate axes. Then, the partition function of the monopole-dimer model on G is

$$2^{16}(a_1^2 + a_2^2 + a_3^2 + a_4^2)^4(a_2^2 + a_3^2 + a_4^2)^4$$

which is not an 8^{th} power. Hence the product formula (2.3.4) does not generalise to higher dimensions in obvious way.

Remark 6.13. Again, note that the oriented d -dimensional Klein grid $Q_{2m_1, \dots, 2m_d}^{\text{Klein}}$ can be regarded as the oriented Cartesian product of $P_{2m_1}, C_{2m_2}, \dots, C_{2m_d}$ (oriented from lower-labelled vertex to higher-labelled vertex) together with some additional dashed edges oriented in the specified manner. We believe that the partition function of the monopole-dimer model remains unchanged regardless of the Pfaffian orientation on the path and cycle graphs.

Chapter 7

Eccentric graph of trees

We talked in Section 2.5 about the interesting properties of the eccentric graph of a tree. In this chapter, we will discuss about the structure of the eccentric graph of a tree and its girth in detail. From now on, we will only consider simple, undirected graphs on *at least* two vertices.

7.1 Structure of eccentric graph of a tree

In this section, we will focus on the structure of the eccentric graph of a tree.

Definition 7.1. Let T be a tree and v be a leaf in T . We define the path from v to the nearest vertex of degree greater than two as the *stem* at v and the *branching vertex* is an endpoint of the stem which has degree greater than two in T .

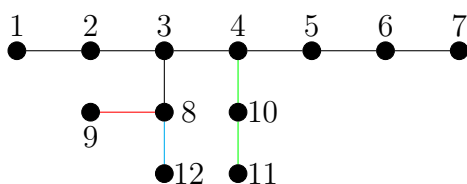


Figure 7.1: A tree T on 12 vertices with different colored stems at vertices 9, 11 and 12.

Note that a path graph P_n has no stems. Recall that a diametrical path (defined in Section 2.5) is a longest eccentric path in the graph G .

Definition 7.2. Let P be a diametrical path in a tree T . We define the *tree induced from the path P* as the subtree of T obtained by removing stems except branching vertices at those leaves (except endpoints of P), which are an endpoint of some diametrical path other than P .

Consider the tree T shown in Figure 7.1. T has three diametrical paths and the subtrees induced by these are shown in Figure 7.2.

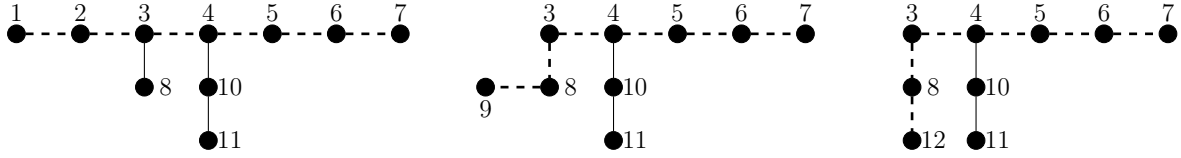


Figure 7.2: Subtrees induced by different diametrical paths (dashed) of the tree in Figure 7.1.

The eccentric graphs of the subtrees in Figure 7.2 are shown in Figure 7.3.

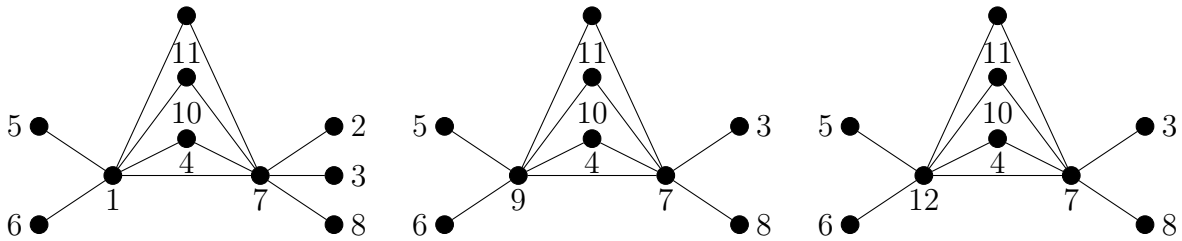


Figure 7.3: Eccentric graphs of the three subtrees in Figure 7.2 of the tree in Figure 7.1.

In general, the structure of the eccentric graph of a subtree induced from a diametrical path in T depends on the diameter of T . In case of an even diameter, it looks as shown in the left of Figure 7.4 and in case of odd diameter, it looks as shown in the right of Figure 7.4.

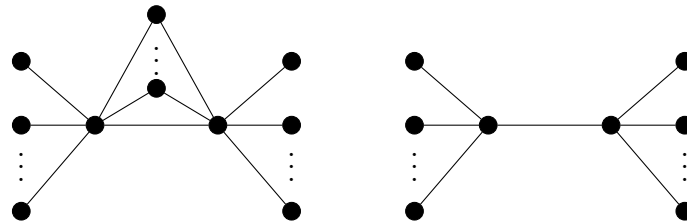


Figure 7.4: Eccentric graphs of subtrees induced by diametrical paths.

The following result shows that the graphs shown in Figure 7.4 are the building blocks for the eccentric graph of a tree. First, recall that the *union* of two graphs G_1 and G_2 , denoted $G_1 \cup G_2$, is the simple graph whose vertex set and edge set are formed by taking the union of the vertex sets of G_1 and G_2 and the edge sets of G_1 and G_2 , respectively.

Theorem 7.3 ([5, Theorem 1]). *Let Q_1, \dots, Q_k be diametrical paths in T with starting point v_0^1, \dots, v_0^k and ending point v_n^1, \dots, v_n^k , respectively. Let T_1, \dots, T_k be induced trees from Q_1, \dots, Q_k , respectively. Then, $Ec(T) = \cup_{i=1}^k Ec(T_i)$.*

Proof. A vertex of T either lies in some diametrical path or lies on a stem in each of the induced trees T_i 's. Thus,

$$V(T) = \cup_{i=1}^k V(T_i).$$

For $i \in [k]$, let e be an edge in the eccentric graph $Ec(T_i)$. As Q_i is the unique diametrical path in T_i , it follows that one of the endpoints of e is either v_0^i or v_n^i , assume that $e = vv_n^i$. Thus, $e_{T_i}(v) = d_{T_i}(v, v_n^i) = d_T(v, v_n^i) = e_T(v)$. Thus, $Ec(T_i)$ is a subgraph of $Ec(T)$.

Now, let $v \sim_{Ec(T)} w$ which implies that one of v or w (say v) is an endpoint of a diametrical path say Q_j ($1 \leq j \leq k$) in T . It is enough to show that v and w both lie on the same tree T_s for some $s \in [k]$. If $w \notin Ec(T_j)$, eccentric graph of the tree induced from Q_j , then w lies on a stem at some leaf z in T . In that case, the path joining from v to z is a diametrical path and the tree induced by this diametrical path T_s contains both v and w . \square

The following example illustrates Theorem 7.3.

Example 7.4. Let T be the tree shown in Figure 7.1. The eccentric graph of T (see Figure 7.5) is the union of the eccentric graphs (shown in Figure 7.3) of the subtrees (shown in Figure 7.2) induced from the three diametrical paths of T .

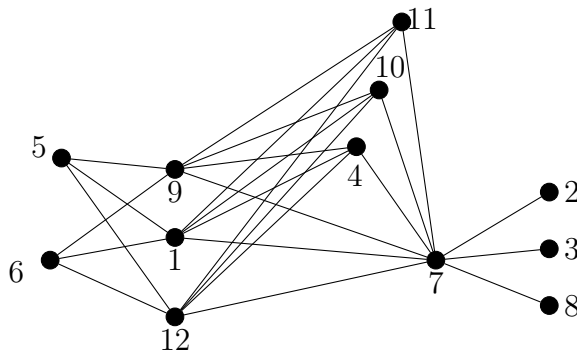


Figure 7.5: Eccentric graph of the tree in Figure 7.1 which is the union of the graphs in Figure 7.3.

Proposition 7.5. *Let T be a tree. There does not exist $v_1, v_2, v_3 \in V(T)$ such that $v_1 \sim_{Ec(T)} v_2$, $v_2 \sim_{Ec(T)} v_3$ and $e_T(v_1) < e_T(v_2) < e_T(v_3)$.*

Proof. On the contrary, assume that such $v_1, v_2, v_3 \in V(T)$ exist. Then $d_T(v_1, v_2) = \min\{e_T(v_1), e_T(v_2)\} = e_T(v_1)$, i.e., v_2 is eccentric to v_1 . Therefore, v_2 is an endpoint of a diametrical path. Again, $d_T(v_2, v_3) = \min\{e_T(v_2), e_T(v_3)\} = e_T(v_2)$, which implies that the path from v_2 to v_3 is a diametrical path and therefore $e_T(v_2) = e_T(v_3)$, a contradiction. \square

Remark 7.6. The essence of Proposition 7.5 can be summarized by saying that the eccentricity of a vertex $v \in V(T)$ is either the smallest or the largest among the eccentricities of its neighbours in the eccentric graph of T .

7.2 Eccentric girth of a tree

In this section, we will determine the eccentric girth of a tree and its potential values. In addition, we will classify the instances in which these possible values of the eccentric girth can be achieved. It is well-known that two paths of maximum length must pass through a common point. Thus, it is evident that two diametrical paths in a tree must intersect at vertices. But this is not true for graphs that are not trees; the graph in Figure 7.6 has two diametrical paths (dashed) but they do not intersect.

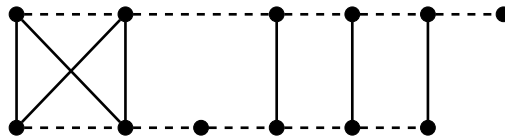


Figure 7.6: A graph having two non-intersecting diametrical paths

Now, we will present the main result of this section which classifies the eccentric girth of a tree.

Theorem 7.7 ([5, Theorem 3]). *Let T be a tree. Then the eccentric girth of T is either zero, three, or four. Moreover,*

$$g(\text{Ec}(T)) = \begin{cases} 3 & \text{if the diameter of } T \text{ is even,} \\ 0 & \text{if the diameter of } T \text{ is odd with unique diametrical path,} \\ 4 & \text{otherwise.} \end{cases}$$

Corollary 7.8. *The only trees T which satisfy $\text{Ec}(T) = T$ are P_2 and P_4 .*

Proof. The proof is divided into the following cases depending on the parity of the diameter of T .

First, let the diameter of T be even and $P = v_0 v_1 \dots v_k v_{k+1} \dots v_{2k}$ be a diametrical path. Note that $e(v_0) = 2k = e(v_{2k})$ and $d(v_0, v_{2k}) = 2k$, therefore $v_0 \sim_{\text{Ec}(T)} v_{2k}$. If $e(v_k) > k$, then one of $e(v_0)$ or $e(v_{2k})$ will be greater than $2k$, which is not possible. Also, $d(v_0, v_k) = k = d(v_k, v_{2k})$, therefore $e(v_k) = k$ and $v_k \sim_{\text{Ec}(T)} v_0$, $v_k \sim_{\text{Ec}(T)} v_{2k}$. Thus, v_0, v_k , and v_{2k} form a triangle in $\text{Ec}(T)$.

Second, If the diameter of T is odd and $P = v_0 v_1 \dots v_k v_{k+1} \dots v_{2k+1}$ is the unique diametrical path in T . It is sufficient to show that for any vertex $i \in V(T)$ exactly one of v_0 or v_{2k+1} is eccentric to i and no other vertex is eccentric to i . Note that, in a tree, if a vertex j is eccentric to some vertex, then j must be a pendant vertex.

Let $i \in V(P)$, if possible, there exists a vertex $j \in V(T)$ other than v_0 and v_{2k+1} which is eccentric to i , that is, $d(i, j) = e(i)$, then j is a leaf of a branch emerging from some vertex $p \in V(P)$. Assume that p is on the left of i in P , then $d(i, j) \geq d(i, v_0)$, which implies $d(v_{2k+1}, j) = d(v_{2k+1}, i) + d(i, j) \geq d(v_{2k+1}, i) + d(i, v_0) = 2k + 1$, which contradicts the fact that P is the only diametrical path. A similar argument can be given when p is on the right of i .

Now suppose that $i \in V(T) \setminus V(P)$ lies on some branch emerging from a vertex $i' \in V(P)$. Again let there exists $j \in V(T)$ other than v_0 and v_{2k+1} which is eccentric to i . Note that j cannot lie on the same branch; otherwise, the eccentricity of one of v_0 or v_{2k+1} will increase. Thus, j must be eccentric to i' which cannot happen as proved in the preceding paragraph. Moreover, because of odd diameter, exactly one of v_0 or v_{2k+1} can be eccentric to i . For illustration, $Ec(T)$ in this scenario is shown in Figure 7.7.

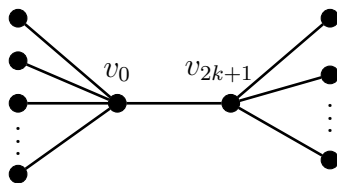


Figure 7.7: Eccentric graph of a tree (of odd diameter) with unique diametrical path.

Third, let the diameter of T be odd and $P = v_0 v_1 \dots v_k v_{k+1} \dots v_{2k+1}$, $P' = w_0 w_1 \dots w_k w_{k+1} \dots w_{2k+1}$ be two diametrical paths in T . As mentioned at the start of Section 7.2, they must intersect. Therefore, it is reasonable to assume that P and P' have one common endpoint say $v_0 = w_0$, otherwise one of the paths joining from v_0 to w_0 or w_{2k+1} (say w_{2k+1}) is a diametrical path and we can create two such diametrical paths by replacing P' with the diametrical path from v_0 to w_{2k+1} . Hence, $(v_0, v_{2k+1}, v_1, w_{2k+1})$ forms a 4-cycle in $Ec(T)$. Now, if there is a triangle (z_1, z_2, z_3) in $Ec(T)$ and $e(z_1) \leq e(z_2) \leq e(z_3)$. Without loss of generality, assume that z_1 is a vertex on some branch emerging from w_p , $1 \leq p \leq k$ (Note that z_1 can be w_0). If z is any vertex eccentric to z_1 , then z must be a vertex on some branch emerging from w_i , for some $k + 1 \leq i \leq 2k$; if not, then $d(z, w_{2k+1})$ is greater than the diameter $2k + 1$. Now z_2 being eccentric to z_1 must lie on some branch emerging from w_q , $k + 1 \leq q \leq 2k$ (Note that z_2 can be w_{2k+1}). Again, as z_3 is eccentric to z_2 , z_3 is a vertex on some branch emerging from w_r , $1 \leq r \leq k$, but then z_3 cannot be eccentric to z_1 . Hence $Ec(T)$ cannot have a triangle. \square

Chapter 8

Eccentric graph of Cartesian products

In this chapter, analogous to Theorem 7.7, we will see the possible values for the eccentric girth of Cartesian product of trees. We will discuss the structure of the eccentric graph of Cartesian product of two path graphs and two cycle graphs. We will also provide a necessary and sufficient condition for the invertibility of the eccentricity matrix of Cartesian product of trees.

8.1 Cartesian product of graphs

In this section, we will examine some properties of the eccentric graph of Cartesian product of general graphs and calculate the eccentric girth of Cartesian product of trees in Section 8.2. Recall Cartesian product of two graphs defined in Definition 2.1. The following equations

$$d_{G_1 \square G_2}((u_1, u_2), (v_1, v_2)) = d_{G_1}(u_1, v_1) + d_{G_2}(u_2, v_2), \quad (8.1.1)$$

and

$$e_{G_1 \square G_2}((u_1, u_2)) = e_{G_1}(u_1) + e_{G_2}(u_2) \quad (8.1.2)$$

follow directly from Definition 2.1 and can be generalised to Cartesian product of k graphs G_1, \dots, G_k denoted as $G_1 \square \dots \square G_k$.

Definition 8.1. Let G_1 and G_2 be two simple connected graphs. The *Kronecker product* of G_1 and G_2 denoted as $G_1 \times G_2$ is a graph with vertex set $V(G_1) \times V(G_2)$, and two vertices (u_1, u_2) and (v_1, v_2) are adjacent if and only if $u_1 \sim_{G_1} v_1$ and $u_2 \sim_{G_2} v_2$.

Lemma 8.2. *Let G_1, \dots, G_k be simple connected graphs and $G = G_1 \square \dots \square G_k$ be their Cartesian product. Let $u = (u_1, \dots, u_k)$, $v = (v_1, \dots, v_k) \in V(G)$ where $u_i, v_i \in V(G_i)$ for $i \in [k]$. Then, v is eccentric to u if and only if v_i is eccentric to u_i for all $i \in [k]$.*

Proof. Let v be eccentric to u , i.e., $d_G(u, v) = \max\{d_G(u, x) : x \in V(G)\}$. Then by (8.1.1) we can express this as:

$$\sum_{i=1}^k d_{G_i}(u_i, v_i) = \max \left\{ \sum_{i=1}^k d_{G_i}(u_i, x_i) : x_i \in V(G_i) \right\}.$$

Which holds only if

$$d_{G_i}(u_i, v_i) = \max\{d_{G_i}(u_i, x_i) : x_i \in V(G_i)\} \text{ for all } i \in [k].$$

Thus, v_i is eccentric to u_i for all $i \in [k]$. Furthermore, we can reverse the steps of this argument to establish the converse part. \square

Remark 8.3. Note that if $(u_1, \dots, u_k) \sim_{Ec(G_1 \square \dots \square G_k)} (v_1, \dots, v_k)$, then $u_i \neq v_i$ for all $i \in [k]$. Also, it is clear from Lemma 8.2 that if $u \sim_{Ec(G)} v$, then $u_i \sim_{Ec(G_i)} v_i$ for all $i \in [k]$, but the converse is not true. For example, $1 \sim_{Ec(P_4)} 3$ and $2 \sim_{Ec(P_4)} 4$, but $(1, 2) \not\sim_{Ec(P_4 \square P_4)} (3, 4)$ (see Figure 8.1).

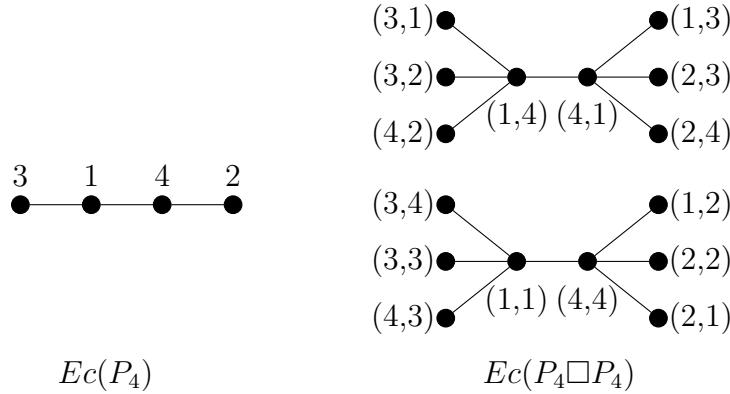


Figure 8.1: Eccentric graphs of naturally labelled P_4 and $P_4 \square P_4$.

Corollary 8.4. *Let G_1 and G_2 be simple connected graphs such that all the vertices in both G_1 and G_2 have the same eccentricities. Then $Ec(G_1 \square G_2)$ is isomorphic to $Ec(G_1) \times Ec(G_2)$, the Kronecker product of $Ec(G_1)$ and $Ec(G_2)$.*

Lemma 8.5. *Let G_1, \dots, G_k be simple connected graphs and $G = G_1 \square \dots \square G_k$. If for some $s, t \in [k]$ there exists $u_s, v_s, w_s \in V(G_s)$ such that $u_s \sim_{Ec(G_s)} v_s$, $v_s \sim_{Ec(G_s)} w_s$ and*

$e_{G_s}(v_s) \geq \max\{e_{G_s}(u_s), e_{G_s}(w_s)\}$, and there exists $u_t, v_t, w_t \in V(G_t)$ such that $u_t \sim_{Ec(G_t)} v_t$, $v_t \sim_{Ec(G_t)} w_t$ and $e_{G_t}(v_t) \leq \min\{e_{G_t}(u_t), e_{G_t}(w_t)\}$, then there exists a 4-cycle in $Ec(G)$.

Proof. Without loss of generality, assume that $s = 1$ and $t = 2$ and for $i = 3, \dots, k$, let $\{u_i, v_i\}$ be an edge in $Ec(G_i)$ such that $e_{G_i}(u_i) \geq e_{G_i}(v_i)$, i.e., u_i is eccentric to v_i for $i = 3, \dots, k$. By the inequalities in the hypothesis, v_1 is eccentric to both u_1 and w_1 , u_2 is eccentric to v_2 and w_2 is eccentric to v_2 . Thus by Lemma 8.2, $a = (u_1, v_2, v_3, \dots, v_k)$, $b = (v_1, w_2, u_3, \dots, u_k)$, $c = (w_1, v_2, v_3, \dots, v_k)$ and $d = (v_1, u_2, u_3, \dots, u_k)$ form a 4-cycle in $Ec(G)$ (see Figure 8.2). \square

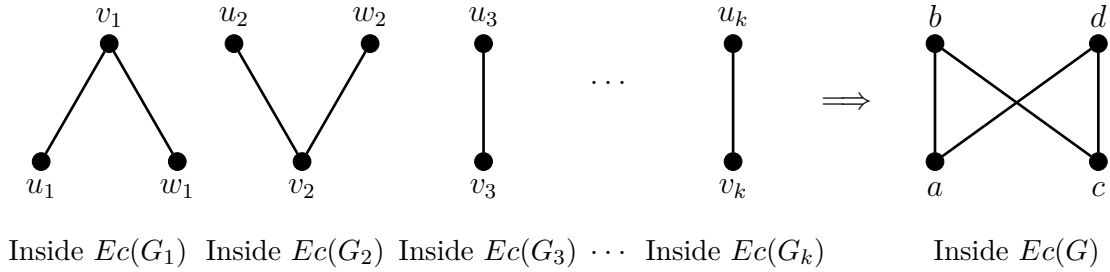


Figure 8.2: Formation of 4-cycle in $Ec(G)$.

We will now prove that there is a triangle in the eccentric graph of Cartesian product of k graphs if and only if there is a triangle in the eccentric graph of each of the individual graphs.

Theorem 8.6. *Let G_1, \dots, G_k be simple connected graphs and G be their Cartesian product. Then the girth of $Ec(G)$ is 3 if and only if the girth of $Ec(G_i)$ is 3 for all $i \in [k]$.*

Proof. First, suppose that there is a triangle in $Ec(G_i)$ for all $i \in [k]$. Let $\{u_i, v_i, w_i\}$ be a triangle in $Ec(G_i)$ such that $e_{G_i}(u_i) \leq e_{G_i}(v_i) \leq e_{G_i}(w_i)$ for all $i \in [k]$. In other words, v_i is eccentric to u_i and w_i is eccentric to both u_i and v_i for all i . Therefore by Lemma 8.2, $(u_1, \dots, u_k), (v_1, \dots, v_k)$ and (w_1, \dots, w_k) form a triangle in $Ec(G)$. Conversely, suppose $(u_1, \dots, u_k), (v_1, \dots, v_k)$ and (w_1, \dots, w_k) form a triangle in $Ec(G)$, then again by Lemma 8.2, $\{u_i, v_i, w_i\}$ forms a triangle in $Ec(G_i)$ for all $i \in [k]$. \square

Theorem 8.7. *Let G_1, \dots, G_k be simple connected graphs such that the eccentric girths of at least two of them are greater than two. Let $G = G_1 \square \dots \square G_k$, then the girth of $Ec(G)$ is four except when the girth of $Ec(G_i)$ is exactly three for all $i \in [k]$.*

Proof. Suppose that $Ec(G_1)$ and $Ec(G_2)$ have girths greater than two and C_1 and C_2 are cycles in $Ec(G_1)$ and $Ec(G_2)$, respectively. Let v_1 be a vertex of the largest eccentricity

on C_1 and v_2 be a vertex of the smallest eccentricity on C_2 . In particular, if u_1, w_1 are neighbours of v_1 in C_1 and u_2, w_2 are neighbours of v_2 in C_2 , then

$$e_{G_1}(v_1) \geq \max\{e_{G_1}(u_1), e_{G_1}(w_1)\} \text{ and } e_{G_2}(v_2) \leq \min\{e_{G_2}(u_2), e_{G_2}(w_2)\}.$$

Hence, the result follows from Theorem 8.6 and Lemma 8.5. \square

Based on the above-stated theorems, it can be concluded that the eccentric girth of Cartesian product of graphs in which at least two have non-zero eccentric girth is either three or four.

8.2 Eccentric girth of Cartesian product of trees

Recall that in Section 7.2, we observed that the eccentric girth of a tree could either be zero, three or four. Now, we will prove that for Cartesian product of trees, it can also be six in addition to the above values. We will now characterize completely the eccentric girth of Cartesian product of trees and present an analogous result to Theorem 7.7.

Theorem 8.8 ([5, Theorem 6]). *Let T_1, \dots, T_k be trees and $G = T_1 \square \dots \square T_k$. Then,*

$$g(Ec(G)) = \begin{cases} 0 & \text{if the girth of } Ec(T_i) = 0 \text{ for all } i \in [k], \\ 3 & \text{if the girth of } Ec(T_i) = 3 \text{ for all } i \in [k], \\ 6 & \text{if } G = T_1 \square P_2 \square \dots \square P_2 \text{ and } Ec(T_1) \text{ is } C_4\text{-free with girth three,} \\ 4 & \text{otherwise.} \end{cases}$$

Proof. First, assume that T_1, \dots, T_k are trees with eccentric girth 0. By Theorem 7.7, there exists a unique diametrical path of odd length in T_i with endpoints u_i and v_i for all $i \in [k]$. Consider the set of vertices $S = \{(x_1, \dots, x_k) : x_i \in \{u_i, v_i\}, i \in [k]\}$ in $V(G)$. Any vertex $u \in V(G) \setminus S$ cannot be eccentric to anyone in G and the vertices eccentric to u lie in S . Moreover, exactly one vertex in S is eccentric to u because each of the T_i 's has a unique diametrical path. Consequently, u is adjacent to exactly one vertex in the eccentric graph $Ec(G)$. Also, note that any two vertices in S are adjacent if and only if they differ at each component, therefore $Ec(G)$ is an acyclic graph with 2^{k-1} connected components.

Second, only one of T_i 's say T_1 has non-zero eccentric girth. Now there are two cases, one is when at least one of T_i , $i = 2, \dots, k$, is not P_2 and the other is $T_i = P_2$ for all $i = 2, \dots, k$.

If suppose that $T_2 \neq P_2$, and since $Ec(T_2)$ has girth zero, by Theorem 7.7 there exists a unique diametrical path with endpoints u_2 and v_2 and $u_2 \sim_{Ec(T_2)} v_2$. Now, as $T_2 \neq P_2$ and $Ec(T_2)$ is connected [34], there is a vertex w_2 , adjacent to either u_2 or v_2 , say $v_2 \sim_{Ec(T_2)} w_2$. Clearly, $e_{T_2}(v_2) \geq \max\{e_{T_2}(u_2), e_{T_2}(w_2)\}$. Additionally, as the girth of $Ec(T_1)$ is nonzero (it is either 3 or 4 by Theorem 7.7), it is possible to choose $u_1, v_1, w_1 \in V(T_1)$ such that $u_1 \sim_{Ec(T_1)} v_1$, $v_1 \sim_{Ec(T_1)} w_1$ and $e_{T_1}(v_1) \leq \min\{e_{T_1}(u_1), e_{T_1}(w_1)\}$. Therefore by Lemma 8.5 and Theorem 8.6, the girth of $Ec(G)$ is four.

Let $T_i = P_2$ with endpoints $\{u_i, v_i\}$ for $i = 2, \dots, k$. If $Ec(T_1)$ contains a 4-cycle, $\{u_1, v_1, w_1, x_1\}$, then $\{(u_1, \dots, u_k), (v_1, \dots, v_k), (w_1, u_2, \dots, u_k), (x_1, v_2, \dots, v_k)\}$ forms a 4-cycle in $Ec(G)$. Therefore the girth of $Ec(G)$ is four as $Ec(G)$ can not contain any odd cycle (because $T_2 = P_2$). If $Ec(T_1)$ doesn't contain a 4-cycle, then by Theorem 7.7, girth of $Ec(T_1)$ is 3. Let $\{u_1, v_1, w_1\}$ be a 3-cycle in $Ec(T_1)$ then $\{(u_1, \dots, u_k), (v_1, \dots, v_k), (w_1, u_2, \dots, u_k), (u_1, v_2, \dots, v_k), (v_1, u_2, \dots, u_k), (w_1, v_2, \dots, v_k)\}$ forms a 6-cycle in $Ec(G)$. If $Ec(G)$ contains a 4-cycle, then so is $Ec(T_1)$ as $T_i = P_2$ for all $i = 2, \dots, k$.

Finally, the rest of the cases follow from Theorem 8.6 and Theorem 8.7. \square

As an illustration, we will now discuss the structure of the eccentric graph of Cartesian product of two path graphs and two cycle graphs. We will also discuss about their eccentric girth.

8.3 Cartesian product of two path graphs

Let the vertices of the grid graph $P_m \square P_n$ be $\{(i, j) : 1 \leq i \leq m, 1 \leq j \leq n\}$. In this chapter, we label a vertex (i, j) by $(i-1)n+j$. Figure 8.3 shows the mentioned labelling for the grid graph $P_3 \square P_5$.

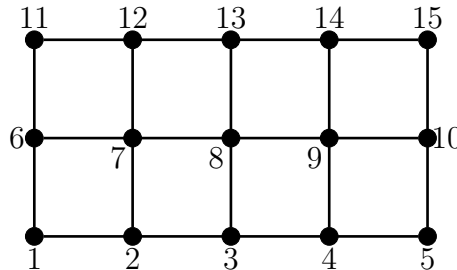


Figure 8.3: The grid graph, $P_3 \square P_5$.

Let $G = P_m \square P_n$ be a grid. Then the eccentricity of each vertex is given by

$$e((i, j)) = \begin{cases} d((i, j), (m, n)) & \text{if } 1 \leq i \leq \lceil \frac{m}{2} \rceil, 1 \leq j \leq \lceil \frac{n}{2} \rceil, \\ d((i, j), (1, 1)) & \text{if } \lfloor \frac{m}{2} \rfloor < i \leq m, \lfloor \frac{n}{2} \rfloor < j \leq n, \\ d((i, j), (m, 1)) & \text{if } 1 \leq i \leq \lceil \frac{m}{2} \rceil, \lfloor \frac{n}{2} \rfloor < j \leq n, \\ d((i, j), (1, n)) & \text{if } \lfloor \frac{m}{2} \rfloor < i \leq m, 1 \leq j \leq \lceil \frac{n}{2} \rceil. \end{cases}$$

Note that $(1, 1)$, $(1, n)$, $(m, 1)$ and (m, n) have the maximum eccentricity, which is $m + n$. Therefore,

$$(i, j) \sim_{Ec(G)} \begin{cases} (m, n) & \text{if } 1 \leq i \leq \lceil \frac{m}{2} \rceil, 1 \leq j \leq \lceil \frac{n}{2} \rceil, \\ (1, 1) & \text{if } \lfloor \frac{m}{2} \rfloor < i \leq m, \lfloor \frac{n}{2} \rfloor < j \leq n, \\ (m, 1) & \text{if } 1 \leq i \leq \lceil \frac{m}{2} \rceil, \lfloor \frac{n}{2} \rfloor < j \leq n, \\ (1, n) & \text{if } \lfloor \frac{m}{2} \rfloor < i \leq m, 1 \leq j \leq \lceil \frac{n}{2} \rceil. \end{cases}$$

From the above adjacency relations, it is clear that the eccentric graph of $P_m \square P_n$ has a specific structure depending on the parity of m and n . Example for each of the three cases, depending on whether both m and n are even, both are odd, or one is even and the other is odd, are presented in Figure 8.4. Further, note that the eccentric girth of $P_m \square P_n$ is zero if both m and n are even, four if exactly one of m and n is even and greater than two, six if exactly one of m and n is two and the other is odd, and three if both m and n are odd.

Moreover, if n is odd and $m > 2$ is even, then

$$\left((1, 1) \left(\frac{n+1}{2}, m-1 \right) (n, 1) \left(\frac{n+1}{2}, m \right) \right)$$

form a 4-cycle in $Ec(P_n \square P_m)$. If n is odd and $m = 2$, then

$$\left((1, 1) \left(\frac{n+1}{2}, 2 \right) (n, 1) (1, 2) \left(\frac{n+1}{2}, 1 \right) (n, 2) \right)$$

form a 6-cycle in $Ec(P_n \square P_m)$. If both n and m are odd, then

$$\left((1, 1) \left(\frac{n+1}{2}, \frac{m+1}{2} \right) (n, m) \right)$$

form a 3-cycle in $Ec(P_n \square P_m)$.

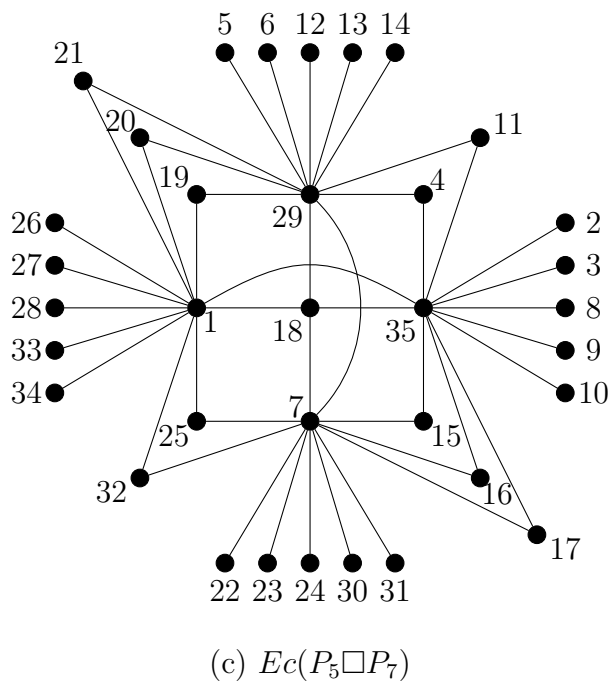
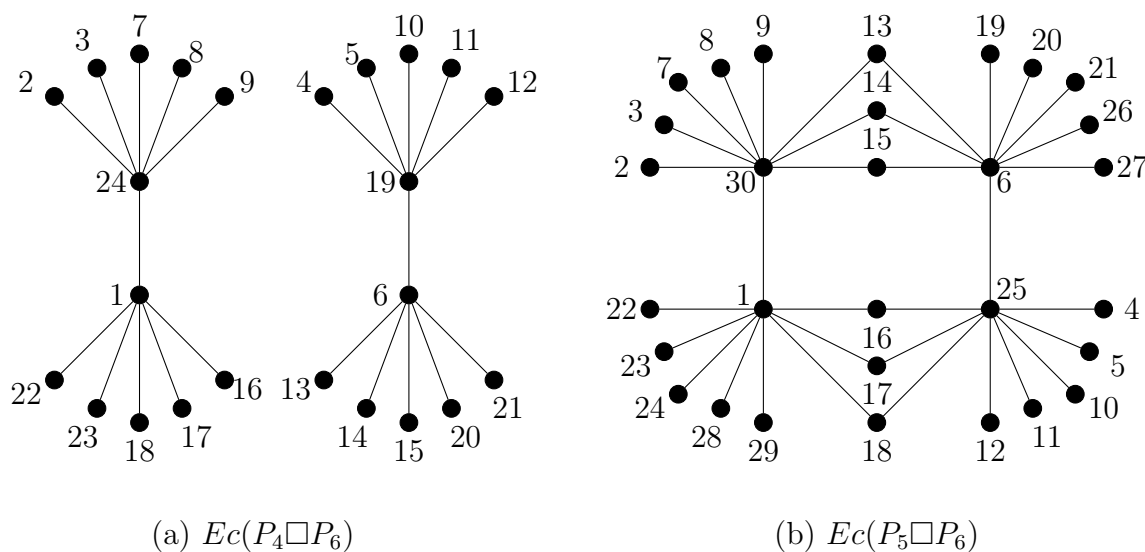


Figure 8.4: Eccentric graphs of different grid graphs.

8.4 Cartesian product of two cycle graphs

In this section, we first give the structure of the eccentric graph of Cartesian product of two cycles and then we discuss about their girth.

Theorem 8.9 ([5, Section 4.3]). *Let C_n and C_m be the cycle graphs on n and m vertices,*

respectively. Then,

$$Ec(C_n \square C_m) = \begin{cases} \frac{nm}{2} \text{ copies of } K_2 & \text{if both } n \text{ and } m \text{ are even,} \\ \frac{n}{2} \text{ cycles of length } 2m & \text{if } n \text{ is even and } m \text{ is odd,} \\ C_n \times C_m & \text{if both } n \text{ and } m \text{ are odd.} \end{cases}$$

Proof. As discussed in Section 2.5, $Ec(C_n)$ is isomorphic to the $\frac{n}{2}$ copies of K_2 for an even n . Thus when n and m both are even, each vertex in $Ec(C_n \square C_m)$ has degree 1. In other words, $Ec(C_n \square C_m)$ is isomorphic to a graph containing $\frac{nm}{2}$ copies of K_2 .

For even n and odd m , each vertex in $Ec(C_n)$ and $Ec(C_m)$ has degree 1 and 2 respectively. Therefore, $Ec(C_n \square C_m)$ is a 2-regular graph. Consequently, $Ec(C_n \square C_m)$ is either a cycle or a union of cycles. Moreover, $Ec(C_n \square C_m)$ consists $\frac{n}{2}$ cycles of length $2m$, namely

$$\left((i, 1) \left(\frac{n}{2} + i, 2 \right) \dots (i, m) \left(\frac{n}{2} + i, 1 \right) (i, 2) \dots \left(\frac{n}{2} + i, m \right) \right)$$

for $i \in \left[\frac{n}{2} \right]$.

The final case follows from Proposition 2.18 and Corollary 8.4. \square

Figure 8.5 shows the eccentric graph of Cartesian product of C_4 and C_3 .

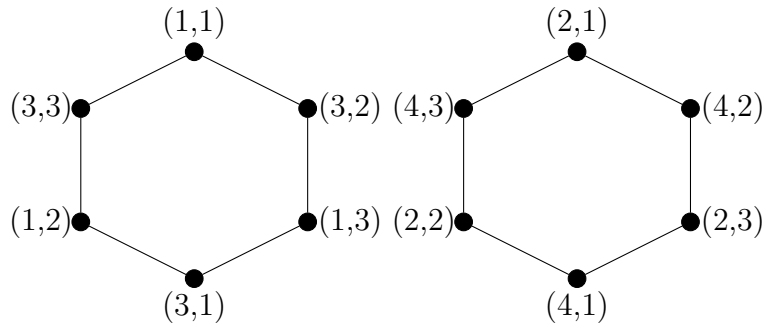


Figure 8.5: Eccentric graph of Cartesian product of C_4 and C_3 .

The eccentric graph of $C_3 \square C_3$ is shown in Figure 8.6 and its girth is 3 by Theorem 8.6, which can be seen in the figure as well. But when both n and m are odd but one of them is not equals to 3, it follows from Theorem 8.7 that the eccentric girth of $C_n \square C_m$ is four and

$$\left(\left(1, \frac{m+3}{2} \right) \left(\frac{n+1}{2}, 1 \right) \left(1, \frac{m+1}{2} \right) \left(\frac{n+3}{2}, 1 \right) \right)$$

form a 4-cycle in $Ec(C_n \square C_m)$.

The following statement summarizes the above discussion: The eccentric girth of Cartesian product of two cycle graphs is even except when both cycles are triangles.

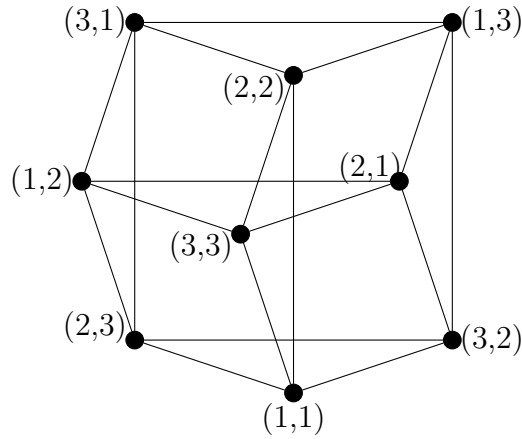


Figure 8.6: Eccentric graph of Cartesian product of a 3-cycle with itself.

Moreover,

$$g(\text{Ec}(C_n \square C_m)) = \begin{cases} 0 & \text{if both } n \text{ and } m \text{ are even,} \\ 3 & \text{if } n = m = 3, \\ 2m & \text{if } n \text{ is even and } m \text{ is odd,} \\ 4 & \text{otherwise.} \end{cases}$$

We will end this section with the following observation.

Proposition 8.10. *For odd n , $\text{Ec}(C_n \square C_n)$ is isomorphic to $C_n \square C_n$.*

Proof. By Corollary 8.4, it is enough to show that $C_n \square C_n$ is isomorphic to $C_n \times C_n$ for an odd n . We assume the natural labelling on the vertices of C_n . Now, we define an isomorphism f from $C_n \square C_n$ to $C_n \times C_n$ as follows

$$\begin{aligned} f((1, 1)) &= (1, 1), \\ f((i, 1)) &= (n + 2 - i, n + 2 - i) \text{ for } i = 2, \dots, n, \\ f((i, j)) &= [f((i, 1)) + (j - 1, 1 - j)] \pmod{n}. \end{aligned}$$

We will write 0 as n in the computation of f . To see f is a bijection, first note that $f((i, 1)) \neq f((j, 1))$ for $i \neq j$. Now assume that $(i, j) \neq (k, l)$, this happens in either of three cases, (a) $i \neq k$ and $j = l$, (b) $i = k$ and $j \neq l$, or (c) $i \neq k$ and $j \neq l$.

Consider the first case $i \neq k$ and $j = l$ and let $f((i, 1)) = (s, s)$ and $f((k, 1)) = (t, t)$, clearly $s \neq t$. Now, if $f((i, j)) = f((k, l))$, then $s + j - 1 \equiv t + j - 1 \pmod{n}$, which leads to $s = t$, a contradiction. Therefore $f((i, j)) \neq f((k, l))$. Similarly, we can show for the second case. Now consider the third case $i \neq k$ and $j \neq l$, and again let $f((i, 1)) = (s, s)$ and $f((k, 1)) = (t, t)$, clearly $s \neq t$. Now, if $f((i, j)) = f((k, l))$, then $s + j - 1 \equiv t + l - 1 \pmod{n}$ and $s + 1 - j \equiv t + 1 - l \pmod{n}$, compatibility with addition

of congruence leads to again $s = t$ (because n is odd), a contradiction. Therefore, f is a bijection.

Now, let $(i, j) \in V(C_n \square C_n)$ and $f((i, j)) = (s, t)$. Then $f((i \pm 1, j)) = (s \pm 1, t \pm 1)(\text{mod } n)$ and $f((i, j \pm 1)) = (s \pm 1, t \mp 1)(\text{mod } n)$. This proves that f preserves the adjacency. \square

8.5 Invertibility of eccentricity matrix of Cartesian product of trees

In this section, we will focus on the invertibility of the eccentricity matrix for Cartesian product of trees. First, recall the definition of the *Kronecker product* of two matrices defined in Definition 2.12.

Lemma 8.11. *Let T_1 be a tree which is not a star or P_4 . Then the eccentricity matrix of $T_1 \square \underbrace{P_2 \square \cdots \square P_2}_{k-1}$ is not invertible.*

Proof. Let $G = T_1 \square P_2 \square \cdots \square P_2$ and the i^{th} graph in this product be the path P_2 with endpoints $\{u_i, v_i\}$ for $i = 2, \dots, k$. Note that a vertex (x_1, x_2, \dots, x_k) is adjacent to (u_1, u_2, \dots, u_k) in $Ec(G)$ if and only if $x_i = v_i$ for $i = 2, \dots, k$ and either x_1 is eccentric to u_1 in T_1 or u_1 is eccentric to x_1 in T_1 . In other words, adjacency with (u_1, u_2, \dots, u_k) in $Ec(G)$ solely depends on the adjacency of u_1 in $Ec(T_1)$. Now we consider three cases.

Case 1: $diam(T_1) = 3$.

Let $P = a_1 b_1 c_1 d_1$ be a diametrical path in T_1 . As $T_1 \neq P_4$, there must be a leaf vertex, say e_1 , adjacent to either b_1 or c_1 . Let us assume that e_1 is adjacent to b_1 . Now we claim that $N_{Ec(G)}((a_1, u_2, \dots, u_k)) = N_{Ec(G)}((e_1, u_2, \dots, u_k))$. If a vertex f_1 is eccentric to a_1 then f_1 is also eccentric to e_1 because $d_{T_1}(a_1, f_1) = d_{T_1}(e_1, f_1)$, and if a_1 is eccentric to some vertex f_1 then so is e_1 because $d_{T_1}(a_1, f_1) = d_{T_1}(e_1, f_1)$. This proves our claim and hence the rows corresponding to these two vertices in \mathcal{E}_G are exactly the same and therefore $\det(\mathcal{E}_G) = 0$.

Case 2: $diam(T_1) = 4$.

Let $P = a_1 b_1 c_1 d_1 e_1$ be a diametrical path in T_1 . Let $\{b_1, d_1, p_1, \dots, p_\ell\}$ be the set of neighbours of c_1 . Note that if a vertex x is eccentric to a neighbour of c_1 then it is also eccentric to c_1 . Further, note that none of c_1 or its neighbours can be eccentric to any vertex in T_1 . Therefore, the row corresponding to (c_1, u_2, \dots, u_k) in the matrix \mathcal{E}_G is a constant multiple of the sum of the rows corresponding to $(b_1, u_2, \dots, u_k), (d_1, u_2, \dots, u_k), (p_1, u_2, \dots, u_k), \dots, (p_\ell, u_2, \dots, u_k)$.

Case 3: $\text{diam}(T_1) > 4$.

Let $P = a_1 b_1 c_1 d_1 \dots z_1$ be a diametrical path in T_1 . A vertex eccentric to b_1 in T_1 is also eccentric to c_1 in T_1 and vice versa. Also, b_1 and c_1 cannot be eccentric to any vertex in T_1 as they are not leaves. Therefore, b_1 and c_1 have same neighbourhood in $Ec(T_1)$. As a result, the rows corresponding to (b_1, u_2, \dots, u_k) and (c_1, u_2, \dots, u_k) in \mathcal{E}_G are constant multiple of each other and hence $\det(\mathcal{E}_G) = 0$. \square

Now, we will present the main result of this section.

Theorem 8.12 ([5, Theorem 7]). *Let T_1, \dots, T_k be trees and $G (= T_1 \square \dots \square T_k)$ be their Cartesian product. Then the eccentricity matrix of G , \mathcal{E}_G , is invertible if and only if one of them is either a star or a P_4 , and the rest are P_2 's.*

Proof. Let T_1, \dots, T_k be trees with at least two vertices and $G = T_1 \square \dots \square T_k$. Assume that T_1 is a star on $n + 1$ vertices and $T_2 = \dots = T_k = P_2$. Then the eccentricity matrix of G is

$$\mathcal{E}_G = \begin{pmatrix} 0 & k & k & \dots & k \\ k & 0 & k+1 & \dots & k+1 \\ \vdots & \vdots & \ddots & & \\ k & k+1 & \dots & 0 & k+1 \\ k & k+1 & \dots & k+1 & 0 \end{pmatrix} \otimes J_{2^{k-1}},$$

where, J_s is a $s \times s$ antidiagonal matrix with all antidiagonal entries as 1.

Note that $\det J_{2^{k-1}} \neq 0$ and

$$\det \begin{pmatrix} 0 & k & k & \dots & k \\ k & 0 & k+1 & \dots & k+1 \\ \vdots & \vdots & \ddots & & \\ k & k+1 & \dots & 0 & k+1 \\ k & k+1 & \dots & k+1 & 0 \end{pmatrix} = (-1)^n n k^2 (k+1)^{n-1}.$$

Therefore $\det \mathcal{E}_G \neq 0$.

Now if $T_1 = P_4$, then the eccentricity matrix of G is

$$\mathcal{E}_G = \begin{pmatrix} 0 & 0 & k+1 & k+2 \\ 0 & 0 & 0 & k+1 \\ k+1 & 0 & 0 & 0 \\ k+2 & k+1 & 0 & 0 \end{pmatrix} \otimes J_{2^{k-1}},$$

Again, $\det \mathcal{E}_G \neq 0$, as

$$\det \begin{pmatrix} 0 & 0 & k+1 & k+2 \\ 0 & 0 & 0 & k+1 \\ k+1 & 0 & 0 & 0 \\ k+2 & k+1 & 0 & 0 \end{pmatrix} = (k+1)^4.$$

For the converse part, let T_1 be neither a star nor P_4 . Thus the diameter of $T_1 > 2$ and let $P = u_1 u_2 \dots u_s$ be a diametrical path in T_1 . If each of T_2, \dots, T_k contains only pendant vertices, then the conclusion follows from Lemma 8.11. Therefore, we can assume without loss of generality that T_2 has a non-pendant vertex v . Now we want to show that $\det \mathcal{E}_G$ is zero. This assertion holds if we can show in general $\det \mathcal{E}_K$ is zero, where K is Cartesian product of T_1 , T_2 and a simple connected graph H . Let $(u_i, v, x) \in V(K)$. Note that (u_i, v, x) cannot be farthest from (and hence, eccentric to) any vertex in K because v is a non-pendant. Consequently, only those vertices are adjacent to (u_i, v, x) (in $E_C(K)$) which are eccentric to (u_i, v, x) . Thus by Lemma 8.2,

$$N_{E_C(K)}(u_i, v, x) = \{(w_i, w, y) : w_i, w, y \text{ are eccentric to } u_i, v, x \text{ respectively}\}. \quad (8.5.1)$$

Now if any vertex is eccentric to u_1 in T_1 , then the same vertex is eccentric to u_2 as well in T_1 leading to

$$N_{E_C(K)}(u_1, v, x) = N_{E_C(K)}(u_2, v, x).$$

Thus, the row corresponding to (u_1, v, x) in \mathcal{E}_K is a constant multiple of that of (u_2, v, x) , proving the non-invertibility of \mathcal{E}_K . \square

Bibliography

- [1] Milton Abramowitz and Irene A Stegun. *Handbook of mathematical functions with formulas, graphs, and mathematical tables*, volume 55. US Government printing office, 1964.
- [2] Jin Akiyama, Kiyoshi Ando, and David Avis. Eccentric graphs. *Discrete Mathematics*, 56(1):1–6, 1985.
- [3] Anita Arora. The monopole-dimer model on high-dimensional cylindrical, toroidal, Möbius and Klein grids. *arXiv:2406.05750*, 2024.
- [4] Anita Arora and Arvind Ayyer. The monopole-dimer model on Cartesian products of plane graphs. *Combinatorial Theory*, 3(3), 2023.
- [5] Anita Arora and Rajiv Mishra. Eccentric graph of trees and their Cartesian products. *Discrete Mathematics*, 347(9):114062, 2024.
- [6] Arvind Ayyer. A statistical model of current loops and magnetic monopoles. *Math. Phys. Anal. Geom.*, 18(1):Art. 16, 19, 2015.
- [7] Arvind Ayyer. Squareness for the monopole-dimer model. *Ann. Comb.*, 24(2):237–255, 2020.
- [8] J. A. Bondy and U. S. R. Murty. *Graph theory*, volume 244 of *Graduate Texts in Mathematics*. Springer, New York, 2008.
- [9] J. G. Brankov and V. B. Priezhev. Critical free energy of a Möbius strip. *Nuclear Physics B*, 400(1):633–652, 1993.
- [10] A. Cayley. Sur les déterminants gauches. (suite du mémoire t. xxxii. p. 119). *Crelle's journal*, 1849(38):93–96, 1849.
- [11] Nishant Chandgotia, Scott Sheffield, and Catherine Wolfram. Large deviations for the 3D dimer model, 2023.

-
- [12] David Cimasoni and Nicolai Reshetikhin. Dimers on surface graphs and spin structures. II. *Communications in Mathematical Physics*, 281:445–468, 07 2008.
- [13] Michael E. Fisher. Statistical mechanics of dimers on a plane lattice. *Phys. Rev.*, 124:1664–1672, Dec 1961.
- [14] Michael E. Fisher and John Stephenson. Statistical mechanics of dimers on a plane lattice. II. Dimer correlations and monomers. *Phys. Rev.*, 132:1411–1431, Nov 1963.
- [15] I. S. Gradshteyn and I. M. Ryzhik. *Table of integrals, series, and products*. Academic Press Inc., San Diego, CA, sixth edition, 2000. Translated from the Russian, Translation edited and with a preface by Alan Jeffrey and Daniel Zwillinger.
- [16] J. M. Hammersley and V. V. Menon. A lower bound for the monomer-dimer problem. *J. Inst. Math. Appl.*, 6:341–364, 1970.
- [17] Ivailo Hartarsky, Lyuben Lichev, and Fabio Toninelli. Local dimer dynamics in higher dimensions, 2023.
- [18] Mark Jerrum. Two-dimensional monomer-dimer systems are computationally intractable. *Journal of Statistical Physics*, 48(1):121–134, 1987.
- [19] S Kaspar, B Gayathri, MP Kulandaivel, and N Shobhanadevi. Eccentric graphs of some particular classes of graphs. *International Journal of Pure and Applied Mathematics*, 119(16):145–152, 2018.
- [20] P. W. Kasteleyn. The statistics of dimers on a lattice: I. the number of dimer arrangements on a quadratic lattice. *Physica*, 27(12):1209–1225, 1961.
- [21] P. W. Kasteleyn. Dimer statistics and phase transitions. *Journal of Mathematical Physics*, 4(2):287–293, 1963.
- [22] P. W. Kasteleyn. Graph theory and crystal physics. *Graph theory and theoretical physics*, pages 43–110, 1967.
- [23] Richard Kenyon. Conformal invariance of loops in the double-dimer model. *Communications in Mathematical Physics*, 326, 05 2011.
- [24] Richard Kenyon and David Wilson. Double-dimer pairings and skew young diagrams. *Electronic Journal of Combinatorics*, 18, 07 2010.
- [25] W. T. Lu and F. Y. Wu. Dimer statistics on the Möbius strip and the Klein bottle. *Physics Letters A*, 259(2):108–114, 1999.

-
- [26] Iswar Mahato, R. Gurusamy, M. Rajesh Kannan, and S. Arockiaraj. On the spectral radius and the energy of eccentricity matrices of graphs. *Linear and Multilinear Algebra*, 71(1):5–15, 2023.
- [27] Iswar Mahato, R. Gurusamy, M. Rajesh Kannan, and S. Arockiaraj. Spectra of eccentricity matrices of graphs. *Discrete Applied Mathematics*, 285:252–260, 10 2020.
- [28] Iswar Mahato and M. Rajesh Kannan. On the eccentricity matrices of trees: Inertia and spectral symmetry. *Discrete Mathematics*, 345:113067, 11 2022.
- [29] Barry M. McCoy and Tai Tsun Wu. *The Two-Dimensional Ising Model*. Harvard University Press, Cambridge, MA and London, England, 1973.
- [30] Milan Randić. Dmax-matrix of dominant distances in a graph. *MATCH - Communications in Mathematical and in Computer Chemistry*, 70:221–238, 01 2013.
- [31] Milan Randić, Rok Orel, and Alexandru Balaban. D-max matrix invariants as graph descriptors. Graphs having the same Balaban index J. *MATCH - Communications in Mathematical and in Computer Chemistry*, 70, 01 2013.
- [32] H. N. V. Temperley and Michael E. Fisher. Dimer problem in statistical mechanics—an exact result. *The Philosophical Magazine: A Journal of Theoretical Experimental and Applied Physics*, 6(68):1061–1063, 1961.
- [33] Glenn Tesler. Matchings in graphs on non-orientable surfaces. *Journal of Combinatorial Theory, Series B*, 78(2):198–231, 2000.
- [34] Jianfeng Wang, Mei Lu, Francesco Belardo, and Milan Randić. The anti-adjacency matrix of a graph: Eccentricity matrix. *Discrete Applied Mathematics*, 251:299–309, 2018.
- [35] Jianfeng Wang, Mei Lu, Maurizio Brunetti, Lu Lu, and Xueyi Huang. Spectral determinations and eccentricity matrix of graphs. *Advances in Applied Mathematics*, 139:102358, 2022.
- [36] F. Wu. Pfaffian solution of a dimer-monomer problem: Single monomer on the boundary. *Physical Review E*, 74(2), 2006.
- [37] Ke Xiang Xu, Yaser Alizadeh, and Kinkar Ch. Das. On two eccentricity-based topological indices of graphs. *Discrete Applied Mathematics*, 233:240–251, 12 2017.

- [38] Ke Xiang Xu, Kinkar Ch. Das, and Ayse Dilek Maden. On a novel eccentricity-based invariant of a graph. *Acta Mathematica Sinica, English Series*, 32(12):1477–1493, 2016.